

Effects of Space Flight on Locomotor Control

(DSO 614)

Jacob J. Bloomberg, Charles S. Layne, P. Vernon McDonald, Brian T. Peters, William P. Huebner, and Millard F. Reschke of the Johnson Space Center, Houston, TX;

Alain Berthoz of the Laboratoire de Physiologie de la Perception et de L'Action, Collège de France, Centre National de la Recherche Scientifique, Paris, France;

Stefan Glasauer of the Ludwig-Maximilians-Universität München, Klinikum Großhadern Neurologische Klinik, München, Germany; Dava Newman and D. Keoki Jackson of the Massachusetts Institute of Technology, Cambridge, MA

BACKGROUND

Locomotor Head-Trunk Coordination Strategies

In the microgravity environment of spaceflight, the relationship between sensory input and motor output is altered [1]. During prolonged missions, neural adaptive processes come into play to recalibrate central nervous system function, thereby permitting new motor control strategies to emerge in the novel sensory environment of microgravity. However, the adaptive state achieved during spaceflight is inappropriate for a unit gravity environment and leads to motor control alterations upon return to Earth that include disturbances in locomotion. Indeed, gait and postural instabilities following the return to Earth have been reported in both U.S. astronauts and Russian cosmonauts [1-17] even after short duration (5- to 10-day) flights. After spaceflight, astronauts may: (1) experience the sensation of turning while attempting to walk a straight path, (2) encounter sudden loss of postural stability, especially when rounding corners, (3) perceive exaggerated pitch and rolling head movements during walking, (4) experience sudden loss of orientation in unstructured visual environments, or (5) experience significant oscillopsia during locomotion.

Russian investigators [3, 6, 7] have studied locomotor behavior in cosmonauts following Soyuz missions lasting from 2 to 63 days. The sequential positions of various body joints and limbs were recorded and analyzed to determine kinematic features of walking, running, long jumps, and high jumps. Their results showed distinct postflight performance decrements in gait and jumping behavior. In most cases, the durations of the postflight performance decrements were related to the length of the flight. Postflight walking was characterized by an exaggerated width in leg placement, shifting the trunk to the side of the supporting leg, and failure to maintain the intended path. To enhance stability, the subjects frequently raised their arms to the side while making small steps of

irregular length. Although both anecdotal and experimental evidence indicate that significant locomotor disturbances occur following spaceflight, little is known about underlying mechanisms contributing to these problems.

Pozzo and Berthoz [18, 19] have demonstrated that during normal locomotion the head is actively stabilized relative to space with a precision of a few degrees. Based upon this result they have speculated that postural and gait motor control mechanisms may utilize a top down control scheme to ensure head stability during body movement. Such a strategy is advantageous because a stable head facilitates the maintenance of gaze stability during locomotion. Grossman et al. [20] have determined that during walking and running, the peak velocities of head rotations in yaw, pitch, and roll are generally maintained below 100°/s and are thus below the saturation velocity (350°/s) of the vestibulo-ocular reflex [21]. Grossman and colleagues [22] have characterized gaze stability during locomotion and have found that the angle of gaze is maintained relatively stable during walking and running. However, individuals with loss of vestibular function and neurological disease experience increased oscillation of the head and instability of gaze during locomotion, leading to impaired visual acuity and instability of the visual scene during locomotion [23-28]. These results underscore the importance of head stability in aiding gaze stabilization during locomotion.

Guitton et al. [29] examined visual, vestibular, and voluntary control of head movement in normal subjects and patients with bilateral vestibular deficits during passive whole body rotation about a vertical axis. Subjects were asked to maintain the position of a head-fixed laser on a stationary target, with vision, without vision in the dark, and during performance of a distraction task such as mental arithmetic. Normal subjects were most accurate when vision was provided. With vision, the vestibular deficit patients performed as well as normal subjects. Performance of the patient group deteriorated when vision was denied, indicating that vestibular information plays a

role in head movement control. Guitton et al. [29] determined that long latency voluntary mechanisms were responsible for head stabilization. However, as head frequency increased (above 2 Hz), they hypothesized that the passive inertial properties of the head-neck system would dominate the response in the higher frequency range. Keshner and Peterson [30] examined head stability during free locomotion and during passive rotations. Their results indicated that head movement during free locomotion was largely restricted to the 1 to 2 Hz range. This falls within the frequency range identified for vestibulocollic and cervicocollic reflex control of head movement characterized during passive rotation. Voluntary, reflexive, and passive mechanisms may all play a role in head movement control during locomotion [31, 32].

Angular head movements can actually contribute to gaze stabilization during locomotion. In humans, both during treadmill and free locomotion, pitch head rotations (in the sagittal plane) aid gaze stabilization by compensating for the vertical trunk translation that occurs with each step during locomotion [13, 19, 28, 33]. In a previous study, we determined that when subjects are asked to visually fixate a target while walking on a treadmill, the magnitude of these pitch head rotations was modulated, depending upon target distance [13]. When an Earth-fixed visual target at optical infinity was brought close (within 30 cm) to the eyes, pitch head movements increased in amplitude in a way consistent with the hypothesis that rotational head movements are driven in part by the requirement to aid in gaze stabilization. In related work, Paige et al. [34] showed that compensatory eye movements during vertical trunk translation were mediated by similar alterations in target distance. The goal-directed response of pitch head movements during concurrent locomotion and visual target fixation suggests that these head movements were not completely dependent on passive inertial and visco-elastic properties of the head-neck system, but could be actively modulated to respond to altered gaze control requirements. Monkeys trained to locomote around the perimeter of a circular platform were found, while running, to produce continuous eye and head nystagmus to maintain gaze stabilization during body movement [35, 36]. Thus, coordinated head and trunk movements play a central role in maintaining clear vision during natural body movements, and may have a strong influence on the organization of postural and locomotor control patterns. Accordingly, one of the objectives of DSO 614 was to determine if exposure to the microgravity environment encountered during spaceflight adaptively modified head-trunk coordination strategies during postflight locomotion.

Lower Limb Kinematics During Treadmill Walking

Both scientific and anecdotal evidence suggest profound changes in perceptual motor functioning after spaceflight

[10]. These changes pose concern for situations in which movements must be executed reliably and accurately. Locomotion, whether on Earth following completion of a U. S. Space Shuttle mission or on a remote planet surface following a lengthy flight, would be subject to compromise by changes in perceptual motor functioning resulting from in-flight adaptation to the microgravity environment.

Postflight locomotor changes of a biomechanical nature include increased angular amplitude at the knee and ankle, and increased vertical accelerations in the center of mass [37]. In addition, Chekirda et al. [6] noted both: (1) apparent change in the contact phase of walking, in which the foot appeared to be thrust onto the support surface with a greater force than that observed before flight, and (2) efforts to preserve stability in which cosmonauts spread their legs far apart, used their arms more, and used shorter steps after flight. Even with these compensatory changes, both Russian and U.S. investigators have observed disturbances in performance, including deviations from a straight trajectory [6] and a tendency toward loss of balance during walking when turning corners [1, 3].

Locomoting through a complex and cluttered environment also involves perceptual demands. A contributing factor to stable and reliable locomotion is the maintenance of stable gaze. Empirical evidence suggests that the head-neck-eye complex operates to minimize angular deviations in gaze during locomotion [19]. Since the head-neck-eye complex is situated on top of the trunk-lower limb complex, the noted postflight biomechanical changes suggest a high potential for negative impact on gaze stabilization strategies. The situation is further compounded by changes in perceptual function. For example, after spaceflight, crew members developed a stronger dependence on visual cues [38], there were changes in the ability to detect accelerations, and otolith organ sensitivity declined throughout the duration of a flight [128]. In addition, changes in vestibulo-ocular reflex (VOR) gain as a function of spaceflight were observed [39, 40], and exposure to microgravity modified eye-head coordination during target acquisition [41, 42] and ocular saccadic performance [43].

When considered together, these biomechanical and perceptual changes point toward a highly probable adaptation of head and gaze control during locomotion after spaceflight. However, strategies used for maintaining gaze stability have not been documented during postflight locomotion. To better understand the functional implications of existing flight related evidence, especially in terms of the strategies used for coordination among the various perceptuo-motor subsystems, we designed the DSO 614 investigation to examine the role of adaptive modification in head movement control during postflight locomotor performance. The investigation was designed to address this problem not only in terms of eye-head-trunk coordination, but rather as a problem from the ground up, inasmuch as lower limb coordination and support surface

dynamics influence gaze control [44]. We contend that an important element of gaze control during locomotion is the management of energy flow through the body, especially during high energy interactions with support surfaces such as those occurring at the moment of heel strike and toe off [45, 46]. The ability to attenuate the transmission of energy through the body is influenced directly by a number of factors. Among these are changes in the characteristics of the musculoskeletal shock absorbers, including the viscoelastic properties of joints [47]. Also important for the management of energy flow through the body is the pattern of joint kinematics seen during locomotion. Of specific relevance is lower limb joint configuration at the moment of heel strike with the support surface. Perry and Lafortune [48] demonstrated that absorption capacity could be reduced by excessive foot pronation, suggesting that the joint configuration of the foot-ankle at heel strike contributes directly to the potential transmission of the heel strike shock wave through the body. Changes in foot activity during the contact phase of locomotion following spaceflight were demonstrated by Chekirda et al. [7].

McMahon and colleagues [49] suggested that the degree of shock wave transmission during locomotion was extremely sensitive to the degree of knee flexion. They discovered that while tibial shock was increased with increased knee flexion, transmission of the shock wave to the head was significantly reduced. However, after a direct investigation of the role of knee angle on axial stiffness of the lower limb, Lafortune et al. [50] suggested that increased knee angle at foot impact was less effective than previously thought in attenuating impact shock. Nevertheless, Hernandez-Korwo et al. [37] noted locomotor changes in both knee and ankle angles following spaceflight.

Grossman et al. [20] recognized that locomotion induces rhythmic oscillations of the trunk and the head. The predominant frequency of these oscillations is equivalent to the step frequency. Since the head contains both the visual and vestibular systems, any irregularities in these step-dependent oscillations could influence locomotor control. Consequently, we determined that it was crucial to examine not only the head-trunk linkage [51], but all the links between the head and the support surface. Appropriate attenuation of the intersegmental energy flow during locomotion minimizes the disturbance of the visual and vestibular systems, and preserves head and gaze stability. However, we suspect that spaceflight adaptation may compromise this ability and thus lead to impaired head and gaze control. To more clearly determine the role of the lower limb joint complex in this phenomenon, we chose to focus attention on two specific locomotor events: heel strike and toe off. High energy transitions between the stance and swing phases were considered the most likely events to illustrate changes in locomotor performance, since any maladapted effort to manage energy flow would result in inappropriate energy transfer among contiguous

body segments and could cause disturbances in both lower limb coordination and head-eye coordination observed during walking after spaceflight.

Neuromuscular Activation Patterns During Locomotion

Astronauts display remarkable flexibility in adapting themselves and their movements to the unique microgravity environment of spaceflight. Despite shifts in many physiological processes, crew members rapidly develop motor control strategies to perform tasks effectively in space. Moreover, astronauts must readapt quickly upon return to Earth in order to regain appropriate coordination strategies, particularly with regard to posture and locomotion.

Spaceflight has been associated with: (1) decreases in muscle strength and tone [5, 52-54], (2) hyperactivity in H- and stretch-reflex characteristics [5, 53, 55], (3) changes in muscle strength velocity profiles [54], (4) changes in lower limb muscle activation patterns [55], (5) changes in proprioceptive and vestibular functioning [5, 53, 56], and (6) oscillopsia [57]. These neurological and physiological alterations could be expected to influence the precise neural control needed for the lower limb muscle activation patterns required for optimal locomotion.

Electromyography (EMG) has long been used to assess the neuromuscular control features associated with both normal and abnormal gait [58-66]. The phasic properties of processed EMG are highly correlated with the changes in muscle tension and joint angular accelerations that occur throughout the gait cycle [60, 67], and a linear relationship exists between muscle tension and EMG amplitude in the range of tension levels found during normal walking [68, 69].

A wide range of compensatory locomotor neuromuscular patterns have been identified in several clinical populations [70-72], suggesting that the sensorimotor system can adapt so as to allow a range of locomotor behavior. Changes in EMG measures reflecting muscle co-contraction, such as simultaneous activation of antagonist muscles, have often been interpreted as representing modifications of neuromuscular control strategies [73, 74]. The learning and development phase of a skilled movement is often associated with a high degree of muscle co-contraction. This co-contraction results in stiff, uncoordinated movement patterns. As skill level increases, segmental motions become smoother and well coordinated, reflecting a decrease in muscle co-contraction. Conversely, increases in co-contraction following spaceflight may result in less coordinated and more variable segmental motions. Additionally, the stiffness resulting from increased co-contraction can alter how the impact forces generated at heel strike are dissipated throughout the body during locomotion. The inability to efficiently manage the energy resulting from heel strike may result in increased head motion, thereby increasing the possibility of gaze

instability. Thus, muscle co-contraction is an important index of how effectively the sensorimotor system is able to control neuromuscular activation in order to produce coordinated movement. On the basis of the above properties, the use of EMG to describe changes in muscle activation patterning and co-contraction levels during locomotion seems well suited for revealing changes in neuromuscular properties resulting from spaceflight. Although much anecdotal information exists, DSO 614 was the first time that the influence of 8- to 15- day spaceflight on lower limb neuromuscular activation during postflight locomotion had been adequately evaluated.

Spatial Orientation

Prolonged stays in the microgravity environment result in changes in both the vestibular and somatosensory systems [10]. Several hypotheses have addressed the question of how the changed sensory inputs are reinterpreted. For example, the otolithic system, which on Earth measures a combination of head orientation through gravity and linear translational acceleration, should reinterpret all linear acceleration in microgravity as being translational [75]. This could lead to misperception of head tilt as translation in the first hours after return to Earth. These changes in perception of vestibular input may affect the ability to spatially orient during locomotion after spaceflight.

In the new paradigm presented here, the astronaut subjects perform a natural task involving both somatosensory and vestibular sensory inputs. Goal-directed locomotion satisfied these requirements and provided information about the spatial orientation capabilities of the subjects. Goal-directed locomotion, with or without vision, is a simple everyday task, in contrast to former investigations that required more artificial tasks such as performing eye movements with the head fixed. This portion of DSO 614 focused mainly on the question of whether exposure to the microgravity conditions encountered during spaceflight was associated with impaired spatial orientation during locomotion following return to Earth, and what role vision played in this process.

Lower Limb and Mass Center Kinematics in Downward Jumping

In addition to changes in posture and locomotor control, astronauts exhibit alterations in the ability to maintain stability following drop landings. Watt et al. [77] tested astronauts subjected to sudden “drops” and reported that all subjects were unsteady postflight, and that one subject fell over backwards consistently.

Such performance decrements may result from various changes in the sensorimotor complex resulting from microgravity exposure. Parker et al. [78] found direct evidence for reinterpretation of graviceptor inputs during spaceflight. Young et al. [79] also provided evidence for

sensory compensation during spaceflight, resulting in interpretation of utricular otolith signals as linear acceleration rather than head tilt, as well as increased dependence on visual cues for perception of orientation. The otolith-spinal reflex, which helps prepare the leg musculature for impact in response to sudden falls, is dramatically reduced during spaceflight [77]. However, postflight results were not significantly different from preflight responses, indicating a rapid course of readaptation upon return to Earth. Other work indicates that spaceflight may affect proprioception of limb position; Watt et al. [77] found a considerable decline in arm pointing accuracy while blindfolded during and immediately following spaceflight. Furthermore, the subject who fell consistently in the drop test reported that his legs were always further forward than he expected them to be.

Other possible explanations for postflight postural instability include atrophy of the antigravity muscles [80], in-flight changes in tonic leg muscle activation patterns, or microgravity-induced alterations in stretch reflexes [81, 82]. Gurfinkel [83] also reported reorganization of higher-level anticipatory postural responses to rapid movements during spaceflight. Altered patterns of leg muscle coactivation may result in changes in the modulation of limb impedance that controls the dynamic interaction of the limb with the environment. McDonald et al. [45] cited postflight changes in the phase-plane description of knee joint kinematics during gait as preliminary evidence for changes in joint impedance resulting from exposure to weightlessness.

The aim of this aspect of the study was to determine the effects of microgravity exposure on the astronauts' performance of two-footed jump landings. This study was intended to elucidate how exposure to an altered gravitational environment affects control of lower limb impedance and preprogrammed motor strategies for impact absorption. The joint kinematics of the lower extremity during the jump landings, as well as the kinematics of the whole-body mass center, were of particular interest. The results suggest that different subjects adopt one of two response modes upon return to 1-g following spaceflight, and that postflight performance differences may result largely from adaptive changes in open-loop lower limb impedance modulation. The altered jumping kinematics seen postflight may reflect decrements in limb proprioception, altered interpretation of otolith acceleration cues, and reduced requirements for maintenance of posture under microgravity conditions.

METHODS

Locomotor Head-Trunk Coordination Strategies

Twenty-three astronauts, 19 males and 4 females, ranging in age from 34 to 51 years, served as subjects in this study. All subjects gave informed consent to testing,

and all protocols were approved by the NASA/Johnson Space Center Institutional Review Board for Human Research. To measure head and trunk movements, passive retroreflective markers, with negligible mass, served as tracking landmarks. These were affixed to the vertex, occipital, right temporal positions of the head and on the seventh cervical vertebrae (C7). The movements of these markers were simultaneously recorded with four video cameras sampling concurrent video images at 60 Hz. The position of each marker in space was uniquely determined with the aid of a video-based motion analysis system (Motion Analysis Corporation, Santa Rosa, CA). Each subject wore spandex shorts, sleeveless shirt, and running shoes. Markers and electromyographic (EMG) electrodes were also placed on the lower limbs for a separate analysis of kinematic and muscle activation patterning. Vertical eye position relative to the head was recorded using standard DC-Electrooculographic (EOG) methods.

During each test session, the astronaut subjects were required to walk, at 6.4 km/h (4 mph), on a motorized treadmill (Quinton™ Series 90 Q55 with a surface area of 51 cm × 140 cm, or 20 in × 55 in) while visually fixating on a centrally located Earth-fixed target. This target consisted of a light emitting diode (LED) positioned either 30 cm or 2 m from the subject, at the height of the subject-perceived eye level. Prior to initiating the trial, the subject straddled the treadmill belt while the speed was increased to the desired speed, at which time the subject was free to begin walking. A few strides were permitted to allow the subject to become comfortable with the treadmill speed and to attain a steady gait. After a verbal ready indication from the subject, data collection was initiated, with the subject continuing to locomote while fixating the target for 20 seconds. The subject maintained fixation of the target for the full duration of the trial. To prevent potential injury through falling, each subject wore a torso harness attached to an overhead frame. During nominal treadmill performance, this harness provided no support and did not interfere with natural movements of head or limbs.

Data were collected before and after Shuttle missions of 8 to 15 days duration. Preflight testing consisted of two sessions, one each at approximately 90 and 10 days prior to launch. Postflight testing was performed 2 to 4 hours after landing and 2, 4 and 8 days following return to Earth. Data collected approximately 10 days before flight (referred to as “preflight”) and on landing day (referred to as “postflight”) were evaluated. Recovery data (R+2, 4, and 8 days) will be covered in future communications.

A variety of challenges to head-trunk coordination were used to delineate adaptive changes in goal directed response characteristics. These included:

1. Far Target Condition (FAR) – Subjects walked on the treadmill while visually fixating the target located 2 m (6.5 ft) from the outer canthus of the eyes. Two trials of 20 s in duration were performed.

2. Near Target Condition (NEAR) – Subjects walked on the treadmill while visually fixating the target located 30 cm (1 ft) from the outer canthus of the eyes. Two trials of 20 s in duration were performed.

3. Intermittent Vision Condition (IV) – To investigate how the head-trunk system dynamically responded to short term (5 seconds) alternating changes in sensory input, subjects walked on the treadmill during intermittent visual occlusion. A 20-second locomotion trial would begin with the eyes open and the subject fixating the visual target. After 5 seconds, subjects were instructed to close their eyes and continue walking while attempting to fixate on the remembered position of the target. Five seconds later, subjects were instructed to open their eyes. The 5-second eyes open/eyes closed periods alternated through the 20-second duration of the IV walking trial. Two trials of 20 seconds in duration were performed. To address safety concerns, subjects lightly placed their index finger on the forward hand rail of the treadmill to gain additional haptic cues regarding body placement. It has been recently shown [84, 85] that a light touch, insufficient to produce mechanical support, contributes significantly to control of postural equilibrium in the absence of vision. Although the light finger touch may have enhanced performance in general, all the eyes-open and eyes-closed epochs in an IV trial occurred under the same haptic conditions. The alternating 5 s epochs of eye closure were confirmed using vertical electrooculography to detect eye closure transitions in EOG baselines.

Three-dimensional translational trajectories of each body-fixed marker were calculated relative to a coordinate frame that was coincident with the surface of the treadmill. The marker trajectories were low pass filtered at 10 Hz using a finite impulse response filter with a Hamming window. Movement of the head in the sagittal plane (head pitch) was characterized by the angle between the horizontal and the line connecting the vertex and occipital markers. Vertical (z-axis) trunk translation was determined from the displacement of the marker placed on the seventh cervical vertebrae (C7).

The degree of association between vertical trunk translation and corresponding compensatory pitch head movement was characterized using the coherence function. The coherence between two signals was defined as:

$$\text{Coherence} = \frac{|\text{cross spectra of signals } x, y|^2}{(\text{power spectra } x)(\text{power spectra } y)} \quad (1)$$

The coherence value could vary between zero and unity. If a perfect linear relationship existed between the two signals at some specific frequency, the coherence

function was equal to unity at that frequency. If the two signals were completely unrelated, the coherence function was zero over all frequencies.

Compensatory pitch head movement wave forms were also subjected to Fourier analysis and the amplitude of the predominant frequency was determined. Each 20-second walking trial was divided into 4 epochs of 4 seconds duration. The frequency spectra of each 4-second epoch was then calculated separately. For each subject, over two walking trials per condition, eight individual epochs were analyzed and the predominant peak determined, allowing the mean peak amplitude to be determined for each subject.

Lower Limb Kinematics During Treadmill Walking

A total of seven subjects were tested from three Shuttle missions, of eight or nine days duration, flown between March 1992 and February 1994. Of the seven subjects, two were first-time fliers and five had flown at least once previously, six were men and one was a woman. Subject height ranged from 1.68 m (5 ft 6 in) to 1.85 m (6 ft 1 in). Subject ages ranged from 35 to 49 years with a mean of 41 years.

Before each testing session, passive retroreflective markers, serving as tracking landmarks, were affixed at vertex, occipital and temporal positions on the head, and at the acromion process, lateral epicondyle of the humerus, midpoint on the dorsal surface of the distal portion of the radius-ulnar, C7, femoral greater trochanter, lateral femoral epicondyle, lateral malleolus, shoe surface coincident with the posterior surface of the calcaneus of both feet, and the fifth metatarsophalangeal joint, on the right side of the body. The movement of these markers was recorded simultaneously with four video cameras sampling images at 60 Hz. Ambient light was adjusted to allow high contrast between the retroreflective markers and the surface to which they were attached. The position of each marker in space was determined with the aid of a video based motion analysis system (Motion Analysis Corporation, Santa Rosa, CA). Each subject wore cycling shorts, a sleeveless shirt, and the same brand of running shoe before and after flight. Foot switches, using Interlink

Electronics™ force sensing resistors, were attached to each shoe at the heel and toe and sampled at 752 Hz through a 12 bit analog/digital (A/D) board.

Subjects were required to ambulate on a treadmill and tested on the same schedule as described earlier.

Table 5.5-1 illustrates the conditions of each data collection session. Trial numbers indicate presentation order within each testing session. Additional walking trials were performed during periodic visual occlusion. Trials 1 and 10 were the standing trials used to calibrate the EOG system. Segmental kinematic data collected during these trials were used to calculate joint configurations during quiet standing. Only data from walking (6.4 km/h or 4 mph) trials during near (30 cm or 1 ft) target visual fixation collected 10 days before flight (preflight) and on landing day (postflight) were evaluated, since this comparison was most likely to reflect any spaceflight induced effects.

Subjects were instructed to maintain ocular fixation of the target at all times. During each trial, the spotter monitored subject location on the treadmill and instructed the subject to move forward or backward if necessary. For the walking trials, subjects stood off the treadmill belt while its speed was increased to the criterion. At this point the subject was free to begin walking. A few strides were permitted to allow the subject to become comfortable with the speed and to attain a steady gait. After a verbal ready indication from the subject, data collection was begun with the subject continuing to walk and fixate the target for 20 seconds.

Data resulted from a direct evaluation of lower limb joint kinematics patterns observed during treadmill walking after short duration spaceflight. Data analyses were designed to determine the potential influence of lower limb kinematics on adaptive strategies utilized for head and gaze control during postflight locomotion. Basic characteristics of the temporal form of the gait pattern were examined, since even while locomoting on a treadmill at a fixed speed, there was an opportunity to trade off step amplitude and step frequency while maintaining the same forward speed. At the same time, the relative duration of the stance and swing components of the step could be adapted. This composition was referred to as the duty factor, a ratio representing the amount of time spent in the stance phase in each step. The duty factor could be

Table 5.5-1. Experiment Conditions

Treadmill Speed	Visual Target at 2 m		Visual Target at 30 cm	
	Continuous Vision	Periodic Occlusion	Continuous Vision	Periodic Occlusion
6.4 km/h	trials 2 and 4	trials 3 and 5	trials 6 and 8	trials 7 and 9
9.6 km/h	trials 11 and 12	Not performed	Not performed	Not performed

identified by analyzing the temporal location of the toe-off between two successive foot falls. The duty factor of bipedal walking was typically reported as approximating 0.6 because the toe-off occurred at about 60% of the step. Step-to-step variation of these temporal measures is presented as a precursor to the joint kinematic analyses. Any changes in these factors could directly influence the frequency and amplitude of the rhythmic oscillations in the trunk and the head.

Several techniques were used to evaluate the lower limb locomotion system comprising the hip, knee, and ankle joints. Representing the periodic motion of these joints on the phase plane, we documented within-cycle variability over discrete epochs of the cycle, and also at two discrete events, heel strike and toe off. These analyses were performed on each joint independently, to document any disturbances in individual joint activity, and to identify where these disturbances occurred relative to gait cycle phases. To quantify cycle-to-cycle stability in gait patterns, a Poincaré map was used to take the continuous dynamics of the joint phase portraits into the discrete regime, based on the event-specific iterations at heel strike and toe off. The states of the phase portraits (angular displacement and angular velocity) of the three lower limb joints were used to define a six-dimensional state space. Such a representation allowed the exploitation of a specific analysis technique to evaluate system stability. This technique evaluated behavior of the three-joint system as a whole, so that any changes in a single joint could be assessed at the system level. Therefore, independent measures of system component variability, and a measure of system stability as a whole are presented. These measures were intended to determine changes in the nature and source of perturbations to the trunk emanating from the lower limbs during the locomotor cycle.

Marker trajectory data were processed to derive three-dimensional translation information relative to a coordinate frame coincident with the surface of the treadmill. Subjects walked toward the +X direction and the belt moved in the -X direction. The vertical axis orthogonal to the treadmill surface was +Z, and the Y axis was orthogonal to the X-Z plane (Figure 5.5-1). Marker trajectories were low pass filtered at 10 Hz using a finite impulse response filter with a Hamming window. The filtered trajectories in X and Z were then used to determine joint angular motions in the sagittal plane for the hip (thigh and knee markers), knee (thigh, knee, and ankle), and the ankle (knee, ankle, toe). Figure 5.5-1 illustrates how these joint angles were determined relative to the coordinate frame of reference. The hip (H) angle was measured with respect to the vertical, with flexion designated as positive and extension as negative. The knee (K) angle was measured from the projection of the thigh link segment to the tibial link segment, with flexion designated positive and extension as negative. The ankle (A) angle was measured as that angle between the tibial link segment and the foot

segment, with plantar flexion being greater than 90 degrees and dorsiflexion less than 90 degrees. These three joint angles were considered to be a satisfactory representation of the lower limb dynamic during the task of treadmill walking.

The equilibrium position was determined for each joint under consideration, to facilitate the modeling of lower limb oscillatory motion. This position was equivalent to the joint angles measured during quiet standing on the treadmill. Hence, the hip, knee, and ankle joint angles were used to determine the equilibrium point about which the joint motions occurred for each subject. This equilibrium point was represented as the origin (0,0) on the phase plane. All subsequent joint angular displacement data were represented with respect to this origin. Having determined the sagittal plane joint angular displacements, joint angular velocities were then determined with a fourth order central difference algorithm.

Foot switch signals allowed determination of the moments of heel strike and toe off in the right limb. However, foot switch information was not available for all subjects. In such cases reliable kinematic correlates for heel strike and toe off were determined from toe marker velocity in the Z direction. Determining heel strike and toe off in this manner matched foot switch information with an error not exceeding ± 16.7 ms.

Phase plane data, using the joint angular displacement and joint angular velocity as the states of the system, were analyzed using three different techniques to evaluate joint dynamics. The first of these techniques was employed to evaluate variability of independent joint motion over the course of the full gait cycle. The second technique was used to evaluate variability of independent joint configuration at two discrete points in the gait cycle. For both of these techniques, a measure was constructed to combine the variability in the joint angular displacement with the variability in the joint angular velocity. After normalizing each gait cycle to 60 samples, the variability in the joint angular kinematics observed over multiple cycles of one trial was quantified using the standard deviation about the mean joint angle, and the mean joint angular velocity at the moment of heel strike and at the moment of toe off. The displacement and velocity standard deviation magnitudes were then used to define the diameter of the two orthogonal axes of an ellipse. The area of this ellipse was presented as an index of the variability on the phase plane. To evaluate variability over the full gait cycle, the cycle was divided into five 20% temporal epochs, and the variability from each of the 12 samples within each epoch was summated. The phase plane variability at heel strike and at toe off was presented using those samples at which the named events occurred. The third technique used phase plane data to evaluate system stability. This technique utilized the three lower limb joints in combination. The idea of using joint kinematics as state variables and Poincaré maps to evaluate the stability of human locomotion was first introduced by Hurmuzlu [86, 87].

First return maps can be represented by the following finite difference equations in an n-dimensional state space:

$$x_{i+1}^k = f_k(x_i) \quad k=1, \dots, n \quad (2)$$

where x is a vector of state variables ($x=[x^1, x^2, \dots, x^n]^T$) and f represents the nonlinear mapping function. The equilibrium values (steady state) of equation (2) are known as fixed points of the map. Assuming that the fixed point of a map is defined as:

$$x^* = x_{i+1} = x_i \quad (3)$$

the stability of a dynamical system can be analyzed by linearizing equation (2) in the neighborhood of the fixed point to obtain:

$$\delta x_{i+1} = J \delta x_i \quad (4)$$

where δx_i and δx_{i+1} represent the perturbations associated with the i 'th and $(i+1)$ 'th elements of the state vectors, and J is a $(n \times n)$ Jacobian matrix. The entries of this matrix are the partial derivatives of the nonlinear mapping functions ($f_i, i=1, \dots, n$) with respect to the state variables, given as:

$$a_{kj} = \left. \frac{\partial f_k}{\partial x^j} \right|_{x^*} \quad j=1, \dots, n, \quad k=1, \dots, n \quad (5)$$

Such a system is considered to be stable around equilibrium if all the eigen values of the Jacobian matrix lie inside the unit circle [88, 89]. Bifurcations occur if the eigen value(s) move outside the unit circle, resulting in structural changes in the system.

Elements of the Jacobian matrix can be obtained easily if the nonlinear mapping functions (f), that return cross sections of the flow to itself, are known. However, the complexity of human locomotion does not permit simple determination of the functions (f) such as in equations (1) or (2). Although mathematical models of locomotion are available in the literature [86], the authors are not aware of any study that identifies an appropriate form of analytical equation or function. Consequently, we experimentally acquired joint kinematics of human gait and constructed the Jacobian matrix by means of least square regression techniques [85].

Following the procedures of Hurmuzlu [85, 86], we first identified the state variables of our system as the hip, knee, and ankle motions in the sagittal plane. This resulted in a six-dimensional state space of the form:

$$X_{space} = \{\Phi_H, \Phi_K, \Phi_A, \dot{\Phi}_H, \dot{\Phi}_K, \dot{\Phi}_A, \} \quad (6)$$

where Φ and $\dot{\Phi}$ represent angular rotations and velocities of the three joints used in defining the conceptual

model of the gait dynamics. These state variables were each sampled at the moment of heel strike and the moment of toe off. The same data were used to construct Poincaré maps. For each trial, a mean value for each state was calculated and designated as the equilibrium value. The steady state value of each state variable at each event, heel strike or toe off, was assumed to be the statistical average (mean) of all samples. Deviation from equilibrium was then measured at each iteration for each state by calculating the difference between the mean state value and the state value at that iteration. To approximate elements of the Jacobian matrix, a multidimensional regression was then performed among the vectors determined relative to the steady state value.

The set of equations that formulate this multidimensional fit can be written as

$$(Q_H)_{i+1} = A_{11}(Q_H)_i + \dots + a_{16}(\dot{Q}_A)_i + p_1 \quad (7)$$

$$(\dot{Q}_H)_{i+1} = A_{61}(Q_H)_i + \dots + a_{66}(\dot{Q}_A)_i + p_6$$

where Q_H, \dots, \dot{Q}_A , represents the column vectors, with a number of rows equal to the number of sampled locomotion steps (e.g., Q_H is a column vector indicating the deviation magnitude of the sagittal hip excursion relative to the steady state hip excursion), a_{ij} 's form the elements of the approximated Jacobian matrix, and p_i ($i=1, \dots, 6$) are the constants of the regression.

Finally, we calculated the eigen values ($\lambda_i, i=1, \dots, 6$) of the Jacobian matrix and statistically averaged them for each individual subject to quantify the dynamic stability exhibited by that subject during treadmill walking. According to stability theory, all eigen values should lie inside the circle, ($|\lambda_i| < 1.0, i=1 \dots 6$) for a stable system [89].

Neuromuscular Activation Patterns During Locomotion

Subjects in this study were 10 astronauts (3 women and 7 men) who had completed Shuttle missions lasting 8 to 15 days. All provided informed consent to participate, as required by the Johnson Space Center Institutional Review Board. Six of the subjects had flown on previous Shuttle missions.

Subjects walked on a motorized treadmill and followed the same testing protocol as described earlier.

After the skin was cleaned with alcohol wipes, pre-amplifier surface EMG electrodes were placed on the subjects over the bellies of the rectus femoris (RF), biceps femoris (BF), tibialis anterior (TA), and gastrocnemius (GA) in parallel to the muscle fibers. Electrodes were attached with hypoallergenic tape and covered with elastic leg wraps to prevent movement on the skin. Analog EMG data were band-passed at 30 to 300 Hz before being

digitized at 752 Hz. Foot switch information, also sampled at 752 Hz, was stored within the EMG data files.

Data analysis focused on characterizing the influence of spaceflight on terrestrial locomotion as soon as possible after landing, early in the readaptation process. Data were analyzed to compare the neuromuscular responses obtained 10 days before launch with those obtained between 2.5 and 4 hours after landing.

The first step in data analysis was to determine whether spaceflight influenced stride time, defined as heel strike to heel strike for the same leg, during locomotion. Trials of 20 to 22 strides were averaged relative to heel strike so that stride times before and after spaceflight could be compared. Stride time was a function of time spent in swing and stance phases, both of which could be controlled by the locomoting subject. Changes in the duty factor, defined as the percentage of the gait cycle spent in stance phase, could reflect changes in the neuromuscular activation patterns [90]. Each subject's stride time and duty factor were calculated for each stride. Values before and after spaceflight were compared with t-tests for correlated data.

EMG data were evaluated for each muscle and for each subject. Data across stride cycles were first time-normalized to 100% of stride by averaging the data between consecutive right heel strikes. Next, to reduce variability among subjects [62], wave forms were magnitude normalized to the mean level of activation across the wave form, so that the mean level of activation within the wave form was 100%. The mean wave forms then were divided into 5% epochs by representing the averaged data within an epoch as a single point [91, 92]. Standard deviations, and coefficients of variation across the mean wave forms, were calculated to assess activation variability. These reduction techniques produced EMG wave forms (referred to as reduced wave forms) that represented the phasic features of each muscle across the stride cycle.

The question of how spaceflight affects the lower limb neuromuscular activation during treadmill locomotion was addressed in five ways:

1. Reduced wave forms were compared before and after flight using Pearson product moment correlations for each muscle and each subject [66, 91, 92]. This analytical approach was extended to determine the degree of activation symmetry between individual muscles of both legs before and after flight.
2. Repeated measures analysis of variance (ANOVA) was used in combination with post hoc testing to compare normalized amplitudes before and after spaceflight at each 5% epoch for each right lower limb muscle.
3. Full wave-rectified EMG records, obtained from individual strides, were used to characterize the phasic pattern of activation from the right lower

limb muscles. This approach was adopted to assess the potential for changes in the time of muscle activation within the time-normalized wave forms. Changes in time of muscle activation within a stride cycle would indicate subtle, but potentially important, modifications in neural control.

4. Potential preflight versus postflight changes in coefficient of variation of the reduced EMG wave forms around the behavioral events of heel strike and toe off were assessed using repeated measures ANOVA with post hoc testing. EMG variability around these two events was evaluated because these periods in the stride cycle have large segmental decelerations (heel strike) or accelerations (toe off) and, therefore, require precise neuromuscular control.
5. Muscle co-contractions between the traditional agonist-antagonist pairs of the BF-RF and TA-GA were evaluated for potential preflight versus postflight differences using repeated measures ANOVAs with post hoc testing. An alpha level of $p < 0.05$ was adopted for all statistical tests.

To evaluate the phasic activity of individual strides, the most significant neuromuscular control feature of each muscle during each stride was determined for each subject. For the RF, BF, and GA, this feature was the temporal onset (relative to heel strike) and duration (as a percent of stride cycle) of the largest amplitude burst of activity. For the RF and BF, the largest burst of activity occurred around heel strike. The largest burst of GA activity occurred in preparation for toe off. For the TA, the most significant neuromuscular control feature was the silent period present in most subjects shortly before toe off. This silent period usually corresponded to a large increase in gastrocnemius activity. Thus, the temporal features of the TA silent period was thought to reflect the sensorimotor system's ability to regulate ankle musculature activity, particularly around the critical time of toe off.

Muscle activation onset time was obtained by displaying the EMG activity of all strides simultaneously on the computer monitor. Visual inspection, in combination with interactive electronic cursors, was used to establish parameters of an algorithm for the identification of temporal onset of the phasic activity of interest in each stride. The algorithm was used to identify onset of muscle activation by noting the first point of a burst that exceeded a fixed amplitude threshold value (approximately two standard deviations above a quiet baseline) for at least 30 ms. A 30 ms minimum was selected on the basis of a report that muscle bursts that last less than 30 ms do not contribute to the force of the moving limbs during locomotion [93]. The algorithm was reversed to obtain muscle activation offsets. Muscle activation durations were obtained by calculating

the temporal difference between activation onset and offset. Duration of the silent period for the TA was calculated as the difference between offset and subsequent onset of muscle activity. To standardize measures across data collection sessions and subjects, temporal measures were expressed as a percentage of stride. The relationship between the ankle joint muscle activation characteristics, in preparation for toe off, was assessed by computing the temporal differences (as percent of stride cycle) between GA offset and TA onset. Paired Student *t*-tests were used to test for preflight-to-postflight changes in the activation features of each muscle for each subject. Although this statistical approach limited generalizations to other populations, it was appropriate for our goal of characterizing the range of individual responses after spaceflight.

Although previous gait investigations have revealed greater variability in motor patterns than in limb kinematics, large changes in EMG activation characteristics have a functional effect as well [66]. Following the convention of Ounpuu and Winter [64], changes in relative amplitude were considered functionally significant if: (1) the difference was statistically significant at $p < 0.05$, (2) the difference between the preflight and postflight measures was greater than the variability of each individual measure, and (3) the muscle was active (i.e., 20% of mean amplitude) during the analyzed epoch. A difference between preflight and postflight phasic patterns was considered functionally significant if the Pearson *r* value was less than or equal to 0.71 [66, 94].

It was plausible that the sensorimotor system may have had difficulty in controlling neuromuscular activation after spaceflight, in preparation for the events of heel strike and/or toe off, as a result of these two events, or a combination of preparation for and reaction to heel strike and toe off. Therefore, preflight versus postflight differences in the coefficient of variation during three epochs of the stride cycle were tested. These epochs were: (1) the 10% preceding the event, (2) the 10% following the event, and (3) the combination of the previous two epochs (i.e., 20% of the stride cycle with the event centered in the middle of the epoch). Only muscles that were active during all three epochs around the particular event were evaluated for preflight versus postflight differences.

Measures of co-contraction were obtained by initially summing the area under the curve of the reduced EMG wave forms and expressing the activity within each of the 20 epochs as a percentage of the summed area. The cross-sectional area of EMG activity for the BF-RF and GA-TA antagonist pairs was then calculated and used as an indicator of co-contraction [95].

Spatial Orientation

Tests were conducted to quantify orientation performance during free walking after spaceflight. Seven astronaut subjects, 5 male and 2 female, from spaceflights of

8 to 14 days' duration, performed two spatial orientation tasks requiring them to negotiate a path consisting of a right triangle with two sides 3 m (10 ft) in length, by walking with and without the aid of vision. Three corners were marked on the floor with targets consisting of 7 cm \times 7 cm (2.75 in \times 2.75 in) crosses (Figure 5.5-2). The task was to walk the triangular path, starting at either corner 1 or corner 3. When the path was completed, the subject was requested to turn and face the original direction. The verbal instructions given were, "walk at a comfortable pace, as accurately as possible around the path. The motion should be continuous. The goal is accuracy, with accuracy defined as your ability to straddle the path." For all experiment sessions, two spotters were present to prevent any collisions during the eyes closed tasks.

To control for directional preferences, the task was performed alternating clockwise (cw) and counterclockwise (ccw) directions, but always approaching the right angle (corner 2) of the triangle first. To minimize visual feedback, (1) vision occluded trials were performed before the eyes open trials, and (2) at the conclusion of each eyes closed trial, the subject was led in a serpentine path, with eyes still closed, to the next starting point. The subject was instructed to look at the path before starting each eyes closed trial. The subjects performed 12 trials eyes closed (6 cw and 6 ccw) and 6 trials eyes open (3 cw and 3 ccw). This protocol was performed 45 days and 15 days before, and 2 hours, 2 days, and 4 days after, spaceflight. This report will only present data from 15 days preflight and 2 hours postflight. Each subject wore a helmet with three retroreflective markers located above the head in approximately the sagittal plane (Figure 5.5-3). This helmet was also equipped with headphones that provided white noise to mask out spatial auditory cues, and blackened goggles to occlude vision.

Head kinematic data were collected with a video based motion analysis system using four CCD cameras (Motion Analysis Corporation, Santa Rosa, CA). Signals from the four cameras were fed to a video processor at a sampling frequency of 60 Hz. The outline of each target was extracted and passed to a system that tracked the three reflective head targets, producing a three-dimensional assessment of each marker.

The coordinates necessary to describe head position in all six degrees of freedom were computed from the three-dimensional positions of the head markers, and were used to: (1) identify translational position, (2) compute linear velocity, (3) express tilt, and (4) compute angular velocity of the head. The rotational head position was expressed as quaternions [96]. An interactive graphical software package assisted in determining the corners of the walked trajectory, and angular head velocity maxima, for each walk. Corner points were used to compute distance errors and mean walking velocity. To evaluate the mean walking direction for each leg of the triangle, lines of minimum least square

distance were fitted to the trajectory between the corners. The angle between two lines gave the amount of turn performed by the subject. Angular deviation from desired trajectory was computed as the difference between angle turned and required turn angle at the respective corner. Due to marker dropouts, not all parts of the trajectory were successfully recorded in all trials. The incomplete parts were marked as being invalid. Statistical analysis, performed on the mean parameter values of each subject, was based on a 3 segments \times 2 directions \times 2 visual conditions \times 2 days repeated measures design.

Lower Limb and Mass Center Kinematics in Downward Jumping

Experiment Design

The subject pool for this study consisted of 9 astronauts. In order to protect the subjects' anonymity, they will henceforth be designated by letter codes (S-1, S-2, ... S-9). The subjects ranged in age from 36 to 50 years. Of the 9 subjects, 8 were male and 1 was female. The first preflight testing (PRE1) took place 2-6 months before launch. Another preflight test (PRE2) occurred 9-15 days before launch, while the postflight tests (POST) were performed within 4 hours of Shuttle landing. Mission lengths varied between 7 and 14 days.

At each data collection session, the jumping protocol consisted of 6 voluntary two-footed downward hops from a 30 cm (1 ft) platform. Three jumps were performed while fixating continuously on a ground target 1 meter forward of the subject's initial toe position. The other three jumps were performed with the eyes closed, and subjects were instructed to look at the ground target then close their eyes and fixate on the imagined ground target position during the jump. Eyes open (EO) and eyes closed (EC) trials were alternated. Because of safety concerns related to subject instability postflight, the first jump was always performed with the eyes open. The subjects were instructed to land on both feet at the same time, although no specific instructions were given regarding the jump takeoff. A safety harness connected to an overhead frame prevented subjects from falling to the floor, but did not interfere with mobility during a normal jump.

Full-body kinematic data were collected with a video-based motion analysis system (Motion Analysis Corporation, Santa Rosa, CA). This system tracked the three-dimensional position of 14 passive reflective markers placed on the body. Markers were placed on the right side of the body at the toe, ankle, maleolus, knee, hip, shoulder, elbow, wrist, and ear. The remaining markers were located at the left heel and along the body centerline at the sacral bone, seventh cervical vertebra, occipital protuberance, and the second and third occipital condyles. For some of the subjects, foot switches located in the shoes underneath the heel and great toe of both feet were used to record the times when the feet were in contact with the ground.

Data Analysis

The motion analysis system provided the marker positions in three dimensions at a sampling rate of 60 Hz. The ankle, knee, and hip joint angles in the right leg were computed using the positions of the markers at the toe, ankle, knee, hip, and shoulder (See Figure 1). It was assumed that the foot, shank, thigh, and trunk were rigid segments. For all three joints, larger positive joint angles represented greater joint flexion while negative values denoted joint extension. In order to account for the possibility of variation in marker placement from session to session, average resting joint angles during quiet standing were calculated for each data collection session. These average resting angles were subtracted from the joint angle time series data for that session. Hence, the data shown here represent deviations from quiet standing posture, and positive joint angles indicate increased flexion from the rest position. Joint angular velocities were found by numerically differentiating the joint angle data using a four point centered difference. Before differentiating, the angle data were smoothed by filtering forward and backward (to eliminate phase shift) using a 3rd order Butterworth filter with a corner frequency of 15 Hz. Impact resulted in large and nearly instantaneous increases in the joint angular velocities. In order to avoid excessive smoothing of this feature, the data segments prior to and following impact were filtered and differentiated separately. Care was taken to minimize startup and ending filter transients by matching initial conditions.

The time of foot impact with the ground was extracted from the foot switch data for those subjects who were tested using the switches. For the other subjects, the impact time was calculated by determining when the downward velocity of the toe marker dropped to less than 10 mm/s. Comparisons of the two methods for finding impact time in the subjects with foot switch data yielded excellent agreement. For each jump, peak flexion angles and flexion rates after impact were computed for the ankle, knee, and hip joints as well as joint angles at the time of impact.

The position of the full-body center of mass (COM) in the sagittal plane was estimated from the marker positions, using an 8-segment body model (feet, shanks, thighs, trunk, upper arms, forearms, neck, and head). Lateral symmetry was assumed, allowing combination of the left and right segments in the arms and legs. The approximate distribution of the body mass among the body segments was found using a regression model based on the subject's weight and height [97, 98]. COM position was computed in an X-Z coordinate system, where the X value represented the fore-aft position and the Z direction corresponded to the gravitational vertical. Positive values for X and Z corresponded to forward and upward, respectively. The velocity of the COM was found using the same numerical differentiation procedure described above for the joint angular velocities.

Initial analysis of the joint and COM kinematics indicated a non-uniform pattern of postflight responses across

Table 5.5-2. Number of significant differences in preflight and postflight variables

Measure	Number of Subjects Exhibiting Significant Change		Ratio of Number of (PRE1 and PRE2 vs.POST)/ (PRE1 vs. PRE2)
	Preflight: PRE1 vs. PRE2	PRE1 and PRE2 vs. POST	
Peak Hip Angle	4	3	0.75
Peak Knee Angle	3	8	2.67
Peak Ankle Angle	5	6	1.20
Peak Hip Rate	2	7	3.50
Peak Knee Rate	2	6	3.00
Peak Ankle Rate	1	1	1.00
Peak COM Deflection	2	4	2.00
Time From Impact to Peak COM Deflection	0	4	•
Peak COM Upward Recovery Velocity	3	3	1.00

the subject pool. Therefore, preflight and postflight data sets were compared for each subject individually for peak joint flexion angles, peak joint flexion rates, and three COM-related measures: (1) maximum downward deflection, (2) time from impact to maximum downward deflection, and (3) peak upward recovery velocity. A two-way analysis of variance (ANOVA) was used to examine the effects of test session (PRE1, PRE2, POST) and vision (EO, EC). Test session effect was computed two ways: (1) PRE1 vs. PRE2, and (2) PRE1 and PRE2 together vs. POST. Tests yielding $p < 0.05$ were considered statistically significant.

Changes preflight to postflight in nine measures (3 peak joint angles, 3 peak joint rates, and 3 COM quantities) were considered for classification of the subjects into groups based on postflight performance. For each quantity, the number of subjects showing a significant change between the two preflight sessions was compared with the number demonstrating a significant difference between preflight and postflight (Table 5.5-2).

Of the nine measures, five were selected for classification purposes because they proved relatively insensitive to day-to-day variations. These measures (peak knee angle, peak hip and knee rates, peak COM deflection, and time to peak COM deflection) showed differences between pre- and postflight in at least twice as many subjects as were shown between the two preflight sessions. The five variables were tested together for the effects of test session and vision, using a two-way multivariate analysis of variance (MANOVA). Again, the contrast for test session effect was computed for pre- vs. postflight. Probabilities were based on Wilks' Lambda (likelihood ratio criterion) and Rao's corresponding approximate (sometimes exact) F-statistic. Subjects who did not exhibit

significant differences between pre- and postflight for the multivariate measure were classified as "No Change" (N-C).

The other subjects were classified as either "Postflight Compliant" (P-C) or "Postflight Stiff" (P-S) by scoring the five individual measures used in the MANOVA. For each measure, the subject received a [+1] for a significant change toward greater compliance postflight, a [-1] for a significant change toward lower compliance postflight, and a [0] for no significant change. The results for the individual measures were summed to get an overall score ranging from -5 to +5. Subjects with positive scores were designated P-C, while negative scores were labeled P-S. All statistical computations were performed using SYSTAT [97].

Model of COM Vertical Motion

A simple mechanical body model was developed to investigate the vertical motion of the COM following impact with the ground. In this single degree-of-freedom model (Figure 5.5-5), the vertical (Z) motion was assumed to decouple from the horizontal motion, which was neglected. The entire body mass was concentrated at the COM, supported by a massless, constant stiffness Hookean spring representing the legs. Similar models have been used by Alexander and Vernon [98] and McMahon and Cheng [99] to examine hopping and running. The upward restoring force exerted by the spring was proportional to the downward displacement of the COM from the uncompressed spring length Z_0 (nominally the height of the COM at the moment of impact). Energy dissipation, or damping, was modeled by a linear dashpot in parallel with the leg spring, which opposed the COM motion with a force proportional to COM velocity.

This model led to a second order linear differential equation that describes the COM motion:

$$M\ddot{z} + B\dot{z} + K(z - Z_0) = Mg \quad (8a)$$

$$\ddot{z} + \frac{B}{M}\dot{z} + \frac{K}{M}(z - Z_0) = g \quad (8b)$$

where z, \dot{z}, \ddot{z} = COM vertical position, velocity, and acceleration, respectively; g = gravitational acceleration; M = body mass; B = damping; and K = spring stiffness. The initial conditions needed to find the time solution of the equations are given by the vertical position and velocity of the COM at the moment of impact. In order to compare the pre- and postflight limb impedance properties for each subject, best fit values for each jump were determined for the coefficients $\frac{K}{M}$ and $\frac{B}{M}$ (the stiffness and damping, respectively, normalized by subject body mass). The best fit values were found using the MatLab System Identification Toolbox (The MathWorks Inc., Natick, MA). Model fitting was accomplished by minimizing a quadratic prediction error criterion, using an iterative Gauss-Newton algorithm [100]. The best fit for the rest spring length Z_0 was determined concurrently, although this parameter was nominally set by the height of the COM at impact. Unfortunately, the sampling rate was too low to provide an adequate estimate of the Z_0 value: with COM velocities greater than 2 m/s (6.5 ft/s) at impact, an uncertainty of one sampling interval in the time of impact could result in errors in Z_0 exceeding 3 cm (1.2 in). Since peak deflection of the COM following impact typically ranged from 8-15 cm (3.1-5.9 in), this level of uncertainty required simultaneous estimation of the spring length, using the MatLab identification routines.

Equation 8 can be rewritten in canonical second order form:

$$\ddot{z} + 2\zeta\omega_n\dot{z} + \omega_n^2(z - Z_0) = g \quad (9)$$

where $\omega_n = \sqrt{\frac{K}{M}}$ = natural frequency

$$\zeta = \frac{B}{2\sqrt{KM}} = \text{damping ratio}$$

The natural frequency is roughly equivalent to the bandwidth of the system and provides a measure of the speed of response, since higher natural frequencies correspond to faster transient responses. Clearly, increasing the stiffness K leads to a higher natural frequency. The damping ratio measures how oscillatory the transient response is, with lower damping ratios indicating more overshoot and oscillation or “ringing” in the system behavior. Increasing the stiffness K decreases the damping ratio, as does reducing the damping coefficient B .

RESULTS

Locomotor Head-Trunk Coordination Strategies

Figure 5.5-6 shows an example from one subject of the relationship between: (1) vertical translation of the trunk that occurred during each step, and (2) the corresponding pitch angular head movement during the NEAR target condition. During preflight testing (Figure 5.5-6a), pitch head movements acted in a compensatory fashion to oppose vertical trunk translation during locomotion. As the trunk translated upward, the head pitched forward/downward, thereby assisting maintenance of target fixation. Four hours after spaceflight (Figure 5.5-6b), there was a significant alteration in coordination between compensatory pitch angular head movements and vertical trunk translation. This was evidenced by a breakdown in the smooth, sinusoidal nature of pitch head movements into a number of sub-components.

The step-to-step variability of vertical trunk translation and corresponding compensatory pitch head movement is depicted for one subject in Figure 5.5-7. Each cycle was aligned at the point just prior to heel strike. Very little variation in vertical trunk translation occurred during locomotion, both before (Figure 5.5-7a) and after (Figure 5.5-7b) spaceflight. Pitch head movements showed more step-to-step variability and were considerably increased after flight.

Figure 5.5-8 shows the mean (± 1 S.E.) preflight and postflight coherence values relating vertical trunk translation and corresponding pitch head movement, for all subjects combined, for both NEAR and FAR target conditions. Using these data, a 2×2 (Target Distance versus Spaceflight Exposure) repeated measures ANOVA on pitch head/trunk coherence was performed. This analysis revealed significant effects for both spaceflight exposure ($F(1, 84) = 38.22, p < 0.0001$) and target distance ($F(1, 84) = 13.04, p = 0.0005$). In addition, a significant interaction occurred between target distance and spaceflight exposure ($F(1, 84) = 5.37, p = 0.0230$). There was a general postflight decrement in coordination between head and trunk in both NEAR and FAR, without a greater decrement in performance for the FAR, target condition.

Figure 5.5-9 displays preflight and postflight examples of Fourier amplitude spectra of pitch head angular displacement for the NEAR target condition for one subject. A predominant peak occurred at 2 Hz in both examples. Following spaceflight, the magnitude of the predominant 2 Hz peak was diminished in this subject, suggesting that a change in compensatory head movement control occurred during postflight locomotion.

Individual mean preflight and postflight variability in predominant peak of pitch head movements magnitude is illustrated in Figure 5.5-10 for the FAR and NEAR target conditions. For the FAR target condition, 8 subjects demonstrated a significant (paired t-test; $p < 0.05$) reduction

in predominant peak magnitude, 11 showed no change, and 4 showed a significant augmentation. For the NEAR target condition, 6 subjects demonstrated a significant (paired t-test; $p < 0.05$) reduction in predominant peak magnitude, 13 showed no change, and 4 showed a significant augmentation. The response variability illustrated in Figure 5.5-10 may reflect discrete head movement control strategies intended to maximize the central integration of veridical sensory information during the postflight recovery process.

Figure 5.5-11 shows the mean magnitude of the predominant peak (± 1 S.E.) of pitch head movements for all subjects, before and after spaceflight. The magnitude of the predominant peak was augmented during both the preflight and postflight NEAR target fixation condition. A 2×2 (Target Distance versus Space Flight Exposure) ANOVA revealed a significant effect for target distance ($F(1, 354) = 23.35, p < 0.0001$). This finding indicates that as the visual target was brought closer to the eyes, larger compensatory pitch head movements were induced to aid gaze stabilization of the near target. Results from the ANOVA showed only a marginally significant effect for spaceflight exposure ($F(1, 354) = 5.64, p = 0.018$), presumably reflecting the individual variability displayed in Figure 5.5-10.

To ascertain whether previous spaceflight experience modified head movement control strategies, data were divided into two groups based on experience. Multi-time fliers were defined as those subjects with at least one previous spaceflight exposure. Fifteen subjects were in this category. First-time fliers were defined as those experiencing their first encounter with actual spaceflight during participation in our study. Eight subjects were in this category.

In Figure 5.5-12, the mean preflight and postflight changes in the magnitude of the predominant peak from the amplitude spectra of pitch head movements for multi-time fliers and first-time fliers, for both FAR and NEAR target conditions, are compared. A 2×2 (Experience Level versus Spaceflight Exposure) ANOVA on peak amplitude revealed a significant effect for experience level for both FAR and NEAR target conditions. Inexperienced astronauts may have adopted different head movement strategies compared to their more experienced counterparts during locomotion following return to Earth.

Figure 5.5-13 displays a preflight example of pitch angular head displacement for 5 individual subjects (A-E) performing the Intermittent Vision (IV) paradigm during fixation of the NEAR target. There was a general reduction in head pitch amplitude during each eye closure period. These subjects were attempting to control the magnitude of head pitch movement during eye closure periods. Amplitude was restored within one or two cycles following restoration of vision. In addition to reducing amplitude, subjects also demonstrated a sustained forward head tilt during eye closure periods. During eye closure periods, head pitch amplitude was actively reduced and then

alter
alter

terized by calculating the Fourier amplitude spectrum of each alternating 5 second eyes open/closed epoch.

Figure 5.5-14a compares the preflight and postflight mean (± 1 S.E.) predominant frequency amplitude of pitch head movements, for all subjects, during alternating 5 second eyes open/closed epochs during locomotion. A 2×2 (Visual Condition versus Spaceflight Exposure) ANOVA revealed a significant effect for visual condition ($F(1, 166) = 52.72, p < 0.0001$), but no effect for spaceflight exposure. The entire subject population, taken as a whole, showed no difference in preflight versus postflight responses for both eyes open (EO) and eyes closed (EC) conditions. However, there was a significant ($p < 0.05$) difference across visual conditions. This confirmed the general trend of head pitch amplitude reduction when vision was denied, during both preflight and postflight testing. Figure 5.5-14b compares the preflight and postflight changes in mean (± 1 S.E.) head tilt, relative to horizontal in the sagittal plane for all subjects, during alternating 5 second eyes open/closed epochs during locomotion. A 2×2 (Visual Condition versus Spaceflight Exposure) ANOVA on head tilt revealed a significant effect for visual condition ($F(1, 166) = 67.8, p < 0.0001$), but no effect for spaceflight exposure. In addition to a reduction in predominant frequency amplitude during eye closure, there was also a static forward head pitch during the eye closure periods during both preflight and postflight locomotion.

Lower Limb Kinematics During Treadmill Walking

Temporal stride measures were evaluated for two reasons: (1) to assess the task-specific performance of the lower limb system, and (2) to evaluate a potential confound of the subject population. Subjects were asked to walk at a fixed speed of 6.4 km/hr (4 mph) on the treadmill. However, preferred walking speed was closely related to subject height. Given the range in subject height, certain subjects may have had to walk at other than their preferred speed. Evidence exists to suggest performance may not be as stable in a non-preferred state [104, 123]. Consequently, we examined several simple temporal characteristics of the gait patterns relative to subject height.

Figure 5.5-15 presents the mean stride time and standard deviation about the mean as a function of subject height. The Pearson correlation of mean stride time and subject height was significantly different from zero and remained so after flight (pre = 0.820, post = 0.681, $p < 0.05$), indicating that mean stride time increased with increasing subject height and was not influenced by flight. The Pearson correlation between standard deviation of stride time and subject height was neither significantly different from zero, nor did it change after flight (pre = -0.117, post = 0.147, $p > 0.05$), confirming that no simple

Table 5.5-3. ANOVA Results of Phaseplane Variability as a Function of Stride Epoch and Flight

	Hip	Knee	Ankle
Epoch	F(1,33)=3.4, p=.074	F(1,33)=1.5, p=.23	F<1.0
Pre vs. Post	F(1,33)=2.4, p=.134	F(1,33)=2.8, p=.10	F(1,33)=7.3, p=.011

linear relationship existed between stride time variability and subject height. Therefore, differences in subject height were assumed not to have influenced postflight results.

Figure 5.5-16 illustrates the similarity of duty factors for each subject before and after flight, and the lack of interaction with subject height. The mean duty factor both before and after flight was approximately 0.59, indicating that toe off occurred 59% of the way through the stride after heel strike. Paired t-tests of both the mean duty factor data and the within trial variability of the duty factor identified no differences ($p>0.05$) preflight versus postflight.

Figure 5.5-17 displays exemplar phase portraits, along with identification of the location of heel strike and toe off, to help illustrate the degree of variability in joint kinematics within a trial. The quantitative analyses that follow use data in this form to evaluate within-cycle fluctuations, changes in variability at discrete points within each cycle, and system stability.

Within-cycle variability on the phase plane is illustrated in Figure 5.5-18, which presents box plots of preflight and postflight data for the hip, knee, and ankle joints, constructed from the seven subjects. In all three joints, the postflight variability was clearly higher than the preflight variability, at all epochs. Moreover, there were apparent differences in variability magnitude at the different stride epochs. The knee joint had elevated variability around heel contact, whereas the ankle joint had elevated variability about the swing phase. However, the sizes of box and whiskers at many epochs, in all joints, indicate quite substantial individual differences in joint variability. Consequently, repeated measures ANOVA on each joint revealed no significant flight or epoch effects at the hip and knee joints. Only the ankle joint displayed significantly higher variability postflight at the 0.05 level. Table 5.5-3 summarizes these results. In general these data indicate that postflight treadmill walking was more variable than preflight, and that the response throughout the course of a gait cycle was joint and subject dependent.

Figure 5.5-19 documents variability on the phase plane at the moment of heel strike and toe off for each of the three lower limb joints. In most instances, variability was seen to increase after flight. However, paired t-tests of these data identified only the postflight increase in knee variability as significant ($p<0.05$) at the moment of heel strike, with only the hip joint postflight variability being significantly higher

($p<0.05$) at the moment of toe off. While the size of the box and whiskers in postflight measures on all three joints is indicative of substantial individual differences, the significant joint-specific changes at heel strike and toe off emphasize the importance of these locomotor events.

Figure 5.5-20 illustrates an index of dynamic stability calculated at the moment of heel strike and toe off during preflight and postflight performance. Paired t-test analyses identified no significant difference between preflight and postflight at either heel strike or toe off. Furthermore, the stability index magnitude across subjects was quite consistent, as seen in the width of the box and whiskers.

The stability index was based on eigen values of the Jacobian matrix. A complete loss of stability was identified specifically by the index exceeding unity. Detection of a statistically significant difference in this stability index, which never exceeded unity, did not denote a qualitative change in the system dynamics from the perspective of nonlinear dynamics. However, such a result could be used to indicate a tendency to less stable behavior. The absence of any notable change in the stability index was indicative of the preservation of lower limb intersegmental coordination.

Neuromuscular Activation Patterns

Neither stride time nor duty factor were affected by spaceflight. The group mean stride time before flight was 957.6 ms (SD 39.5), and the postflight mean was 959.1 (SD 38.2). The duty factor was 57.8% of stride cycle before flight (SD 2.2) and 58.6% (SD 1.3) afterward. Although postflight values were statistically different from preflight values for all but one subject, the magnitude of these changes was often small (1-2%). The difference was within the variability of treadmill control, and, therefore, did not have functional significance. Because treadmill belt speed could vary by up to 5% across data collection sessions, we chose to consider preflight versus postflight differences in stride time of less than 5% to be within the normal range of variation for this task. After flight, all of the subjects were able to reproduce preflight kinematic temporal features within 5%.

With few exceptions, preflight and postflight patterns of muscle activity were highly correlated, suggesting that the temporal features of lower limb neuromuscular activation 2.5 to 4 hours after landing were similar to preflight

characteristics. Pearson *r* correlations between preflight and postflight muscle activation in the left and right lower limbs are summarized in Table 5.5-4. The grand ensemble reduced wave form patterns for each muscle before and after flight, illustrated in Figure 5.5-21, reveal few differences in the phasic characteristics of the wave forms. Since there were no differences between the activation patterns of the muscles of the right and left lower limbs, the frequency distribution for preflight versus postflight activation pattern correlations was combined for the right and left lower limbs (Table 5.5-4). To make sure that our data reduction technique did not produce artificially high correlations, correlations were assessed between the mean wave forms developed from all of the digital samples contributing to those wave forms for three subjects. Correlations using all of the available data always revealed relationships as strong as or stronger than those found using the reduced wave forms.

In 70 of the 78 comparisons (90%), symmetry between the left and right lower limb muscle activation patterns, both before and after flight, exceeded a Pearson *r* value of 0.71 (Table 5.5-5). Therefore, the lower limb musculature was activated symmetrically, and this symmetry was not affected by spaceflight.

Despite observing no change in the temporal features of the overall wave form, analysis of the normalized mean amplitude of activation revealed significant functional differences before, versus after flight, around toe off and heel strike (Figure 5.5-22). Specifically, the RF, BF, and TA activation amplitudes were different around the heel strike, and RF and TA activation levels were different around toe off.

Table 5.5-4. Frequency Distribution of Preflight-to-Postflight Muscle Activation Correlation Coefficients for the Combination of the Right and Left Lower Limbs

	<i>BF</i>	<i>RF</i>	<i>GA</i>	<i>TA</i>	<i>Total</i>
1.00-0.91	12	9	17	14	52
0.90-0.81	5	5	1	5	16
0.80-0.71	1	3	2	1	7
0.70-0.61	1	1	0	0	2
0.60-0.51	1	0	0	0	1
0.50-0.00	0	0	0	0	0
Total no. of comparisons	20	18*	20	20	78

*Postflight RF data could not be obtained for two subjects.

Ranges of Pearson Product Moment correlations are presented in the left column.

BF - Biceps Femoris RF - Rectus Femoris
 GA - Gastrocnemius TA - Tibialis Anterior

Table 5.5-5. Frequency Distribution of Right vs. Left Lower Limb Muscle Activation Correlation Coefficients Combined for Preflight and Postflight Conditions

	<i>BF</i>	<i>RF</i>	<i>GA</i>	<i>TA</i>	<i>Total</i>
1.00-0.91	11	10	16	12	49
0.90-0.81	6	3	1	4	14
0.80-0.71	2	2	3	2	9
0.70-0.61	0	1	0	1	2
0.60-0.51	0	0	0	0	0
0.50-0.00	1	2	0	1	4
Total no. of comparisons	20	18*	20	20	78

*Postflight RF data could not be obtained for two subjects.

Table 5.5-6 presents muscle activation onset and duration for the RF, BF, and GA. Offset of activation and duration of the TA silent period are given in Table 5.5-7. Many of the preflight-to-postflight comparisons for individuals were statistically different, although the absolute differences were small. Figure 5.5-23 graphically represents the differences between GA activation offset and TA onset before and after flight. All but two subjects showed changes in the postflight temporal relationship between GA offset and TA onset relative to before flight. For some subjects, GA offset preceded the TA onset (i.e., the difference was negative). For other subjects the difference was positive. Moreover, the direction of the difference was changed after spaceflight for half of the subjects, indicating a complete reversal of the activation/deactivation sequence for the ankle musculature in preparation for toe off. The average preflight-to-postflight difference in this temporal relationship was 7.1 percent of the stride cycle. Because mean stride time across subjects was approximately 950 ms, each percentage point represented roughly 9.5 ms. Therefore, the average postflight difference between the GA offset and TA onset changed by approximately 67 ms (7.1% * 9.5 ms) relative to preflight values. Even accounting for slight changes in stride cycle time between the preflight and postflight measures, the magnitude of this difference indicates that at least some subjects experienced considerable changes in neuromuscular control of their ankle musculature in preparation for toe off.

Although there was a trend toward increased variability for all the active muscles around both heel strike and toe off, only the activation variability of the TA around toe off was significantly increased after spaceflight. The magnitude of co-contraction of the GA-TA muscles increased after flight, during the epochs immediately before toe off (at 45-55% of the stride cycle), but decreased just before heel strike (95% of the stride cycle).

Table 5.5-6. Onset and Duration (as Percent of Stride Cycle) of Muscle Activation Before and After Space Flight

Subject	Rectus Femoris Onset, % of Stride Time			Rectus Femoris Duration, % of Stride Time		
	Preflight	Postflight	p value	Preflight	Postflight	p value
A	87.8 (2.1)	89.8 (1.6)	0.001	29.0 (3.9)	26.8 (3.0)	0.024
B	88.4 (1.4)	89.7 (1.2)	0.001	77.0 (4.1)	74.4 (4.0)	0.021
C	87.3 (2.7)	86.9 (3.3)	0.356	24.5 (2.9)	28.0 (4.3)	0.003
D	88.0 (1.6)	86.8 (1.9)	0.019	26.4 (1.9)	27.9 (3.7)	0.050
E	90.9 (2.6)	85.3 (4.0)	<0.000	23.4 (3.2)	30.9 (4.1)	<0.000
F	93.3 (3.0)	91.1 (1.7)	0.002	16.5 (3.4)	24.6 (2.5)	<0.000
G	88.1 (2.7)	89.5 (2.9)	0.033	26.7 (3.3)	32.4 (4.0)	<0.000
H	89.0 (1.4)	88.2 (1.3)	0.024	26.6 (2.6)	33.9 (4.2)	<0.000
I	88.1 (3.1)	89.1 (2.4)	0.083	24.2 (5.1)	31.3 (12.0)	<0.000
J	91.9 (1.9)	94.5 (1.8)	<0.000	21.0 (2.4)	18.4 (1.7)	<0.000
Mean	89.3 (3.0)	89.0 (3.3)		29.5 (17.0)	32.9 (15.3)	
Median	88.9	88.9		25.45	29.45	
Subject	Biceps Femoris Onset, % of Stride Time			Biceps Femoris Duration, % of Stride Time		
	Preflight	Postflight	p value	Preflight	Postflight	p value
A	82.0 (0.5)	81.9 (0.6)	0.365	51.9 (4.2)	44.6 (10.1)	0.002
B	77.4 (1.2)	78.7 (3.4)	0.066	28.1 (4.4)	28.2 (4.5)	0.482
C	82.9 (0.7)	83.2 (0.8)	0.141	25.4 (3.3)	29.7 (4.2)	0.000
D	79.6 (1.1)	80.9 (1.4)	0.002	63.7 (2.8)	62.8 (1.9)	0.124
E	86.7 (4.3)	81.2 (1.5)	<0.000	23.6 (5.2)	33.2 (8.0)	<0.000
F	76.8 (2.3)	84.6 (6.7)	<0.000	24.6 (2.3)	24.7 (6.8)	0.480
G	84.3 (7.1)	82.4 (0.9)	0.125	43.1 (7.7)	42.2 (9.2)	0.380
H	81.5 (0.6)	80.3 (1.0)	<0.000	43.4 (6.2)	46.6 (3.0)	0.020
I	75.4 (2.2)	73.3 (5.0)	0.035	29.6 (3.7)	35.9 (5.4)	<0.000
J	77.0 (4.7)	81.4 (1.7)	<0.000	43.6 (6.5)	39.8 (11.0)	0.099
Mean	80.4 (4.7)	80.8 (4.2)		37.7 (13.6)	38.8 (11.1)	
Median	81.0	81.2		36.4	37.9	
Subject	Gastrocnemius Onset, % of Stride Time			Gastrocnemius Duration, % of Stride Time		
	Preflight	Postflight	p value	Preflight	Postflight	p value
A	94.7 (0.7)	6.6 (9.6)	<0.000	71.9 (4.8)	48.7 (10.5)	<0.000
B	25.8 (2.7)	96.3 (4.1)	<0.000	31.8 (5.4)	55.2 (5.6)	<0.000
C	22.7 (6.9)	87.7 (2.7)	<0.000	28.1 (7.9)	85.9 (3.1)	<0.000
D	27.8 (2.6)	93.8 (2.4)	<0.000	24.7 (4.3)	67.5 (5.2)	<0.000
E	94.3 (2.9)	17.3 (5.0)	<0.000	59.2 (4.6)	35.8 (6.5)	<0.000
F	91.7 (2.4)	96.5 (6.3)	<0.000	57.8 (3.6)	53.3 (6.2)	<0.000
G	99.5 (7.3)	95.3 (2.5)	0.009	52.6 (7.8)	63.5 (8.7)	<0.000
H	16.4 (4.2)	20.2 (3.2)	0.005	41.5 (7.6)	39.7 (4.3)	0.171
I	92.1 (2.4)	94.8 (2.7)	<0.000	56.8 (2.7)	55.8 (4.5)	0.200
J	0.4 (6.5)	90.9 (3.8)	<0.000	54.8 (7.3)	66.0 (4.7)	<0.000
Mean	6.6 (14.8)	99.9 (11.5)		47.9 (15.6)	57.1 (14.6)	
Median	97.8	95.7		53.7	55.5	

Numbers in parentheses are S.D. Note that 0.00% and 100.00% represent heel strike.

Table 5.5-7. Offset and Duration (as Percent of Stride Cycle) of Tibialis Anterior Activations Before and After Space Flight

Subject	Tibialis Anterior Offset, % of Stride Time			Tibialis Anterior Silent Period Duration, % of Stride Time		
	Preflight	Postflight	p value	Preflight	Postflight	p value
A	44.1 (4.1)	51.2 (1.1)	<0.001	14.7 (3.9)	8.0 (1.3)	<0.000
B	14.4 (7.7)	16.2 (11.2)	0.268	39.6 (7.2)	39.2 (11.1)	0.452
C	48.8 (3.0)	51.0 (3.3)	0.022	9.5 (3.5)	6.7 (2.8)	0.010
D	47.4 (1.4)	47.8 (1.5)	0.218	7.4 (1.4)	7.4 (3.5)	0.473
E	46.7 (2.1)	49.7 (2.5)	<0.000	9.8 (1.6)	8.3 (2.8)	0.021
F	33.2 (16.0)	46.4 (1.6)	<0.000	18.0 (15.9)	11.2 (1.6)	0.030
G	45.4 (6.2)	50.3 (2.1)	0.001	11.4 (5.8)	7.1 (1.6)	0.002
H	46.7 (2.5)	46.1 (2.5)	0.194	9.2 (2.0)	9.9 (2.6)	0.155
I	44.4 (2.9)	46.7 (2.9)	0.013	10.5 (1.9)	7.3 (2.5)	<0.000
J	49.4 (2.0)	51.1 (0.8)	0.012	5.5 (2.5)	4.3 (1.1)	0.095
Mean	42.0 (12.0)	45.4 (11.0)		86.8 (10.0)	89.2 (10.2)	
Median	46.3	48.5		89.4	91.9	

Numbers in parentheses are S.D.; 0.00% and 100.00% represent heel strike.

Co-contraction of the BF-RF muscles increased in the two epochs immediately before heel strike (90-100% of the stride cycle).

Spatial Orientation

Two different ways of describing distance errors were used: (1) the two-dimensional distance error of each corner point to the required corner at the end of a segment (arrival error), and (2) the difference between required length of a segment and actual distance covered (length error). The arrival error gave an absolute estimate of both directional and longitudinal deviations from the required path. The length error showed purely longitudinal errors in reproducing segments. Arrival error was cumulative over the walk, while length error was not. Figure 5.5-24 shows pre- and postflight walking trajectories for one subject during the eyes closed condition.

For all subjects combined, the four-way ANOVA revealed a significant effect of segment ($F(2,6)=8.74$; $p=0.017$) and a segment vision interaction ($F(2,6)=5.86$; $p=0.039$) on length error. Length error was increasing from segment 1 to 3 for the eyes closed condition, while it was largest for segment two in the eyes open condition, due to the fact that subjects tended to walk around corner 1 and 2 with open eyes. The segment effect could partly be explained by the different length of segment 3, while the interaction illustrated that errors increased more from one segment to the next in the eyes closed condition. The segment effect could partly be explained by the different length of segment 3, while the interaction illustrated that errors increased more from one segment to the next in the eyes closed condition.

Two-dimensional distance error was slightly larger after flight (0.74 ± 0.53 m) than before flight (0.61 ± 0.42 m). However, the difference was far from being significant. Only vision ($F(1,3)=12.66$; $p=0.038$) and the segment vision interaction ($F(2,6)=12.83$; $p=0.006$) had significant effects. The effect of vision was the result of much smaller errors in the eyes open condition (0.22 ± 0.11 m preflight, 0.27 ± 0.12 m postflight).

The directional error was described as the difference between: (1) the mean walking direction during each segment with respect to the previous segment, and (2) the required angle of turn from one segment to the next. Therefore, the directional error of the first segment only gave the heading error toward corner 1, while the directional errors during segments 2 and 3 gave the errors of angular turn with respect to the preceding path segment. Directional error, as defined here, was not cumulative because it was computed in relative coordinates.

Directional error was tested only for segment 2 and 3. Mean errors for the eyes closed conditions were -7.01 ± 9.77 degrees preflight, and -9.28 ± 8.23 degrees after flight, showing a trend to underestimate turns. The vision factor ($F(1,3)=14.45$; $p=0.031$) and the interaction segment-direction ($F(1,3)=36.72$; $p=0.009$) were significant.

The absolute mean directional error was tested to assess absolute errors. Here, sample day was found to be a significant factor ($F(1,3)=15.25$; $p=0.030$), caused by larger absolute errors in the postflight testing. The two-way interactions segment direction and segment vision were also significant. The segment direction interactions were due to individual differences between the clockwise and counterclockwise conditions. The effect of day on absolute directional error showed that postflight directional deviations were larger than before flight.

Mean walking velocity was computed by dividing walked length by the time needed for one segment to be walked. Subjects walked slower postflight for both eyes closed (0.73 ± 0.10 m/s preflight, 0.66 ± 0.10 m/s postflight) and eyes open (0.84 ± 0.08 m/s preflight, 0.81 ± 0.10 m/s postflight) conditions. All of the main factors, except direction, were significant, i.e., segment ($F(2,6)=21.68$; $p=0.002$), vision ($F(1,3)=28.28$; $p=0.013$) and day ($F(1,3)=12.26$; $p=0.039$). The interaction between direction and day ($F(1,3)=10.62$; $p=0.047$) was the only significant two-way interaction. Walking velocity for segment 3, with eyes closed, was slower after spaceflight.

Lower Limb and Mass Center Kinematics in Downward Jumping

Joint Kinematics

Phase plane plots, where joint angular velocities (degrees per second) are plotted against the joint angles (degrees), yield the best format for comparing the joint kinematics of several jumps. Figure 5.5-25 (top) shows phase portraits for subject S-1, comparing a time synchronized average of 12 preflight and 6 postflight jumps for the hip, knee, and ankle joints. The time of impact is marked by an open circle (○) on each plot, and the plots are traversed in the clockwise direction through the impact absorption and recovery to an upright posture. In general, after impact the peak flexion rate is reached rapidly; the peak flexion rate is the uppermost point on the phase portrait. Moving further along the phase diagram, the joint angular velocities drop to zero as the muscles act to decelerate the body's downward motion. When the joint flexion rate reaches zero, the joint is at its peak flexion angle, the rightmost point on the plot. After this point, the flexion rate becomes negative, indicating joint extension as the subject recovers to the upright resting posture. These plots depict averages of the jumps for the preflight and postflight sessions, with the time scales for each data series synchronized at the time of foot impact with the ground.

The plots for subject S-1 clearly illustrate expanded postflight phase diagrams for each joint with respect to the preflight measurements. Postflight, this subject exhibits greater peak joint flexion angles than during the preflight jump landings, indicating that the subject reached a more crouched body position postflight while absorbing the impact from the jump. Furthermore, the peak joint angular velocities seen postflight are greater than the joint rates observed preflight. In contrast, the phase-plane diagrams for subject S-9 in Figure 5.5-25 (bottom) demonstrate the opposite effect; the postflight portraits are consistently smaller than the plots of the preflight jumps. This postflight contraction of the phase diagrams denotes a decrease in peak joint flexion postflight, indicating that this subject retained a more upright posture while absorbing the impact. In addition, this subject showed smaller peak joint flexion rates in postflight testing than in the preflight jumps.

Center of Mass (COM) Kinematics

As with the joint angle data, the kinematics of the COM are plotted in a phase-plane format. Figure 5.5-26 shows the COM motion for subject S-1. Once again, the plots depict averages of the 12 preflight and 6 postflight trials. Figure 5.5-26 (left) shows the average motions of the COM in the X-Z (sagittal) plane. Figures 5.5-26 (middle) and 5.5-26 (right) present the phase-plane trajectories in the X (fore-aft) and Z (vertical) directions traversed in the clockwise direction, respectively. The open circles (○) denote the moment of impact coinciding with peak downward COM velocity. Deceleration of the COM downward motion takes place until the COM is at its lowest point and the Z velocity is zero. Then the Z velocity becomes positive as the COM recovers to the steady-state value for standing posture. The peak upward velocity occurs at the uppermost point on the trajectory. The trajectory may spiral in around the equilibrium point if there is oscillation about the final steady-state position.

Subject Classification

The joint angle phase diagrams for these two astronauts suggest that the subjects who exhibit postflight changes in joint kinematics compared to preflight values may be divided into two distinct groups. Using the analogy of a spring of variable stiffness, the first group is denoted "postflight compliant," or P-C. Just as a more compliant spring compresses more under a given load, this group generally exhibited greater joint flexion postflight than preflight, accompanied by increased postflight flexion rates. The second group is labeled "postflight-stiff," or P-S, indicating lower peak flexion and flexion rates for the jump landings following spaceflight.

The COM kinematics provide complementary information for classification of subject performance following spaceflight. If the legs are considered to be roughly spring-like in supporting the mass of the upper body, the maximum downward deflection of the COM following impact gives a measure of the stiffness of the lower limb "spring" (e.g., an increase in the downward deflection of the mass center indicates a decrease in the spring stiffness). The time from impact to the point of peak downward deflection also provides an indicator of the effective stiffness of the lower limbs. A decrease in the time between impact and maximum deflection implies an increase in the stiffness.

Table 5.5-8 contains the scoring of the five measures used to classify each subject. Positive entries indicate significant changes toward greater compliance postflight, corresponding to increases in peak joint angles or peak joint flexion rates, greater downward COM deflection, or longer times from impact to maximum COM vertical deflection. Negative entries represent significant differences in these quantities that indicate greater stiffness postflight. The statistical significance for the preflight/postflight MANOVA contrast of the five measures are shown for each subject. As previously mentioned, subjects with significant

Table 5.5-8. Subject Classification Based on Kinematic Measurements

Subject	S-1	S-2	S-3	S-4	S-5	S-6	S-7	S-8	S-9
Peak Knee Flexion	+1	+1	+1	+1	+1			-1	-1
Peak Knee Flexion Rate	+1	+1	+1	+1	+1				-1
Peak Hip Flexion Rate	+1	+1	+1	+1	+1		+1		-1
Peak COM Deflection	+1	+1	+1					-1	
Time to Peak COM Deflection	+1	+1	+1						-1
Overall Score	+5	+5	+5	+3	+3	0	+1	-2	-4
p-value	0.005	0.003	0.002	0.003	0.277	0.275	0.051	0.002	4×10^{-6}
Classification	P-C	P-C	P-C	P-C	N-C	N-C	N-C	P-S	P-S

MANOVA results were denoted P-C or P-S based on positive or negative overall scores respectively for the five classification measures; the remainder were designated “No Change” (N-C).

Four subjects (S-1, S-2, S-3, S-4) were classified P-C. All four had significantly increased peak knee flexion combined with significantly greater peak knee and hip flexion rates postflight; for three of the four (all except S-4), COM downward deflection and the time from impact to peak COM downward deflection also increased postflight. Both of the subjects designated P-S (S-8 and S-9) exhibited significantly decreased peak knee flexion postflight. Subject S-9 also showed significant decreases in peak hip and knee flexion rates after spaceflight, as well as a decrease in the average time from impact to peak COM downward deflection. Peak COM downward deflection was significantly reduced for subject S-8. The remaining three subjects (S-5, S-6, S-7) did not show a significant change between preflight and postflight, based on the multivariate criterion.

Because the measures of peak joint angle, peak joint rate, and maximum COM vertical deflection are affected by the magnitude of the impact force as well as lower limb stiffness, the changes observed cannot be attributed to limb impedance changes unless the impact loading is the same pre- and postflight. For this reason, the COM vertical velocity at the moment of impact was compared for each subject’s pre- and postflight jumps. Only two subjects (S-9 and S-2) showed significant differences between pre- and postflight impact velocities at the $p < 0.05$ level. For subject S-9, the average postflight impact velocity was

reduced by almost 20% compared to the preflight jumps. This change probably contributed to the decrease in knee flexion, joint rates and COM displacement observed for this subject. Subject S-2 also exhibited a significant postflight decrease of about 5% in impact velocity. In spite of the postflight reduction in impact loading, subject S-2 exhibited consistent increases in peak joint flexion, flexion rate and COM downward deflection. Thus, the impact velocity result actually adds support to the P-C classification for S-2. All other P-C and P-S subjects showed small, non-significant differences between pre- and postflight COM impact velocity.

In summary, the P-C subjects exhibited significant increases in postflight joint flexion and flexion rates; the P-S subjects showed the opposite effect, although the trend was less apparent in subject S-8. Figure 5.5-27a compares the average preflight and postflight values for maximum knee flexion, based on two preflight sessions of six jumps each and one postflight session of six jumps. Figures 5.5-27b and 27c contain pre- and postflight peak flexion rates for the knee and hip joints, respectively. Figures 5.5-28a and 28b show the preflight and postflight values for the two COM-related measures: peak downward COM deflection and time from impact to peak deflection. With the exception of subject S-4, all of the P-C and P-S subjects demonstrated a significant change in one or both of the COM measures, supporting their classification.

The error bars are standard errors, and significant differences between the pre- and postflight data are denoted with asterisks (*). Cases marked by a “†” indicate a significant test day effect for the contrast between the two

Table 5.5-9. Stiffness and Damping in Second Order Model

Subject	Stiffness, K/M, 1/s ²				Damping, B/M, 1/s			
	Preflight	Postflight	Percent Change	p-value	Preflight	Postflight	Percent Change	p-value
S-1	217.2	98.3	-54.7	0.0001	14.2	12.8	-9.7	0.1490
S-2	132.0	76.6	-42.0	0.0007	14.0	14.0	+0.1	0.7150
S-3	247.2	150.7	-39.1	0.0001	16.2	12.5	-22.9	0.0030
S-4	208.2	159.9	-23.2	0.0240	13.7	12.5	-8.6	0.0740
S-5	178.6	108.9	-39.0	0.0100	12.3	13.4	+9.5	0.2630
S-6	158.3	106.3	-32.8	0.1990	14.6	14.8	+1.8	0.6590
S-7	247.1	265.4	+7.4	0.3230	15.2	16.2	+6.5	0.3030
S-8	170.5	207.8	+21.9	0.0510	14.4	13.6	-5.9	0.2280
S-9	101.4	150.4	+48.3	0.1720	12.8	13.7	+7.1	0.4620

preflight sessions. Group averages for pre- and postflight data were also calculated for the P-S subjects, the P-C subjects, and all subjects taken together, and are shown at the right in Figures 5.5-27 and 28. Taken as a group, the P-C subjects show significant increases in all five measures. Grouping the two P-S subjects reveals significant decreases in peak knee flexion and maximum COM downward deflection.

Modeled COM Vertical Motion

Figure 5.5-29 shows predicted COM model responses using parameters estimated for representative pre- and postflight jumps for P-C subject S-1. Model fits for the 12 preflight (Fig. 5.5-29a upper) and 6 postflight (Fig. 5.5-29a lower) trials are staggered along the vertical axis. Figure 29b shows preflight (upper) and postflight (lower) average COM vertical trajectories; the shaded region indicates ± 1 standard deviation. Simulated model results using the pre- and postflight stiffness and damping averages are included as well. The COM motion in the preflight jump exhibited a substantial overshoot above the final equilibrium posture, indicating a fairly low damping ratio. The postflight jump showed a much slower response with little overshoot. Thus, the postflight response was consistent with a decreased natural frequency and increased damping ratio, in comparison to the preflight jump. P-S subjects, in contrast, demonstrated the opposite trend toward faster responses postflight, with greater overshoot.

Table 5.5-9 summarizes the stiffness and damping coefficients that were estimated for each subject, and shows an excellent match with the subject classification based on kinematics. Note that these values have been normalized by the subject body mass, and modeled stiffnesses are shown in Figure 5.5-30. All four P-C subjects (S-1, S-2, S-3, and S-4) and S-5 showed large (23%-55%), statistically significant decreases in postflight stiffness

compared to preflight values. Stiffness increases for P-S subjects S-8 and S-9 were not significant. The surprising lack of a significant postflight stiffness increase for subject S-9 (considering the consistent P-S changes in the joint and COM kinematics) may have been due to this subject's postflight decrease in impact velocity. The change in impact loading is explicitly accounted for in the COM motion model. In contrast with the changes in stiffness, examination of the damping coefficients revealed few differences between pre- and postflight performance, with only subject S-3 exhibiting a significant change (decrease). Furthermore, there was no apparent pattern of increases or decreases in the level of damping that corresponds to either subject classification or the changes in stiffness.

From the definitions of ω_n and z in Equation 2, a decrease in stiffness for a constant damping level should result in a lower natural frequency and a higher damping ratio. The calculated values for ω_n and z are shown in Table 5.5-10. As anticipated, the four P-C subjects, as well as S-5, all exhibited significant decreases of 13%-33% in the natural frequency, and hence reduced bandwidth postflight. Four of these subjects had increased damping ratios postflight as well, although significant changes were seen only for subjects S-1, S-2, and S-5. The P-S subjects demonstrated the opposite trend: increased natural frequency postflight, combined with decreases in the damping ratio (significant only for S-8 damping ratio).

Table 5.5-10. Second Order Response Parameters

Subject	Natural Frequency, ω_n				Damping Ratio, z			
	Preflight	Postflight	Percent Change	p-value	Preflight	Postflight	Percent Change	p-value
S-1	14.7	9.8	-33.3	0.0001	0.49	0.66	+36.5	0.0004
S-2	11.4	8.6	-24.6	0.0003	0.61	0.83	+35.4	0.0010
S-3	15.7	12.3	-21.8	0.0001	0.52	0.51	-2.5	0.7600
S-4	14.4	12.6	-12.7	0.0200	0.48	0.50	+5.6	0.2850
S-5	13.3	10.3	-22.5	0.0090	0.47	0.67	+43.0	0.0100
S-6	14.3	10.1	-18.0	0.1870	0.61	0.74	+20.7	0.1020
S-7	15.7	16.2	+3.4	0.3260	0.49	0.50	+3.0	0.5920
S-8	13.0	14.4	+10.5	0.0540	0.56	0.48	-14.7	0.0090
S-9	9.8	11.7	+20.0	0.1500	0.68	0.61	-10.4	0.2600

DISCUSSION

Locomotor Head-Trunk Coordination Strategies

Head-Trunk Coordination During Locomotion

We have characterized the deterioration in coordination between vertical trunk translation and compensatory pitch head movements during locomotion by determining the change in coherence between these two wave forms. The results demonstrated that exposure to the microgravity environment of spaceflight induced adaptive modification in coordination between vertical trunk translation and compensatory pitch head movements during locomotion. This change in head-trunk coordination strategy may account, in part, for the reported oscillopsia during locomotion following spaceflight, and may have contributed to disruption in descending control of locomotor function.

One of the interesting features of our data set concerns individual subject differences, illustrated by the individual responses shown in Figure 5.5-10. The variability between subjects may have been caused by individual susceptibility to adaptive neural modification. Alternatively, this variability may reflect the response of a control system looking for a new equilibrium point by assessing the veracity of multiple sensory inputs. Indeed, the requirement to maintain gaze stability may not fully account for the variety of head movement strategies observed during locomotion. Head movement strategies adopted during locomotion may reflect specific task constraints and the need to rely on specific sources of sensory information for the effective organization of coordinated movement. Nashner [105] described two possible head-trunk coordination strategies observed during the maintenance of dynamic postural equilibrium. The first strategy (“strap down”) calls for the head to be fixed to the trunk during body movement, so that in essence the head and trunk can be considered a single unit. Adopting this strategy means

that head-trunk control is simplified. However, the ability to resolve complex movements into their linear and angular components by the otoliths and semicircular canals becomes complex. Alternatively, the “stable platform strategy” fixes orientation of the head with respect to the gravito-inertial force vector, essentially stabilizing the head in space while the body moves underneath. The advantage of this strategy is that larger sustained rotations of the head are actively nulled, permitting simplification of the otolithic process responsible for detecting linear acceleration and static orientation of the head. The cost incurred by this strategy is that complex head-trunk patterns of coordination are required to successfully execute this control scheme.

The significant postflight reduction in predominant frequency amplitude of pitch head movements observed in some of our subjects (Figure 5.5-10) may have been caused by attempts to reduce angular head movement during locomotion and, therefore, reduce potential canal-otolith ambiguities during the critical period of terrestrial readaptation. This action may have further simplified coordinate transformation between head and trunk, presumably allowing an easier determination of head position relative to space. However, this strategy was not optimal for gaze stabilization because it resulted in a disruption in the regularity of the compensatory nature of pitch head movements during locomotion. This strategy also restricted behavioral options for visual scanning during locomotion. Consequently, there may have been tradeoffs between head movement strategies, depending on the imposed constraints. Once significant readaptation took place, a decrease in constraints on the degrees of freedom of head movement was likely to occur, returning performance to preflight levels. Importantly, head movement restriction during locomotion was also shown by patients suffering from vestibular deficits [106] and by children prior to development of the mature head stabilization response [51].

Some subjects showed a significant increase in predominant frequency amplitude of pitch head movements following spaceflight, in both the FAR and NEAR target conditions. These subjects may have been at the very early phase of their individual readaptation path prior to the establishment of a normal, or head restrictive, strategy. Therefore, the observed strategies may not have been subject specific, but rather a snapshot from a recovery curve that contained a continuum of responses. Consequently, immediately after spaceflight, some subjects experienced excessive head instability and the associated postural and gait dysfunctions. In response, a head restrictive strategy was adopted and maintained until normal control could be attained.

Various compensatory head movement strategies may play a central role in facilitating optimal sensorimotor transformations between the head and trunk, required for descending control of locomotion. Zangemeister et al. [107] demonstrated that normal locomotion, performed with the head in a retroflexed position, induced alterations in lower limb muscle activity patterns. They concluded that a functional linkage exists between otolith signals generated by various head positions and the muscle activity patterns generated in the lower limbs during locomotion. Given this functional linkage, it can be argued that if spaceflight induced adaptive modification in head-trunk coordination, this in turn could cause a disruption in the organization of coordinated body movement during post-flight terrestrial locomotion. It follows that active body movement in the unique inertial environment encountered during spaceflight may have required subjects to adaptively acquire novel head-trunk control strategies. However, these strategies may have been maladaptive for locomotion in a terrestrial environment, leading to impairment of locomotor function during the readaptation period following return to Earth.

Effects of Target Distance on Head Movement Control During Locomotion

DSO 614 results confirmed our previous findings which demonstrated that the amplitude of compensatory pitch head movements occurring during locomotion were modified by changes in the distance of the eyes from the visual target [13]. Specifically, when the target was brought closer to the eyes (30 cm vs. 2m, or 1 ft vs. 6.5 ft), the amplitude of pitch head movements increased in accordance with the greater angular gaze deviation per vertical trunk translation required to stabilize the near target. Therefore, we can conclude that the pitch head movements observed during locomotion, in the present context, were goal directed and dependent on the requirement to stabilize gaze, and were not completely a result of the passive inertial and viscoelastic properties of the head-neck system. That is not to say that passive properties did not play a role. However, the response was subject to neural mediation. We can infer that the observed changes in

head-trunk coordination following spaceflight reflected sensorimotor modification, in addition to passive mechanical changes, in the head-neck system following extended exposure to the microgravity environment. However, it is possible that as flight duration is extended from weeks to months, head control may be compromised by both changes in sensorimotor function and atrophy of the neck musculature responsible for maintaining the head upright against gravity. Investigations conducted with Russian cosmonauts, exposed to extremely long duration spaceflight of up to 175 days, indicated a decrease in neck strength of up to 40% following flight [108]. Therefore, it is likely that additional factors may have played a role in changing the dynamics of head movement control during locomotion following long duration spaceflight.

Postflight coherence decrements were observed in both the FAR and NEAR target conditions, with the decrease being greater during the FAR target condition. The apparent difference in head-trunk coordination between the FAR and NEAR ocular fixation conditions may have resulted from enhanced visual feedback of the head-trunk coordination breakdown during the NEAR target condition. During NEAR target fixation, the degree of apparent target motion was greater, resulting in a greater sensitivity to apparent target motion and oscillopsia. Greater sensitivity to target motion could then be used as feedback to enable subjects to actively modify their performance to permit better target stabilization. This would translate into enhanced head movement control during NEAR target fixation. Such enhancement in performance was observed by Dijkstra et al. [109] in standing human subjects asked to maintain postural stability in a moving visual environment. They found that a moving visual environment induced postural sway in subjects, with specific temporal characteristics linked to the presented visual information. Specifically, if the mean distance to a virtual sinusoidally moving wall was varied, the temporal relationship between the wall and induced body sway was dependent on the distance between the wall and the observer. As the distance of the subject to the wall increased, the tight relationship between body sway and wall movement decreased, suggesting a distance effect in action-perception coupling.

Effects of Transient Visual Occlusion on Head Movement Control

To investigate how the head-trunk system dynamically responded to short term (5s) alternating changes in visual input, we asked subjects to walk on the treadmill during intermittent visual occlusion (IV Condition). The results clearly demonstrated that during visual occlusion periods, in both preflight and postflight data sets, pitch head movement amplitudes were minimized. Importantly, this strategy was abandoned almost immediately once vision was restored. These results support the conclusion that the reduction in head pitch amplitude, observed in

some subjects during postflight trials performed with vision, was a goal-directed behavioral strategy produced in response to adaptive alterations in sensorimotor function and not exclusively an outcome of passive head-neck dynamics. When the subject population was considered as a whole, spaceflight had no effect on the predominant frequency amplitude of pitch head movements and static head tilt during the IV Condition. This lack of effect may have been due to enhanced locomotor stability afforded by the light finger touch on the handrail, similar to the enhanced postural stability produced, in the absence of vision, by precision contact of the subject's index finger with a stationary bar [85, 86]. Thus, the light touch could have provided an alternate path for veridical haptic information to contribute to, and enhance, postflight locomotor control.

It is reasonable to predict that both during readaptation to unit gravity and during visual occlusion, different head-trunk coordination strategies may emerge that are appropriate for maximizing input from the sensory modalities providing veridical information. Pozzo et al. [19, 28] demonstrated that during free locomotion in darkness, the mean head position was tilted downward. They hypothesized that the downward head tilt could help minimize head movements by locking the head to the trunk as well as serving to enhance otolithic sensitivity by maximizing the shear force acting on the otoconial membrane. Another rationalization that may account for the reduction in pitch head movement during visual occlusion and during postflight readaptation comes from an observation made by Bernstein [110]. He speculated that in the early stages of motor skill acquisition, subjects reduced available degrees of freedom in an attempt to simplify the control problem. As learning progressed, the restriction placed on degrees of freedom was eventually reduced and the full behavior was manifested. Recent work by Vereijken et al. [111] provided empirical evidence that support Bernstein's concepts. Our data show that restriction of head movement may simply have been a manifestation of a general phenomenon associated with the relearning of appropriate terrestrial motor strategies following spaceflight.

Enhanced Motor Response Flexibility: A Potential Training Tool?

Comparison of responses from multi-time and first-time astronauts indicates that multi-time astronauts demonstrated less postflight alteration in head control strategies than did subjects on their first flight. Postflight behavioral differences between astronauts based on their experience level were previously observed in tests of dynamic postural equilibrium control [8, 9, 112-114]. In these tests, inexperienced astronauts showed greater postflight decrement in postural stability than their more experienced counterparts. Such differences may have been the result of many factors. However, they did indicate a prolonged retention of learned strategies in experienced astronauts

that enabled quicker adaptive transition from microgravity to unit gravity. The identification of a learned enhancement in the capacity for flexible motor responses to altered sensory input and its association with a reduced decrement in postflight motor control suggests that preflight training regimes may be designed to promote development of motor response flexibility. This increased capability for motor response flexibility might aid in mitigating postflight motor disturbances. This concept is supported by the work of Kennedy et al. [115] who examined whether motor behavior could be adapted by exposing subjects to inter-sensory conflict involving vestibular input, and determining if the resultant adaptation was transferred to a different visual-vestibular conflict situation. In this study, one group of subjects was exposed to a visual-vestibular conflict (Purkinje stimulation) and allowed to adapt. A control group was not exposed to any sensory conflict training. The two groups were then exposed to a different visual-vestibular conflict situation (pseudo-Coriolis). Those subjects pre-exposed to sensory conflict experienced less dizziness and locomotor difficulties than the control group. The concept of enhanced motor flexibility or "learning to learn" was confirmed by Welch and colleagues [116], who exposed subjects to prismatic displacement of the visual scene. Using a pointing task as the dependent measure for adaptation, they found that previous exposure to prism displacement enhanced the ability to adapt to novel or previously unexposed visual displacements.

Similarly, astronauts could be exposed to visual-vestibular conflict situations during locomotion as part of a training regime designed to enhance the ability to reorganize motor control responses during sensory conflict situations. Such a training program would provide crew members with preflight experience in solving motor control problems and formulating workable solutions for each encountered situation. This solution might include learning to ignore some sensory input and becoming more reliant on others, and by attending more closely to vision and less to vestibular signals. In essence, this approach would train inexperienced crew members to rapidly reorder their motor control strategies, thereby increasing their chances for improved early postflight postural and locomotor performance.

Lower Limb Kinematics During Treadmill Walking

This aspect of DSO 614 was designed to evaluate lower limb joint kinematics during treadmill walking after spaceflight, with specific reference to head and gaze control. Basic temporal features of the gait cycle, such as stride time and duty cycle, remained unchanged following flight. However, specific and consistent changes in joint phase plane dynamics were identified at the moment of heel strike and toe off. In general, variability was greater

after flight. Although dynamic stability of the lower limb system, during transitions between stance and swing phases, did not seem to change following flight, individual responses to flight should be investigated further.

We expected joint angular dynamics to be significantly perturbed by spaceflight. However, stride epoch data indicated an overall, but statistically insignificant, increase in phase plane variability at all three joints. The lack of significance was partly attributed to the substantial individual differences. The expectation was that susceptibility of the gait cycle to disturbance would be greatest around heel strike and toe off. These events represented significant energy exchange with the support surface, either through exaggerated impact at heel strike or through an exaggerated effort to propel the body forward at toe off. Generally, variability was higher in the heel contact epoch of the knee joint, both before and after flight, and was exacerbated in much of the postflight data. Similarly, postflight variability in the ankle joint was higher for the epoch containing toe off, both before and after flight, and also was exacerbated after flight. These data lend some indirect support to the possibility that these peak energetic events were the source of postflight disturbances in gait. Since the head and eyes are located atop a multi-segmental system, any disturbance can propagate through these segments. Consequently, disturbances identified in the lower limbs may have been related to the reported oscillopsia during walking after flight [57].

Confirmation of the significance of these gait events was sought with analyses focusing on joint variability at the precise moments of toe off and heel strike. At toe off, the initiation of the swing phase, hip joint phase plane variability was significantly greater after flight than before. At the beginning of the swing phase, the hip was flexing and accelerating to maximum angular velocity, and therefore was a strong candidate for perturbations of the trunk. At the moment of heel strike, the initiation of the stance phase, the knee joint phase portrait variability was also significantly greater after flight. McMahon and colleagues demonstrated that, while exaggerated knee flexion during running was energetically inefficient, this strategy changed the joint stiffness and consequently reduced transmission of heel strike energy to the head [49]. The increased variability observed in our data may have been the result of attempts by crew members to adjust lower limb configuration about the moment of heel strike, indicating both a postflight increase in susceptibility to perturbations at heel strike, and explicit attempts to modulate head perturbations resulting from the impact force of heel strike.

In addition to changes in joint variability, we anticipated noticeable changes in system stability following spaceflight, indicating at least a decrease of system stability, if not a qualitative change in system dynamics. These changes did not occur, because increased individual joint variability was not sufficient to interfere with the

basic pattern of lower limb coordination. The absence of significant changes in the index used to evaluate system stability at both toe off and heel strike was consistent with the subjects successfully walking on the treadmill after flight. However, in light of the retained system stability, the relationship between joint coordination pattern and the observed joint variability should be investigated further. Relatedly, variability seen in the lower limbs may have been propagated through the trunk to the head, where the consequences could be more profound for the strategies engaged in maintaining head and gaze stability.

We decided to use a treadmill protocol because it permitted parallel evaluation of full body segmental kinematics and head movement control during locomotion. Only in this manner was it possible to evaluate head and gaze control strategies during locomotion. However, the use of the treadmill also subjected the locomotor performance to certain constraints. Some evidence suggests that treadmill walking is inherently less variable than over-ground walking. Nelson and colleagues observed that treadmill running was characterized by less variable vertical and horizontal velocities than over-ground running [117]. Similarly, a comparison of the mechanical energies of over-ground and treadmill walking by Woolley and Winter [118] found that the stride-to-stride variability of all work measures was significantly greater over ground, suggesting that the treadmill constrained walking more rigidly.

We found the temporal characteristics of gait patterns to be remarkably robust, as demonstrated by the lack of any significant change in either the mean duty factor, or the variability of the duty factor. Consequently, subjects seemed to maintain a consistent stance-to-swing ratio, even on landing day. The basic stride data did illustrate a linear correlation between stride time and subject height. This was not surprising, given the well documented allometric relationships found in animal locomotion [103]. However there was no such relationship between stride time variability and subject height, and no spaceflight influence on this feature could be detected. On a treadmill, the appropriate locomotory state is well defined, with a specific unvarying speed and little opportunity for directional error. Since treadmill walking is associated with low tolerance for error, variation beyond the acceptable state results in a complete failure in performance. In comparison, over-ground walking is much more forgiving, with much more opportunity for variance in speed and direction.

Some subjects opted not to attempt the treadmill protocol after spaceflight. This suggests that there may have been gross changes in locomotor control, beyond the relatively subtle changes we observed, in some individuals. Subjects from whom we acquired data on treadmill walking at the criterion speed had, by definition, attained a relatively high and consistent level of coordination. The possibility of observing qualitative coordination changes

in the lower limb may have been extremely slight, given this constraint. Moreover, subjects were additionally constrained by fixating and maintaining their gaze on a visual target, further regulating their performance.

Our data were also subject to the unique constraints of spaceflight related research. Specifically, crew members began to readapt to the presence of unit gravity between the moment of Shuttle landing and the time when postflight data were collected (usually 2 to 4 hours after landing). Postflight data were evaluated with the knowledge that the readaptation rate during this time was particularly high [8, 9]. In addition, first-time fliers often displayed more difficulty with postural control after flight than did experienced fliers [8, 9]. Although some subtle, but consistent, changes in postflight lower limb dynamics during treadmill walking were identified, our data confirmed the heterogeneous nature of human adaptation after spaceflight. The significant changes at the moment of heel strike and toe off were encouraging for the hypothesized change in the attenuation capacity of the musculoskeletal system.

Neuromuscular Activation Patterns

In general, the overall phasic activation characteristics of lower limb muscles were only minimally affected by short duration spaceflight. However, when analysis focused on muscle activation characteristics around heel strike and toe off, a variety of preflight versus postflight differences were observed. These changes in neuromuscular activation associated with spaceflight are discussed below in relation to observed changes in head and lower limb gait control strategies after spaceflight and the possible neurophysiological adaptations that contributed to these control strategies.

Perforations in the skin were used to measure muscle activation patterns during treadmill locomotion before and after flight revealed that spaceflight had a minor impact on the overall temporal activation patterns. Dickey and Winter [66], using activation pattern correlations to evaluate the effect of ischemic block on lower limb muscle activation during locomotion, considered correlations less than or equal to 0.71 to represent a significant change in the pattern of muscle activation. Gabel and Brand [92] recommended using an r^2 value of 0.50 (differences between muscle activation patterns). Using this criterion, only 4 of our 78 single limb muscle activation patterns differed after flight, compared to the preflight baseline. However, several subjects in this study had obvious postflight gait abnormalities as they entered the testing room. These included widened support base, shuffling (cautious) gait, and reluctance to move their heads relative to their trunks. Despite these problems, the phasic characteristics of muscle activation during postflight treadmill locomotion were remarkably similar to preflight patterns. This lack of difference was consistent with the observed

minimal preflight-to-postflight difference in stride duration and duty factor. However, evaluating single stride phasic muscle activation characteristics, as a percentage of stride duration for each subject, revealed many statistically significant differences between preflight and postflight locomotion. Although these changes may represent slight modifications in neuromuscular control strategies, they indicate that the sensory motor system generally could reproduce the major phasic activity of each muscle involved in locomoting effectively on a treadmill. However, our subjects did report oscillopsia after flight, suggesting they may have exchanged clear vision for dynamic postural stability during postflight treadmill locomotion. This trade-off was not particularly surprising, given that the consequences of locomotor instability during this task (ie, falling) were severe. Conversely, the safety consequences of unclear vision, while tracking an Earth-fixed target during our task, were minimal.

Given the inherent locomotion constraints on a motor-driven treadmill, this preflight-to-postflight stability could also reflect the task itself. Arsenault et al. [119] found treadmill locomotion to limit the variability in lower limb neuromuscular activation patterns normally present in over-ground locomotion. The minimal requirement for over-ground locomotion was translation from one point to another, which allowed much greater flexibility in the coordination pattern used to accomplish the task than that allowed during treadmill locomotion. The minimal requirement of upright treadmill locomotion was to coordinate body segments in a symmetrical manner that kept the subject within a limited gait width, while keeping pace with belt movement. Deviations from these requirements could result in falling. Moreover, the wide stance and shuffling gait used during over-ground locomotion after spaceflight would be ineffective during our treadmill task. In fact, some Shuttle astronauts have opted not to participate in previously scheduled treadmill testing on landing day, suggesting that these individuals were not confident in their ability to adopt the strategies necessary for successful treadmill locomotion.

Rapidity of readaptation after landing was another potential reason for the similarity between preflight and postflight neuromuscular activation patterns. Although many subjects displayed clinical abnormalities in postural control 2.5 hours after landing, they improved substantially one hour later. [8, 9] These results substantiated numerous anecdotal reports that although astronauts frequently have had problems with postural control immediately following Shuttle landing, they quickly readapt.

One discrete event in the gait cycle that required precise neuromuscular control was toe off. This fine motor skill is achieved by rapid exchanges between a large plantar flexor moment late in the stance to a large dorsiflexor moment at toe off. This exchange normally produces toe clearance during the swing phase of less than 1 cm (0.39 in), with a horizontal velocity greater than 4 m/sec

(13 ft/sec) [61]. Immediately before toe off, the GA actively contributes to the peak plantar flexor moment, with reciprocal inhibition of the TA. TA inhibition contributes to the ability of the GA to produce the necessary peak moment. Immediately before toe off, GA activity ceases and the TA is activated to produce a large dorsiflexion moment to provide appropriate toe clearance. In our study, eight of ten subjects displayed a significant change, after spaceflight, in the relationship between the offset of the GA and the subsequent onset of the TA. Moreover, the relative amplitude of the TA at toe off was reduced after flight, and GA-TA co-contraction magnitude was increased just prior to toe off. This further supported the idea that the precise neuromuscular control necessary to achieve proper toe clearance was compromised after spaceflight. These subtle changes could well explain the excessive foot scraping on the treadmill noted during postflight testing, and are consistent with the shuffling gait often noted during over-ground locomotion after flight.

The excessive foot scraping observed in our subjects may have been a maladaptive strategy that resulted from an inability of the sensorimotor system to efficiently activate ankle musculature. It may also have resulted from an exploratory behavioral mode designed to increase proprioceptive and cutaneous feedback. Pozzo et al. [28] suggested that patients with bilateral vestibular deficits, whose shoes displayed excessive wear on the soles, may have used such a strategy. Since proprioception was altered as a result of spaceflight [5, 53], it is plausible that our subjects were scraping their feet along the treadmill belt to obtain increased feedback. However, the cost of this strategy was to increase the possibility of tripping during postflight locomotion.

At heel strike, the sensorimotor system must effectively absorb the energy generated as the result of the sudden impact of the heel with the support medium, while controlling a kinematic strategy that ensures dynamic stability. During this yielding portion of the gait cycle, the hip joint angle is maintained in approximately 10 degrees of flexion while the knee joint rapidly flexes and the ankle joint plantar-flexes. This kinematic and associated neuromuscular strategy serves to keep the head, arm, and trunk segment (HAT) erect to within 1.5 degrees and attenuates potential head accelerations during locomotion [61]. This tight regulation of the HAT helps maintain the dynamic stability necessary to maintain a safe forward trajectory while contributing to stable gaze. The observed postflight differences in the EMG amplitudes of the RF, BF, and TA relative to preflight values, and increased BF-RF co-contraction around heel strike, indicated some disruption in the neuromuscular control needed to ensure optimal control during this critical behavioral event. This finding was consistent with those of McDonald et al. [45], who reported increased kinematic variability in the lower limb around heel strike during treadmill locomotion after spaceflight. Bloomberg et al. [14, 15] also reported the

presence of modified head control strategies after flight that may not have been as effective as preflight strategies in stabilizing gaze. The presence of these strategies could indicate that the energy introduced into the system, and transmitted to the head at heel strike, may not have been damped as effectively after spaceflight as before. Reductions in energy damping could have exacerbated oscillations during postflight locomotion. Subjects in this study consistently reported that the static target they were asked to visually fixate on during the locomotion task seemed to move more after flight than it did before.

Several neurophysiological changes associated with spaceflight could have been responsible for disruptions in lower limb neuromuscular control occurring around toe off and heel strike. Kozlovskaya et al. [5, 53] reported a generalized trend toward increased proprioceptive hyperreactivity after spaceflight. This was manifested by decreased tendon tap reflex thresholds, increased H reflex amplitudes, and increased vibrosensitivity of the soles of the feet. Other evidence of this phenomenon included increased tendon tap reflex amplitude after spaceflight [55]. Associated with these changes were reductions in the ability to perform graded muscle contractions and decreases in muscle stiffness, particularly in the triceps surae [54]. Shuttle crew members experienced a change in strength ratio between ankle plantar flexors and dorsiflexors. The plantar flexors lost significant strength while the dorsiflexors actually increased strength [120]. This change in relative strength was thought to result from the use of foot loops to maintain orientation relative to the work station. The foot loops were designed so that dorsiflexor activation was primarily required to maintain the proper orientation, as opposed to plantarflexor activation which was generally used to maintain the upright position on Earth. Therefore, increase in dorsiflexor strength and decrease in plantar flexor strength after spaceflight was not unexpected. Additionally, Zangemeister et al. [107] suggested that otolith input could influence TA activation characteristics during locomotion. Thus, spaceflight related adaptive modifications in neural processing of vestibular input could also negatively influence ankle joint muscle control after flight. These neurophysiological changes probably contributed to the inability of subjects in our study to achieve optimal transitions between the plantar and dorsiflexor muscle moments required around toe off, resulting in foot scraping on the treadmill after flight.

During spaceflight, dorsiflexors assumed a larger role than on Earth in regulating the orientation of the individual relative to the environment. Conversely, plantar flexors had a reduced role in orientation control compared with Earth-bound control strategies. Roll et al. [56] suggested that these in-flight adaptations in the respective roles of the ankle musculature eventually resulted in the reinterpretation of ankle proprioceptive input. With increasing mission duration, ankle proprioception was no longer interpreted as coding anterior-posterior body sway while upright, but rather, as coding either whole body axial

transportation (i.e., pushing off the support surface) or foot movement [56]. Although the adaptive ankle musculature control strategy and associated sensory input reinterpretations were appropriate in microgravity, they were maladaptive upon return to the terrestrial environment. It is quite possible that during testing on landing day, these maladaptive ankle control strategies contributed to the disordered EMG activation characteristics observed in this study.

The cautious gait shown when subjects entered the testing room after flight undoubtedly reflected the effects of sensorimotor adaptations. However, these subjects could, and did, organize effective neuromuscular activation strategies that allowed them to complete the task of treadmill locomotion. Nonetheless, subtle alterations were present, both in temporal activation features and in relative activation levels, of several muscles after spaceflight. These changes were particularly prominent around the important behavioral events of heel strike and toe off. Although the sensorimotor system could effectively develop and execute functional behavioral strategies during the goal-directed task of treadmill locomotion, changes in the neuromuscular activation characteristics observed during the task probably contributed to the observed difficulty in over-ground locomotion after landing.

Spatial Orientation

Repeating a previously seen trajectory without vision has been examined since Thomson's experiment on locomotor pointing [121]. However, most of the work has concentrated on walking toward one target. Subjects were able to reproduce previously seen distances correctly by walking two different segments, one straight ahead and the second perpendicular to it [122].

A similar task to the one presented here was called triangle completion. The subject was guided over two legs of the course, and then attempted to return directly to the point of origin [123, 124]. Walked segment length and sustaining angles were varied. Measured parameters were: (1) error in turning toward the origin after walking the first two legs, and (2) error in the distance walked to complete the third leg. A pattern of systematic regression to the mean was shown in both of these errors. Subjects tended to over-respond when the required distance or turn was small, and to under-respond when they were large. These responses were similar for both blind and normal subjects [124].

In blindfolded individuals, triangle completion has one major drawback in indicating disturbances in complex spatial understanding. Some errors made during both the guided walk and return walk were not seen in the results. Imagine a subject over-estimating the walked distance by a certain factor but making no other errors. This subject would perfectly perform the triangle completion, but fail to reach the first and second corners in our task. Therefore, we have chosen the reproduction of a previously seen path by means of locomotion. In this way, the locomotor

pointing performance allowed us to quantify misperception of linear and angular self-displacement.

Astronauts have reported anecdotally about problems in walking straight paths or going around corners when visual information was suppressed [10]. However, little is known about the influence of these modifications on spatial orientation during free locomotion following spaceflight. In DSO 614 we tried to assess this question by having subjects walk a triangular path before and after flight, with and without visual information. The subjects showed inter-individual differences, especially for directional deviations from the path in the vision occluded condition, even before spaceflight. The characteristics of these differences persisted throughout all sessions. However, the absolute directional errors turned out to be larger after flight, meaning that the subjects had larger directional errors, but in different directions. There was a trend toward larger under-estimation of the angle turned at each corner in the postflight condition. In contrast to directional errors, the length of the legs walked was similar before and after flight. If this trend was verified within additional subjects, it would suggest that the perception of self-displacement during turning, but not during linear motion, had been changed as a result of the stay in microgravity. This could have been due to a mismatch between information from otoliths and semicircular canals during whole body turns in microgravity, and could have been responsible for disturbances in locomotion experienced by returning astronauts.

Previous experiments [126] showed that angular as well as linear path integration performance heavily depended on velocity. All changes found could have been caused by the most significant finding, the lower walking velocity during postflight testing. The observed correlation between angular and linear velocity suggests that post-flight decrease in velocity, as found, for example for saccades [127], was a general effect of spaceflight.

The question of why subjects walk more slowly after spaceflight remains unanswered. It appears that a classic speed/accuracy tradeoff was achieved by walking more slowly. Another possible explanation might be that a task as simple as walking toward a previously seen target required a larger cognitive effort after spaceflight, which would slow down motor performance. This implies that mechanisms like computing self-displacement from somatosensory and/or vestibular inputs and updating of spatial information, were disturbed by spaceflight and had to be reacquired after return to Earth.

Lower Limb and Mass Center Kinematics in Downward Jumping

Pre- and postflight comparisons of the joint kinematics during jump landings indicate that the astronaut subjects may be separated into two different classes based on examination of the phase-plane descriptions, namely, P-C and P-S. The P-C group exhibited expanded phase-plane

portraits postflight in comparison to preflight baseline data, and the P-S group showed the contrary. The lower leg musculature may be thought of as contributing a resistance to joint displacements, or stiffness (modeled as a torsional spring-like element), as well as a resistance to joint angular velocity, or damping (represented by a viscous damper or dashpot). These stiffness and damping elements represent the displacement- and velocity-dependent components of the joint impedance, respectively.

Using this description, the P-C group exhibited postflight increases in the majority of both peak joint flexion angles and rates, indicating a reduction in stiffness about the joints following microgravity exposure. In these subjects, increases in joint flexion provided quantitative support for the reports of Watt et al.'s [128] astronaut subjects that their legs were bending more during drop landings postflight. These changes were also consistent with reductions in joint torques and a reduction in the bandwidth of the postural control system as a whole. In contrast, two of the subjects demonstrated an opposite, postflight-stiff response after returning from spaceflight. Their postflight contraction in the phase-plane plots indicated increases in limb stiffness and bandwidth of the postural controller.

A number of possible explanations exist for the observed changes in joint impedance during these jump landings, including loss of strength in the antigravity musculature, altered sensory feedback (muscle stretch reflexes, vestibular, or visual), and changes in open-loop modulation of limb stiffness. Since the stiffness and damping that can be exerted about a joint are directly related to the forces in the muscles acting about the joint, significant strength decreases in the antigravity muscles of the legs could well account for the expanded phase-plane portraits observed in the P-C group of astronauts. However, the P-S subjects exhibited postflight increases in stiffness, indicating increased joint torques; thus, the results from these subjects undermine the hypothesis that loss of muscle strength alone can account for the observations in this study.

Sensory Feedback

Sensory feedback pathways also contribute to the stiffness and damping of the closed-loop postural control system. Feedback quantities that could play a role in the jump landings include postural muscle stretch (modulated through spinal reflexes), vestibular sensing of head orientation and angular velocity, and visual inputs. The stretch reflexes effectively increase the stiffness about the joints by recruiting additional muscle fibers to counteract perturbations to the muscle lengths; the stretch reflexes in concert with Golgi tendon organ force feedback probably serve to modulate the tension-length behavior (impedance) of the muscles. Gurfinkel [83] reported decreases in the strength of the stretch reflex in tibialis anterior following spaceflight; Kozlovskaya et al. [5] found amplitude reductions in Achilles tendon stretch reflexes after long-duration flight. Such decreases could have the effect of

reducing the stiffness about the leg joints, and hence the stiffness of the leg "spring" supporting the body mass. However, Melvill Jones and Watt [129] demonstrated that the monosynaptic stretch response (occurring approximately 40 ms after forcible dorsiflexion of the foot) did not contribute to gastrocnemius muscle tension. Rather, the development of force was found to correspond to a sustained EMG burst with a latency of 120 ms following dorsiflexion stimuli, that they termed the "functional stretch reflex." Since the peak joint angle deflections in the jump landing occur only 100 ms after impact, stretch reflex activity is unlikely to play a major role in the impact absorption phase.

Studies by Allum and Pfaltz [130] and Greenwood and Hopkins [131] found vestibulo-spinal reflex latencies for postural muscles of 80 ms. Visual influences were found to be delayed 80 ms and 100 ms, respectively, by Allum and Pfaltz [130] and Nashner and Berthoz [132]. These latencies comprise most of the interval from impact to peak joint deflections, indicating that sensory feedback information from these sources following impact cannot be expected to contribute significantly to the impact absorption phase of jump landings. However, vestibular and visual inputs during the takeoff and flight phases of the jump may contribute to the motor activity during impact absorption. Interestingly, in the current study the eyes were closed in half of the jumps without a measurable effect on performance, indicating that vision's effect during the jump landings was minimal. This qualitative finding is intriguing in light of evidence for increased dependence on visual cues following spaceflight, for posture control and perception of body orientation and self-motion [10]. However, McKinley and Smith [133] describe jump-down behavior in normal and labyrinthectomized cats with and without vision, and conclude that normal cats that jumped from a known height did not rely on visual input to program pre-landing EMG responses, but when jump height was uncertain and visual input was absent, they speculate that vestibular input became more important. In our study, the astronaut subjects had full knowledge of the jump height after the first jump, which was always conducted with the eyes open. Furthermore, even in the EC jumps, the subjects had visual information about the jump height, even though they closed their eyes immediately before jumping. Therefore, the apparent ability to program pre-landing responses without vision may account for the lack of difference in jumps with and without vision.

Limb Stiffness

The limitations on the sensory feedback pathways indicate that the stiffness properties of the lower limbs may be largely predetermined before impact. The stiffness about the joints is determined by the level of muscle activation, and the overall impedance of the leg to COM motion is also affected by the configuration of the limbs

at impact (in general, less joint flexion results in greater vertical stiffness, due to the reduction of the moment arm about the joint centers). McKinley and Pedotti [134] found that the knee extensor muscles (rectus femoris and vastus lateralis) were activated slightly before impact, while the ankle plantarflexors (gastrocnemius and soleus) were continuously active from midflight during jumps. Furthermore, the legs reached their largest extension before impact, and were already slightly flexed again by the time of impact. Other investigators [135,136] have determined that the timing of the preparatory muscle activation and limb configuration is keyed to the expected time of impact. For downward stepping and repetitive hopping, Melvill Jones and Watt [129] found that muscular activity commenced from 80-140 ms before ground contact, and concluded that the deceleration associated with landing was due to a pre-programmed neuromuscular activity pattern rather than stretch reflex action.

Melvill Jones and Watt [137] demonstrated activation of both gastrocnemius and tibialis anterior approximately 75 ms following an unexpected fall; this reflex activity is most likely due to vestibular system otolith inputs. Such activation of antagonist muscles would contribute to stiffening of the limbs before impact. Furthermore, Watt et al. [128] showed that the amplitude of this response is markedly decreased during spaceflight. However, Watt's tests on landing day showed that the response had returned to normal almost immediately postflight, so changes in the otolith-spinal reflex may not account for the changes observed in the jumps described here. Reschke et al. [138] used the H-reflex to examine the effect of drops on the sensitivity of the lumbosacral motoneuron pool, which is presumably set by descending postural control signals. A large potentiation of the H-reflex (recorded in the soleus muscle) was found beginning approximately 40 ms following an unexpected drop. Furthermore, the investigators found that on the seventh day of spaceflight, the potentiation of the H-reflex during drops vanished. Immediately following spaceflight, 2 of 4 subjects demonstrated a significant increase in potentiation during the drop compared to preflight testing. While an increase or decrease in the sensitivity of the motoneuron pool might correspond to respective increases or decreases in the leg stiffness via a gain change in the spinal reflex pathway, the link to preprogrammed muscular activity is not clear.

In addition to the muscular commands linked to the flight and impact phases of the jump, the underlying tonic activation in the leg musculature may contribute to the impedance in the lower limbs during jump landing. Clément et al. [76] found an increase in tonic ankle flexor activity combined with a decrease in tonic extensor activity during spaceflight that, if carried over postflight, could lead to a reduction in the stiffness about the ankle joint against gravitational loads. It is well established that suppression of vestibular function results in depression of the gamma-static innervation to the leg extensors, causing

reduction in extensor tone [139]. However, because relative enhancement of the knee flexor was not observed, Clément's group viewed the changes at the ankle as a "subject initiated postural strategy" rather than a functional deafferentation of the otoliths caused by exposure to microgravity. Regardless of the origin, significant changes in leg muscle tone could well contribute to altered leg stiffness postflight.

Modeled Stiffness

The hypothesis that the joint impedance characteristics transform into lumped leg stiffness and damping parameters governing the vertical COM motion following impact provides the basis for the mechanical model postulated in this paper. These parameters are assumed to remain constant through the impact absorption and recovery to upright stance. McMahon and Cheng [101] summarized evidence indicating that the legs behave much like a linear spring of near-constant stiffness over a wide range of forces and running speeds. Based on those arguments and the generally close fits to experimental data obtained for the jumps in the present study, the simplifying assumptions of constant stiffness and damping appear reasonable. The constant leg stiffness value that best described human running in McMahon and Cheng's 1990 model was approximately 150 (N/m)/kg, falling well within the range of stiffness computed for the jump landings here.

Comparison of the pre- and postflight fits for this model indicates that variations in the model parameters can adequately predict the alterations in COM motion seen in astronaut jump landings following spaceflight. More specifically, changes in the leg stiffness alone appear to govern the differences in transient response observed upon return to earth. The postflight decreases and increases in the vertical leg stiffness found for these subjects correspond to the classifications of P-C and P-S made previously on the basis of kinematics alone.

In the model, decreases in leg stiffness lead to decreases in bandwidth, with slower and less oscillatory time responses. In contrast, increased stiffness results in faster, higher bandwidth performance with greater overshoots. These decreases and increases in leg stiffness postflight match the changes found in the transient performance for the P-C and P-S subjects, respectively. Interestingly, the model fits did not show changes in the leg damping to play a significant role in the postflight differences. This result is counterintuitive, since an increase in antagonist muscle activation to raise the limb stiffness might be expected to cause a corresponding increase in the mechanical damping properties of the muscles as well. Furthermore, changes in damping in accordance with increases or decreases in stiffness would help to prevent large deviations in the damping ratio (see equation 9), which is often desirable from a control system standpoint. Regardless, the evidence presented here indicates that the damping properties of the limbs can be modulated independently of the stiffness, or simply that the

damping characteristics are largely constant in the face of large changes in leg stiffness.

The final equilibrium positions predicted by the model lie somewhat below the actual final COM rest values, implying that the stiffness for these model fits is less than the values that would have been calculated from the final equilibria alone. In many cases, it was not possible to find parameter values that gave good predictions for both the transient portion of the response and the steady-state equilibrium. Because this study focused on impedance modulation during the impact absorption phase of the jump, the parameter estimation procedure was designed to find best fits for the transient portion of the response, often resulting in differences between the predicted and actual equilibrium positions. Interestingly, the pattern seen in Figure 5.5-29 was consistent across the subject pool: on average, predicted equilibria lay below the actual values. This result was attributed to a transition in control mode and limb posture from the impact absorption phase to the maintenance of upright posture near equilibrium. In equilibrium posture control, the flexed joints and greater compliance used in impact absorption give way to the more upright resting stance, where the alignment of the leg joints results in high vertical stiffness.

The changes in the model parameters corresponding to altered joint and mass center kinematics observed in the astronauts postflight were likely due to changes in the preprogrammed muscle activity prior to impact, which sets the limb impedance in an open-loop fashion by controlling the muscle tension-length properties and the limb configuration. The changes observed in this study in the impact absorption phase support the notion that spaceflight contributed to altered neuromuscular activity during the flight phase of the jump, even though EMG records were not available. The presumed alterations in muscle activation patterns following spaceflight could reflect changes in the relative recruitment of antagonist muscles, or differences in the timing of activation (e.g., failure to activate antigravity muscles early enough during the flight phase to stiffen the limbs for impact).

From an operational standpoint, the results of this study are important for understanding how microgravity exposure might impair astronauts' abilities to perform tasks such as an emergency egress from the Space Shuttle, or even locomotion on another planet following an extended duration spaceflight. The postflight changes in the kinematics of astronaut jump landings reported here have been attributed to changes in the control of the lower limb impedance resulting from exposure to the microgravity conditions of spaceflight. The decreased stiffness of the posture control system observed in the P-C group of subjects may reflect in-flight adaptation to the reduced requirements for posture control in the absence of gravitational forces. On the ground, the nature of the body's compound inverted pendulum structure requires the maintenance of a certain minimum stiffness for stability

in an upright position. In space, the body need not be stabilized against gravity, and the control bandwidth and stiffness may therefore be reduced without compromising postural stability. In flight, an overall reduction in postural stiffness may be observed as reduction in extensor tone and decreases in stretch reflex gain, and may be related to the loss of drop-induced H-reflex potentiation. Compliant postflight behavior may result from a residual decrement in the stiffness of the postural control system following return to Earth. In contrast, stiff postflight behavior may indicate overcompensation for reduced in-flight stiffness upon return to Earth, similar to the "rebound" effect observed by Reschke et al. [138] for the H-reflex. Thus, stiff responses postflight may be related to the observation by Young et al. [79] that some subjects were able to maintain balance only within a narrow "cone of stability" postflight, especially with the eyes closed. By using a stiffening strategy postflight, the subject minimizes deviations from equilibrium to avoid approaching the boundaries of the cone of stability. Such stiffening in turn requires a commensurate increase in postural control bandwidth.

In summary, this study provides evidence for modulation of lower limb impedance by astronauts in response to exposure to the microgravity of spaceflight. The results reported here, interpreted in light of other studies, indicate that this impedance modulation may result from a combination of altered tonic muscular activity and changes in the pre-programmed neuromuscular activity observed prior to and during impact absorption. Simulations using a simple mechanical model of the COM vertical motion indicate that changes in the lumped leg stiffness cause the differences in postflight jumping performance seen in the joint and COM kinematics. The reduced requirements for maintenance of posture under microgravity conditions probably contribute to the changes seen postflight, in concert with decrements in limb proprioception and altered interpretation of otolith acceleration cues.

REFERENCES

1. Homick JL, Reschke MF. Postural equilibrium following exposure to weightless space flight. *Acta Otolaryngol* 1977; 83:455-64.
2. Kenyon RV, Young LR. M.I.T./Canadian vestibular experiments on the Spacelab-1 mission: 5. Postural responses following exposure to weightlessness. *Exp Brain Res* 1986; 64:335-46.
3. Bryanov II, Yemel'yanov MD, Matveyev AD, Mantsev EI, Tarasov IK, Yakovleva IYa, Kakurin LI, Kozrenko OP, Myasnikov VI, Yeremin AV, Pervushin VI, Cherepakhin MA, Purakhin YuN, Rudometkin NM, Chekidra IV. Characteristics of statokinetic reactions. In: Gzenko OG, Kakurin LI, Kuznetsov AG, editors. *Space flights in the soyluz spacecraft:*

- biomedical research. Redwood City, CA: Leo Kanner Associates. Translation of Kosmicheskiye Polety na Korablyakh "Soyuz" Biomeditsinskiye Issledovaniya. Moscow: Nauka Press; 1976. p 1-416.
4. Kozlovskaya IB, Aslanova IF, Barmin VA, Grigorieva LS, Gevlich GI, Kirenskaya AV, Sirota MG. The nature and characteristics of gravitational ataxia. *Physiologist (Supplement)* 1983; 26:108-9.
 5. Kozlovskaya IB, Kriendich YV, Oganov VS, Koserenko OP. Pathophysiology of motor functions in prolonged manned space flights. *Acta Astronautica* 1981; 8:1059-72.
 6. Chekirda IF, Bogdashevskiy AV, Yeremin AV, Kolosov IA. Coordination structure of walking of Soyuz-9 crew members before and after flight. *Kosmicheskaya Biologiya i Meditsina* 1971; 5:48-52.
 7. Chekirda IF, Yeremin AV. Dynamics of cyclic and acyclic locomotion of the Soyuz-18 crew after a 63-day space mission. *Kosmicheskaya Biologiya i Aviakosmicheskaya Meditsina* 1977; 4:9-13.
 8. Paloski WH, Reschke MF, Black FO, Doxey DD, Harm DL. Recovery of postural equilibrium control following space flight. In: Cohen B, Tomko DL, Guedry F, editors. *Sensing and controlling motion: vestibular and sensorimotor function*. Ann NY Acad Sci 1992; 682:747-54.
 9. Paloski WH, Reschke MF, Doxey DD, Black FO. Neurosensory adaptation associated with postural ataxia following spaceflight. In: Woolacott M, Horak F, editors. *Posture and gait: control mechanisms*. Eugene, OR: University of Oregon Press; 1992. p 311-15.
 10. Reschke MF, Bloomberg JJ, Paloski WH, Harm DL, Parker DE. Physiologic adaptation to space flight: Neurophysiologic aspects: sensory and sensory-motor function. In: Nicogossian AE, Leach CL, Pool SL, editors. *Space Physiology and Medicine*. Philadelphia: Lea & Febiger; 1994. p 261-85.
 11. McDonald PV, Layne CS, Bloomberg JJ, Merkle L, Jones G, Pruett CJ. The impact of space flight on postflight locomotion. *Soc Neurosci Abstr* 20, Part 1 1994; 792.
 12. Layne CS, Bloomberg JJ, McDonald PV, Jones G, Pruett CJ. Lower limb electromyographic activity patterns during treadmill locomotion following space flight. *Aviat Space and Environ Med* 1994; 65:449.
 13. Bloomberg JJ, Huebner WP, Reschke MF, Peters BT. The effects of space flight on eye-head coordination during locomotion. *Soc Neurosci Abstr* 18, Part 2 1992; 1049.
 14. Bloomberg JJ, Reschke MF, Peters BT, Smith SL, Huebner WP. Head stability during treadmill locomotion following space flight. *Aviat Space and Environ Med* 1994; 65:449.
 15. Bloomberg JJ, Reschke MF, Huebner WP, Peters BT, Smith SL. Locomotor head-trunk coordination strategies following space flight. *J Vestib Res* 1997; 7:161-77.
 16. Layne CS, McDonald PV, Bloomberg JJ. Neuromuscular activation patterns during locomotion after space flight. *Exp Brain Res* 1997; 113:104-16.
 17. McDonald PV, Basdogan C, Bloomberg JJ, Layne CS. Lower limb kinematics during treadmill walking after space flight: implications for gaze stabilization. *Exp Brain Res* 1996; 112:325-34.
 18. Berthoz A, Pozzo T. Intermittent head stabilization during postural and locomotor tasks in humans. In: Amblard B, Berthoz A, Clarac F, editors. *Posture and gait: development, adaptation and modulation*. Amsterdam: Elsevier; 1988. p 189-98.
 19. Pozzo T, Berthoz A, Lefort L. Head stabilization during various locomotor tasks in humans. 1. Normal subjects. *Exp Brain Res* 1990; 82:97-106.
 20. Grossman GE, Leigh RJ, Abel LA, Lanska, DJ, Thurston SE. Frequency and velocity of rotational head perturbations during locomotion. *Exp Brain Res* 1988; 70:470-76.
 21. Pulaski PD, Zee DS, Robinson DA. The behavior of the vestibulo-ocular reflex at high velocities of head rotation. *Brain Research* 1981; 222:159-65.
 22. Grossman GE, Leigh RJ, Bruce EN, Huebner WP, Lanska DJ. Performance of the human vestibulo-ocular reflex during locomotion. *J Neurophysiol* 1985; 62:264-72.
 23. Taguchi K, Hirabayashi C, Kikukawa. Clinical significance of head movement while stepping. *Acta Otolaryngol (Stockh)* 1984; 406:125-28.
 24. Gresty M, Leech J. Coordination of the head and eyes in pursuit of predictable and random target motion. *Aviat Space Environ Med* 1977; 48:741-44.
 25. Takahashi M, Hoshikawa H, Tsujita N, Akiyama. Effect of labyrinthine dysfunction upon head oscillation and gaze during stepping and running. *Acta Otolaryngol (Stockh)* 1988; 106:348-53.
 26. Grossman GE, Leigh RJ. Instability of gaze during locomotion in patients with deficient vestibular function. *Annals of Neurology* 1990; 27:528-32.
 27. Takahashi M. Head stability and gaze during vertical whole-body oscillations. *Annals of Otology, Rhinology and Laryngology* 1990; 99:883-88.
 28. Pozzo T, Berthoz A, Lefort L, Vitte E. Head stabilization during various locomotor tasks in humans. II. Patients with bilateral peripheral vestibular deficits. *Exp Brain Res* 1991; 85:208-17.
 29. Guitton D, Kearney RE, Wereley N, Peterson BW. Visual, vestibular and voluntary contributions to human head stabilization. *Exp Brain Res* 1986; 64:59-69.

30. Keshner EA, Peterson BW. Multiple control mechanisms contribute to functional behaviors of the head and neck. In: Berthoz A, Graf W, Vidal PP, editors. *The head-neck sensory motor systems*. New York: Oxford University Press; 1992. p 381-86.
31. Keshner EA, Peterson BW. Mechanisms controlling human head stabilization. I. Head-neck dynamics during random rotations in the horizontal plane. *J Neurophysiol* 1995; 73:2293-301.
32. Keshner EA, Cromwell RL, Peterson BW. Mechanisms controlling human head stabilization. II. Head-neck characteristics during random rotations in the vertical plane. *J Neurophysiol* 1995; 73:2302-12.
33. Hirasaki E, Takeshi K, Nozawa S, Matano S, Matsunaga T. Analysis of head and body movements of elderly people during locomotion. *Acta Otolaryngol (Stockh)* 1993; 501:25-30.
34. Paige GD. The influence of target distance on eye movement responses during vertical linear motion. *Exp Brain Res* 1989; 77:585-93.
35. Solomon D, Cohen B. Stabilization of gaze during circular locomotion in light. I. Compensatory head and eye nystagmus in the running monkey. *J Neurophysiol* 1992; 67:1146-57.
36. Solomon D, Cohen B. Stabilization of gaze during circular locomotion in darkness. II. Contribution of velocity storage to compensatory eye and head nystagmus in the running monkey. *J Neurophysiol* 1992; 67:1158-70.
37. Hernandez-Korwo R, Kozlovskaya IB, Kreydich YV, Martinez-Fernandez S, Rakhmanov AS, Fernandez-Pone E, Minenko VA. Effect of seven-day space flight on structure and function of human locomotor system. *Kosm Biol Aviakosm Med* 1983; 17:37-44.
38. Anderson, DJ, Reschke MF, Homick JL, Werness SAS. Dynamic posture analysis of Spacelab-1 crew members. *Exp Brain Res* 1986; 64:380-91.
39. Berthoz A, Grantyn A. Neuronal mechanisms underlying eye-head coordination. *Prog Brain Res* 1986; 64:325-43.
40. Vieville T, Clément G, Lestienne F, Berthoz A. Adaptive modifications of the optokinetic vestibulo-ocular reflexes in microgravity. In: Keller EL, Zee DS, editors. *Adaptive processes in visual and oculomotor systems*. New York: Pergamon Press; 1986. p 111-20.
41. Kozlovskaya IB, et al. The effects of real and simulated microgravity on vestibulo-oculomotor interaction. *The Physiologist* 1985; 28(6):51-56.
42. Thornton WE, Moore TP, Uri JJ, Pool SL. Studies of the vestibulo-ocular reflex on STS 4, 5 and 6. *NASA Technical Memorandum* 1988; 100(461):42.
43. Uri JJ, Linder BJ, Moore TP, Pool SL, Thornton WE. Saccadic eye movements during space flight. *NASA Technical Memorandum* 1989; 100(475):9.
44. Jones GM, Gordon C, Fletcher W, Weber K, Block E. Adaptation in the non-visual control of locomotor trajectory. *Third International Symposium on the Head/Neck System*. Vail, CO, 1995.
45. McDonald PV, Basdogan C, Bloomberg JJ, Layne CS. Lower limb kinematics during treadmill walking after space flight: implications for gaze stabilization. *Exp Brain Res* 1996; 112:324-34.
46. McDonald PV, Bloomberg JJ, Layne CS. A review of adaptive change in musculoskeletal impedance during space flight and associated implications for postflight head movement control. *J Vestib Res* 1997; 7:239-50.
47. Voloshin AS, Wosk J, Brull M. Force wave transmission through the human locomotor system. *Transactions of the American Society of Mechanical Engineers Journal of Biomechanical Engineering* 1981; 103:48-50.
48. Perry SD, Lafortune MA. Effect of foot pronation on impact loading. *International Society of Biomechanics 14th Congress*. Paris, France, 1993.
49. McMahan TA, Valiant GA, Frederick EC. Groucho running. *J Appl Physiol* 1987; 62:2326-37
50. Lafortune MA, Hennig EM, Lake MJ. Dominant role of interface over knee angle for cushioning impact loading and regulating initial leg stiffness. *J Biomech* in press. 1996.
51. Assaiante C, Amblard B. Ontogenesis of head stabilization in space during locomotion in children: influence of visual clues. *Exp Brain Res* 1993; 93:499-515.
52. Thornton WE, Rummel JA. Muscular deconditioning and its prevention in space flight. In: Johnston RS, Dietlein LF, editors. *Biomedical results of Skylab, NASA SP-377*. U.S. Government Printing Office: Washington, DC; 1977. p 191-97.
53. Kozlovskaya IB, Kreidich YV, Rakhman OV. Mechanisms of the effects of weightlessness on the motor system of man. *Physiologist* 1981; 24:59-64.
54. Grigoryeva LS, Kozlovskaya IB. Effect of weightlessness and hypokinesia on velocity and strength properties of human muscles. *Kosm Biol Aviakosm Med* 1987; 21(1):27-30.
55. Harris BA, Billica RD, Bishop SL, Blackwell T, Layne CS, Harm DL, Sandoz GR, Rosenow EC. Physical examination during space flight. *Mayo Clin Proc* 1997; 72:301-08.
56. Roll JP, Popov K, Gurfinkel VS, Lipshits M, Andre-Deshays C, Gilhodes JC, Quoniam C. Sensorimotor and perceptual function of muscle proprioception in microgravity. *J Vestib Res* 1993; 3:259-73.
57. Hillman EJ, Bloomberg JJ, McDonald PV, Cohen HS. Dynamic visual acuity while walking in normals

- and labyrinthine deficient patients. *J Vestib Res* 1998; In press.
58. Milner M, Basmajian JV, Quanbury AO. Multifactorial analysis of walking by electromyography and computer. *Arch Phys Med Rehabil* 1971; 50:235-58.
 59. Dubo HIC, Peat M, Winter DA, Quanbury AO, Hobson DA, Steinke T, Reimer G. Electromyographic temporal analysis of gait: normal human locomotion. *Arch Phys Med Rehabil* 1976; 57:415-20.
 60. Winter DA. Pathologic gait diagnosis with computer-averaged electromyographic profiles. *Arch Phys Med Rehabil* 1984; 65:393-98.
 61. Winter DA, MacKinnon, Ruder GK, Wieman C. An integrated EMG/biomechanical model of upper body balance and posture during human gait. In: Allum JHJ, Allum-Mecklenburg DJ, Harris FP, Probst R, editors. *Progress in Brain Research* 1993; 97:359-67.
 62. Winter DA, Yack HJ. EMG profiles during normal human walking: stride-to-stride and inter-subject variability. *Electroencephalogr Clin Neurophysiol* 1987; 67(5):402-11.
 63. Shiavi R, Bugle HJ, Limbird T. Electromyographic gait assessment, part 1: adult EMG profiles and walking speed. *J Rehabil Res Dev* 1987; 24(2):13-23.
 64. Ounpuu S, Winter DA. Bilateral electromyographical analysis of the lower limbs during walking in normal adults. *Electroencephalogr Clin Neurophysiol* 1989; 72:429-38.
 65. Kameyama O, Ogawa R, Okamoto T, Kumamoto M. Electric discharge patterns of ankle muscles during normal gait cycle. *Arch Phys Med Rehabil* 1990; 71: 969-74.
 66. Dickey JP, Winter DA. Adaptations in gait resulting from unilateral ischaemic block of the leg. *Clinical Biomechanics* 1992; 7(4):215-25.
 67. Crosby PA. Use of surface electromyography as measure of dynamic force in human limb muscles. *Med Biol Eng Comput* 1978; 16:519-24.
 68. Komi PV. Relationship between muscle tension, EMG and velocity of contraction under concentric and eccentric work. In: Desmedt JE, editor. *New developments in electromyography and clinical neurophysiology*, vol. 1. Karger & Basel; 1973. p 596-606.
 69. de Jong RH, Freund FG. Relation between electromyogram and isometric twitch tension in human muscle. *Arch Phys Med Rehabil* 1967; 48:539-42.
 70. Bogardh E, Richards CL. Gait analysis and relearning of gait control in hemiplegic patients. *Physiotherapy Canada* 1981; 33:223-30.
 71. Peat M, Woodbury MG, Ferkul D. Electromyographic analysis of gait following total knee arthroplasty. *Physiotherapy Canada* 1984; 36:68-72.
 72. Richards CL, Wesse J, Malouin F. Muscle activation patterns in gait of rheumatoid arthritic patients. *Physiotherapy Canada* 1985; 37:220-28.
 73. Moore SP, Marteniuk, RG. Kinematic and electromyographic changes that occur as a function of learning a time-constrained aiming task. *J Mtr Beh* 1986; 18:397-426.
 74. Normand MC, Lagesse PP, Rouillard CA, Tremblay LE. Modifications occurring in motor programs during learning of a complex task in man. *Brain Res* 1982; 241:87-93.
 75. Young LR, Oman CM, Watt DGD, Money KE, Lichtenberg BK. Spatial orientation in weightlessness and readaptation to earth's gravity. *Science* 1984; 225: 205-8.
 76. Clément G, Gurfinkel VS, Lestienne F, Lipshits MI, Popov KE. Adaptation of posture control to weightlessness. *Exp Brain Res* 1984; 57:61-72.
 77. Watt DGD, Money KE, Bondar RL, Thirsk RB, Garneau M, Scully-Power P. Canadian medical experiments on Shuttle flight 41-G. *Canadian Aeronautics and Space Journal* 1985; 31(3):215-26.
 78. Parker DE, Reschke MF, Arrott AP, Homick JL, Lichtenberg BK. Otolith tilt-translation reinterpretation following prolonged weightlessness: implications for preflight training. *Aviat Space Environ Med* 1985; 56:601-6.
 79. Young L, Oman C, Watt D, Money K, Lichtenberg B, Kenyon R, Arrott A. M.I.T./Canadian vestibular experiments on the Spacelab-1 mission: 1. Sensory adaptation to weightlessness and readaptation to one-g: an overview. *Exp Brain Res* 1986; 64:291-98.
 80. Martin TP, Edgerton VR, Grindeland RE. Influence of spaceflight on rat skeletal muscle. *J Appl Physiol* 1988; 65:2318-25.
 81. Gurfinkel V. The mechanisms of postural regulation in man. *Soviet scientific reviews, section F: physiology and general biology reviews* 1994; 7(5):59-89.
 82. Layne CS, McDonald, PV, Pruett CJ, Jones G, Bloomberg JJ. Preparatory postural control after space flight. *Society of Neuroscience Abstracts* 1995; 21:138.
 83. Gurfinkel V. The mechanisms of postural regulation in man. *Soviet scientific reviews, section F: physiology and general biology reviews*; 7(5):59-89.
 84. Jeka JJ, Lackner JR. Fingertip contact influences human postural control. *Exp Brain Res* 1994; 100: 495-502.
 85. Holden M, Ventura J, Lackner JR. Stabilization of posture by precision contact of the index finger. *J Vestibular Res* 1994; 4:285-301.

86. Hurmuzlu Y, Basdogan C. On the measurement of dynamic stability of human locomotion. *Journal of Biomechanical Engineering, Transactions of the American Society of Mechanical Engineers* 1994; 116:30-36.
87. Hurmuzlu Y, Basdogan C, Carollo JJ. Presenting joint kinematics of human locomotion using phase plane portraits and Poincaré Maps. *J Biomech* 1994; 27:1495-99.
88. Parker TS, Chua LO. *Practical numerical algorithms for chaotic systems*. New York: Springer; 1989.
89. Guckenheimer J, Holmes P. *Nonlinear oscillations, dynamical systems, and bifurcations of vector fields*. New York: Springer-Verlag; 1983.
90. Kadaba MP, Wootten ME, Gainey J, Cochran GVB. Repeatability of phasic muscle activity: Performance of surface and intramuscular wire electrodes in gait analysis. *J Orthop Res* 1985; 3:350-59.
91. Yang JF, Winter DA. Electromyographic amplitude normalization methods: improving their sensitivity as diagnostic tools in gait analysis. *Arch Phys Med Rehabil* 1984; 65:517-21.
92. Yang JF, Winter DA. Surface EMG profiles during different walking cadences in humans. *Electroencephalogr Clin Neurophysiol* 1984; 60:485-91.
93. Bogey RA, Barnes LA, Perry J. Computer algorithms to characterize individual subject EMG profiles during gait. *Arch Phys Med Rehabil* 1992; 73:835-41.
94. Gabel RH, Brand RA. The effects of signal conditioning on the statistical analyses of gait EMG. *Electroencephalogr Clin Neurophysiol* 1994; 93:188-201.
95. Dietz V, Zijlstra W, Duysens J. Human neuronal interlimb coordination during split-belt locomotion. *Exp Brain Res* 1994; 101:513-20.
96. Tweed DW, Cadera, Vilis T. Computing three-dimensional eye position quaternions and eye velocity from search coil signals. *Vision Res* 1990; 30:97-110.
97. McConville J, Churchill T, Kaleps I, Clauser C, Cuzzi J. Anthropometric relationships of body and body segment moments of inertia. Anthropology Research Project, Inc., Aerospace Medical Division, AFSC Technical Report AFAMRL-TR-80-119. 1980.
98. Young J, Chandler R, Snow C. Anthropometric and mass distribution characteristics of the adult female. Civil Aeromedical Institute, Federal Aviation Administration, Report FAA-AM-83-16.
99. Wilkinson L. SYSTAT: the system for statistics. Evanston, IL: SYSTAT, Inc.; 1989.
100. Alexander R McN, Vernon A. Mechanics of hopping by kangaroos (Macropodidae). *J Zoology* 1975; 177:265-303.
101. McMahon TA, Cheng GC. The mechanics of running: how does stiffness couple with speed? *J Biomechanics* 1990; 23(Suppl. 1):65-78.
102. Ljung L. *System identification toolbox user's guide*. Natick, MA: The MathWorks, Inc.; 1993.
103. Kugler PN, Turvey MT. *Information, natural law, and the self assembly of rhythmical movement: theoretical and experimental investigations*. Hillsdale, NJ: Erlbaum; 1987.
104. Turvey MT, Schmidt RC, Rosenblum LD, Kugler PN. On the time allometry of co-ordinated rhythmic movements. *J Theor Biol* 1988; 130:285-325.
105. Nashner LM. Strategies for organization of human posture. In: Igarashi M, Black FO, editors. *Vestibular and visual control on posture and locomotor equilibrium*. Houston, TX: Karger & Basel; 1985. p 1-8.
106. Keshner EA. Postural abnormalities in vestibular disorders. In: Herdman SJ, editor. *Vestibular rehabilitation*. Philadelphia: FA Davis; 1994. p 47-67.
107. Zangemeister WH, Bulgheroni MV, Pedotti A. Normal gait is differentially influenced by the otoliths. *J Biomed Eng* 1991; 13:451-58.
108. Kozlovskaya IB. Personal communication. 1996.
109. Dijkstra TMH, Schöner G, Gielen CCAM. Temporal stability of the action-perception cycle for postural control in a moving visual environment. *Exp Brain Res* 1994; 97:477-86.
110. Bernstein N. *The coordination and regulation of movements*. New York: Pergamon Press; 1967.
111. Vereijken B, Van Emmerik REA, Whiting HTA, Newell KM. Free(z)ing degrees of freedom in skill acquisition. *J of Mot Behav* 1992; 24:133-42.
112. Paloski WH, Harm DL, Reschke MF, Doxey DD, Skinner NC, Michaud LJ, Parker DE. Postural changes following sensory reinterpretation as an analog to spaceflight. Fourth European Symposium on Life Sciences Research in Space; Trieste Italy, May 28-June 1, 1990.
113. Paloski WH, Black FO, Reschke MF. Vestibular ataxia following shuttle flights: effects of transient microgravity on otolith-mediated sensorimotor control of posture. *Am J Otolaryngology* 1993; 1:9-17.
114. Paloski WH, Bloomberg JJ, Reschke MF, Harm DL. Spaceflight-induced changes in posture and locomotion. *Proc Biomech XIVth I.S.B. Congress*; Paris France, 1993. p 40-41.
115. Kennedy RS, Berbaum KS, Williams MC, Brannen J. Transfer of perceptual-motor training and space adaptation syndrome. *Aviat Space and Environ Med* 1987; 58:A29-33.

116. Welch RB, Bridgeman B, Sulekha A, Browman KE. Alternating prism exposure causes dual adaptation and generalization to a novel displacement. *Perception and Psychophysics* 1993; 54:195-204.
117. Nelson RC, Dillman CJ, Lagasse P, Bickett P. Biomechanics of overground versus treadmill running. *Med Sci Sports Exerc* 1972; 4:233-40.
118. Woolley SN, Winter DA. Mechanical energies in overground and treadmill walking. 3rd Annual Conference of the American Society of Biomechanics; University Park PA, 1979.
119. Arsenault AB, Winter DA, Marteniuk RG. Treadmill versus walkway locomotion in humans: an EMG study. *Ergonomics* 1986; 29(5):665-76.
120. Hayes JL, McBrine JJ, Roper ML, Stricklin MD, Siconolfi SF, Greenisen MC. Effects of space shuttle flights on skeletal muscle performance. *FASEB J* 1992; 6(5):A1770.
121. Thomson JA. How do we use visual information to control locomotion? *Trends Neurosci* 1980; 3:247-50.
122. Loomis JM, Da Silva JA, Fujita N, Fukusima SS. Visual space perception and visually directed action. *J Exp Psychol: Human Perception and Performance* 1992; 18:906-21.
123. Worchel P. Space perception and orientation in the blind. *Psychological monographs: general and applied*. 1951. 65L1-27 (Whole No. 332).
124. Loomis JM, Klatzky RL, Golledge RG, Cicinelli JG, Pellegrino JW, Fry PA. *Journal of Experimental Psychology: General* 1993; 122(1):73-91.
125. Fujita N, Klatzky RL, Loomis JM, Golledge RG. The encoding-error model of pathway completion without vision. *Geographical Analysis* 1993; 25(4): 295-314.
126. Mittelstaedt ML, Glasauer S. Idiopathic navigation in gerbils and humans. *Zool Jb Physiol* 1991; 95:427-35.
127. Glasauer S, Reschke M, Berthoz A, Michaud L, Huebner W. The effect of space flight on gaze control strategy. *Proc 5th Eur Symp on Life Science Research in Space* 1984; Arcachon France. ESA SP-366 1994; p 339-44.
128. Watt DGD, Money KE, Tomi LM. M.I.T./Canadian vestibular experiments on the Spacelab-1 mission: 3. Effects of prolonged weightlessness on a human otolith-spinal reflex. *Exp Brain Res* 1986; 64:308-15.
129. Melvill Jones G, Watt DGD. Muscular control of landing from unexpected falls in man. *J Physiol* 1971; 219:729-37.
130. Allum JHJ, Pfaltz CR. Visual and vestibular contributions to pitch sway stabilization in the ankle muscles of normals and patients with bilateral peripheral vestibular deficits. *Exp Brain Res* 1985; 58:82-94.
131. Greenwood R, Hopkins A. Muscle responses during sudden falls in man. *J Physiol* 1976; 354:507-18.
132. Nashner LM, Berthoz A. Visual contributions to rapid motor responses during postural control. *Brain Res* 1978; 150:403-07.
133. McKinley P, Smith J. Visual and vestibular contributions to replacing EMG during jump-downs in cats. *Exp Brain Res* 1991; 52:439-48.
134. McKinley P, Pedotti A. Motor strategies in landing from a jump: The role of skill in task execution. *Exp Brain Res* 1992; 90:427-40.
135. Dyhre-Poulsen P, Laursen AM. Programmed electromyographic activity and negative incremental muscle stiffness in monkeys jumping down. *J Physiol* 1984; 350:121-36.
136. Thompson HW, McKinley PA. Effect of visual perturbations in programming landing from a jump in humans. *Society for Neuroscience Abstracts* 1988; 14:66.
137. Melvill Jones G, Watt DGD. Observations on the control of stepping and hopping movements in man. *J Physiol* 1971; 219:709-27.
138. Reschke MF, Anderson DJ, Homick JL. Vestibulo-spinal response modification as determined with the H-reflex during the Spacelab-1 flight. *Exp Brain Res* 1986; 64:367-79.
139. Molina-Negro P, Bertrand RA, Martin E, Gioani Y. The role of the vestibular system in relation to muscle tone and postural reflexes in man. *Acta Otolaryngol* 1980; 89:524-33.

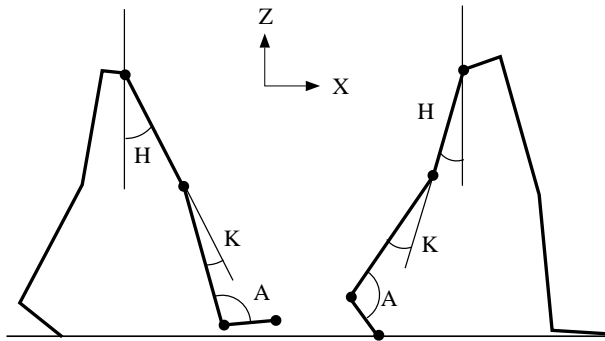


Figure 5.5-1. The convention for joint angle measurements (H = hip angle K = knee angle; A = ankle angle).

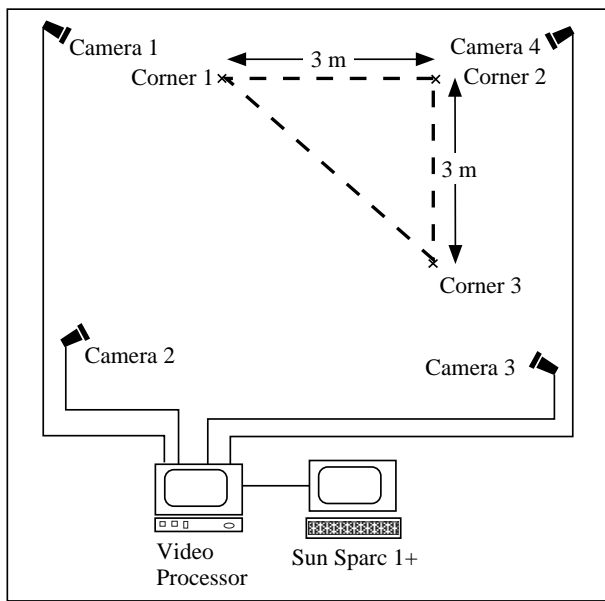


Figure 5.5-2. Map view of the experiment set up. Four cameras connected to a video processor recorded subject path. Three corners of the triangular path (dashed lines) were marked on the floor by white crosses.

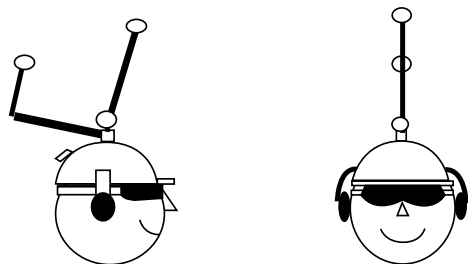


Figure 5.5-3. Subject head sets were used in the locomotor spatial orientation study. Three reflective markers were fixed to the helmet. Head phones and blackened goggles were used to mask auditory cues and occlude vision.

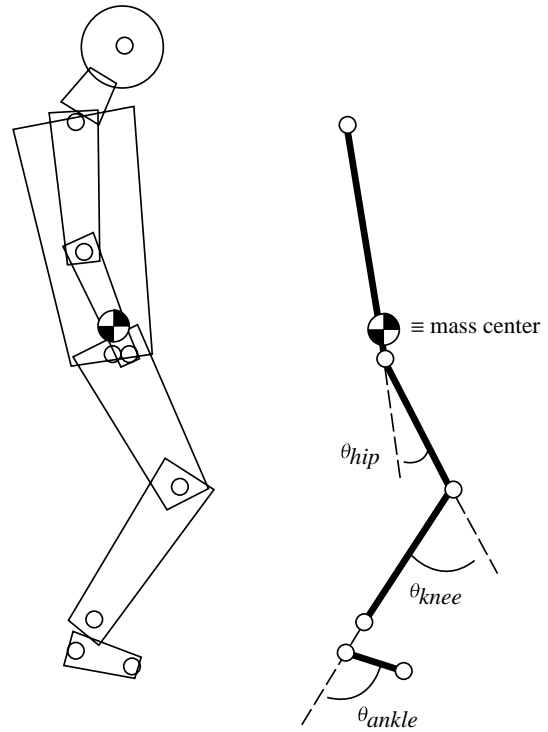


Figure 5.5-4. Sagittal plane body model. The joint angle convention is shown at right. The eight segments used for COM calculation (feet, shanks, thighs, trunk, forearms, upper arms, neck and head) are shown schematically on the left. Reflective marker positions are denoted by "O".

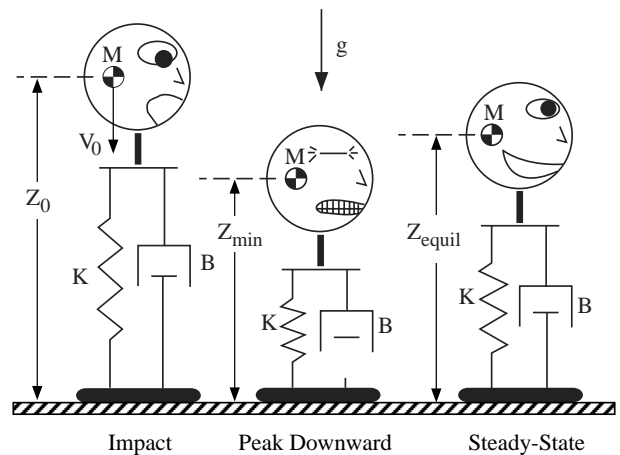


Figure 5.5-5. One degree of freedom, second order model of vertical (Z) COM motion following impact. Body mass (M), located at the COM, is supported by linear spring (K) and dashpot (B). The unloaded length of the spring is Z_0 (nominally the height of the COM at impact), minimum spring length is Z_{min} , and the spring length at the final equilibrium is Z_{equil} .

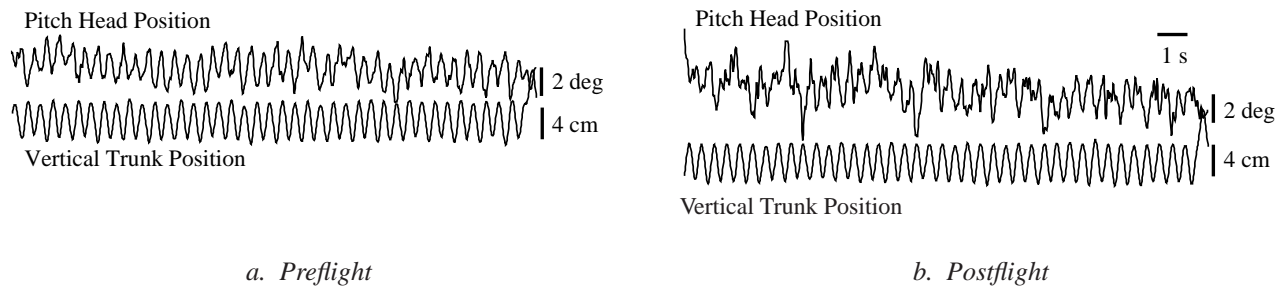


Figure 5.5-6. Waveforms from one subject showing the relationship between vertical translation of the trunk and corresponding pitch angular head movement for the NEAR target condition during pre- (a) and postflight (b) locomotion.

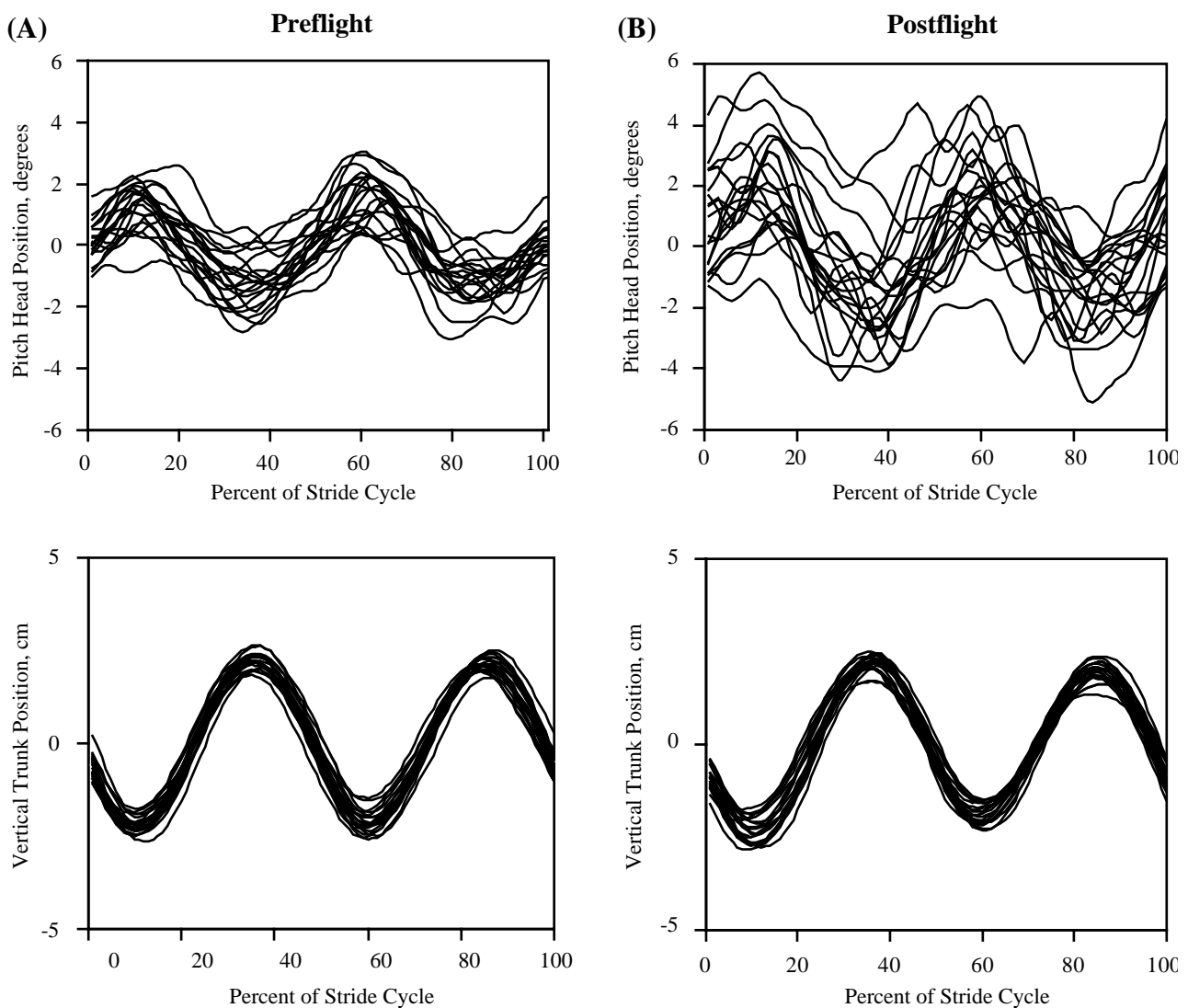


Figure 5.5-7. To show the step-to-step variability, each cycle in the waveforms depicting vertical trunk translation and compensatory pitch head movements were aligned at the point of heel strike in one subject. (a) Preflight and (b) Postflight pitch head movements and corresponding vertical trunk translations during locomotion. Note the increased variability in postflight pitch head movements despite little change in vertical trunk translation.

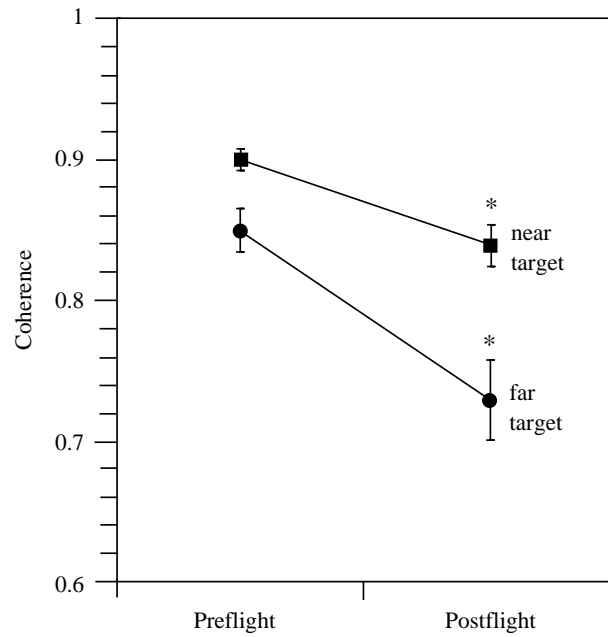


Figure 5.5-8. Mean (± 1 S.E.) pre- and postflight coherence values relating vertical trunk translation and corresponding pitch head movement for all subjects combined, for both FAR and NEAR target conditions. * denotes a significant difference ($p < 0.05$) between pre- and postflight mean coherence values.

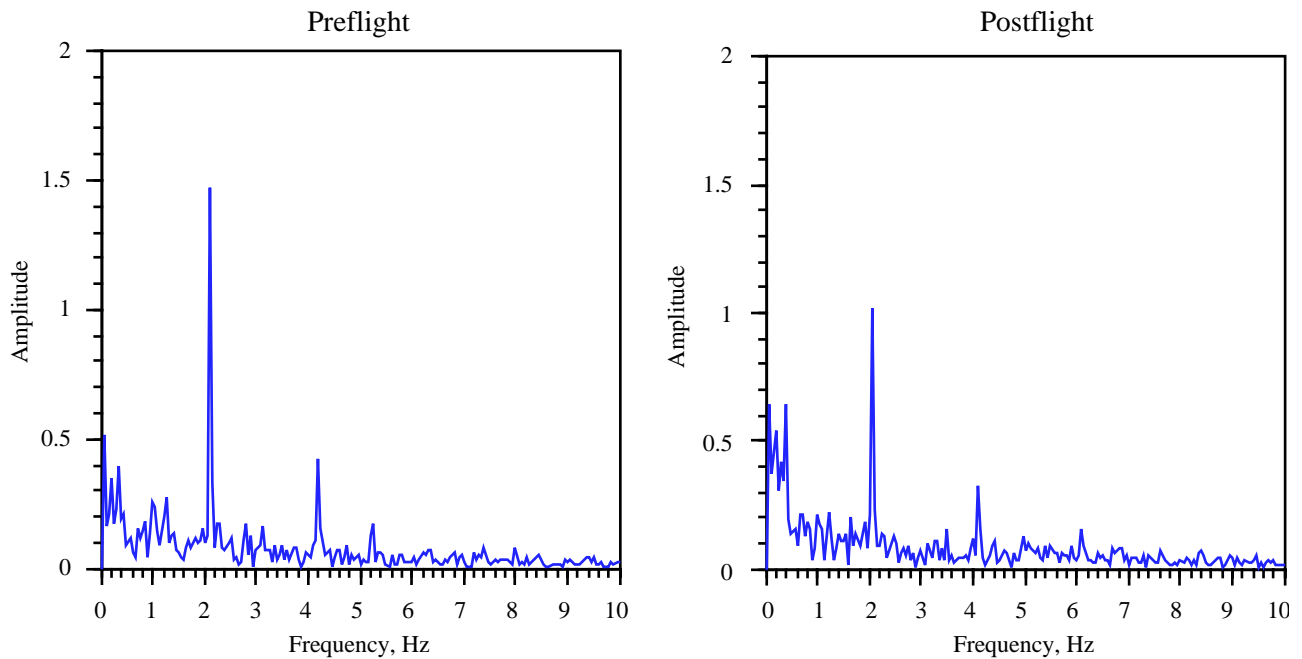


Figure 5.5-9. One pre- and postflight example of Fourier amplitude spectra of pitch head angular displacement for the NEAR target condition for one subject during locomotion. Note the decrease in the amplitude of the predominant frequency component at 2 Hz.

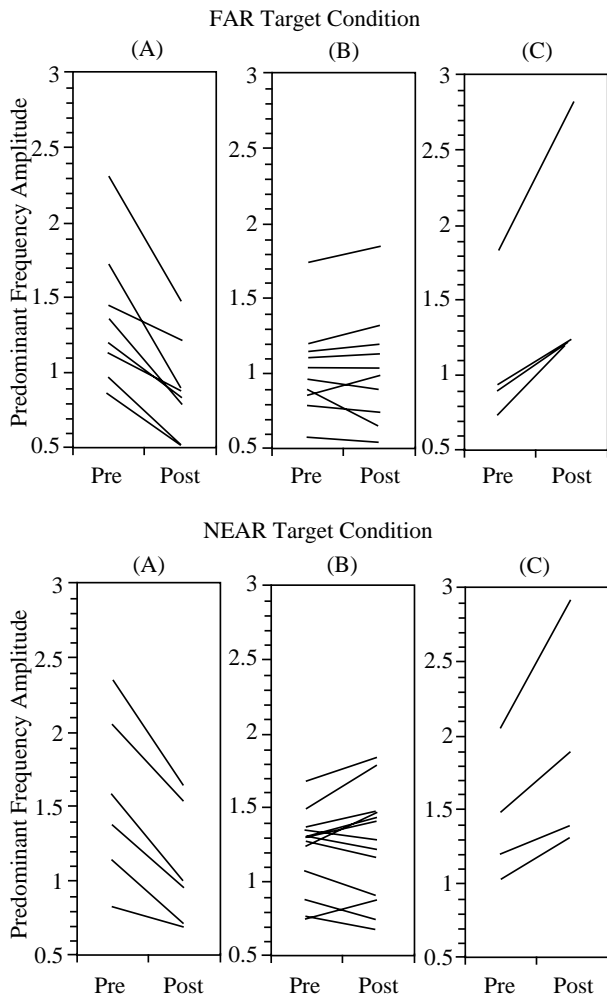


Figure 5.5-10. Individual mean pre- and postflight changes in the magnitude of the predominant peak of pitch head movements for the FAR (top) and NEAR (bottom) target conditions. Individually, subjects show significant ($p < 0.05$) reduction (a), no significant change (b), and augmentation (c) and in predominant peak of pitch head movements during locomotion.

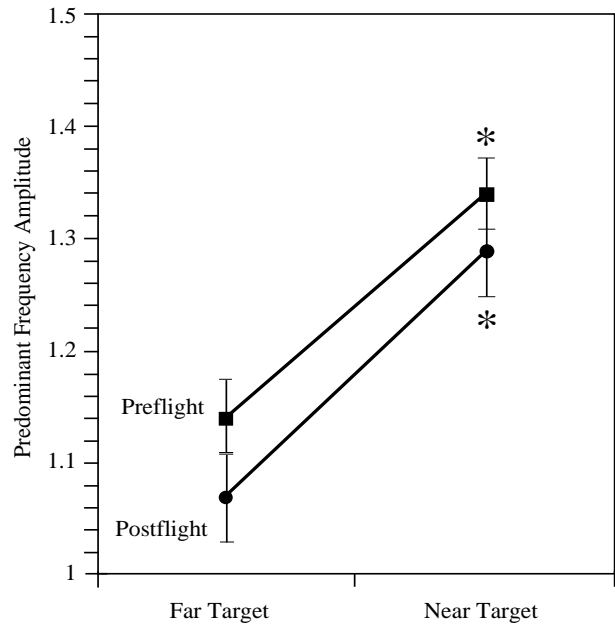


Figure 5.5-11. Mean (± 1 S.E.) magnitude of the predominant peak of pitch head movements for all subjects for the FAR and NEAR target conditions during both pre- and postflight testing. Note the increase in magnitude of predominant peak during visual fixation of the NEAR target. * denotes a significant difference between FAR and NEAR target conditions during both pre- and postflight testing.

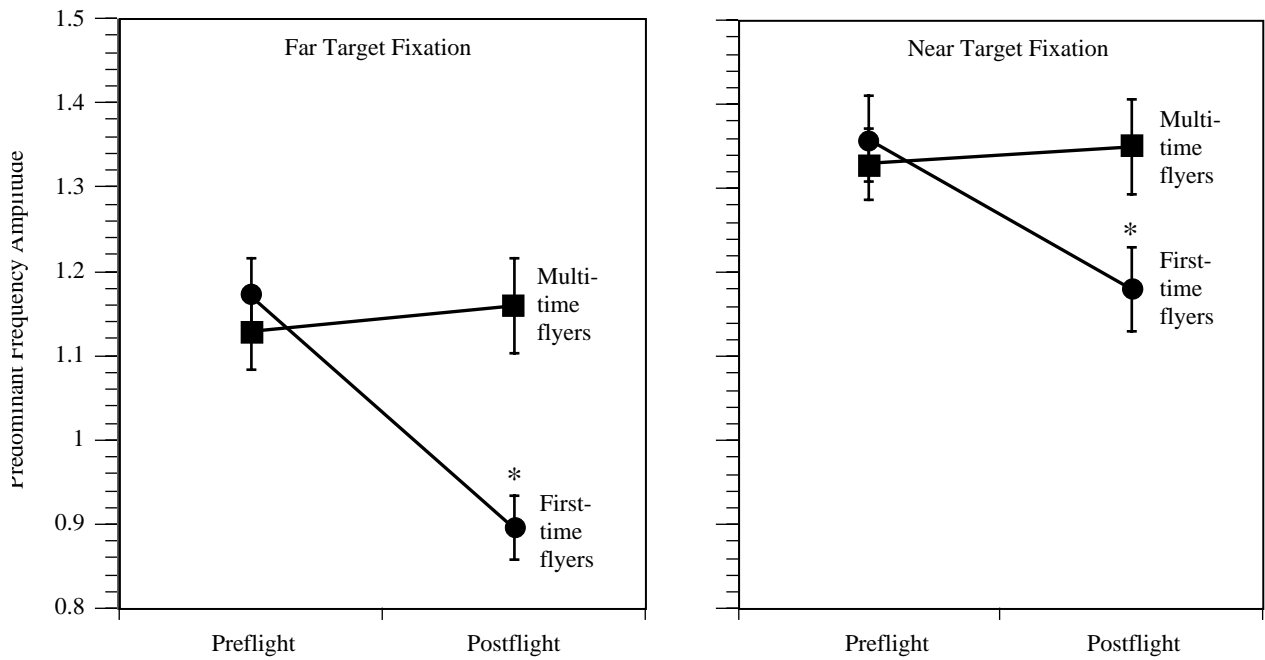


Figure 5.5-12. Comparison between first- and multi-time fliers of the mean (± 1 S.E.) magnitude of the predominant peak of pitch head movements during the FAR and NEAR target conditions. *Note that in both target conditions, first-time fliers display significant ($p < 0.05$) reduction in the predominant peak of pitch head movements while multi-time fliers show no significant changes in pitch head response following space flight.

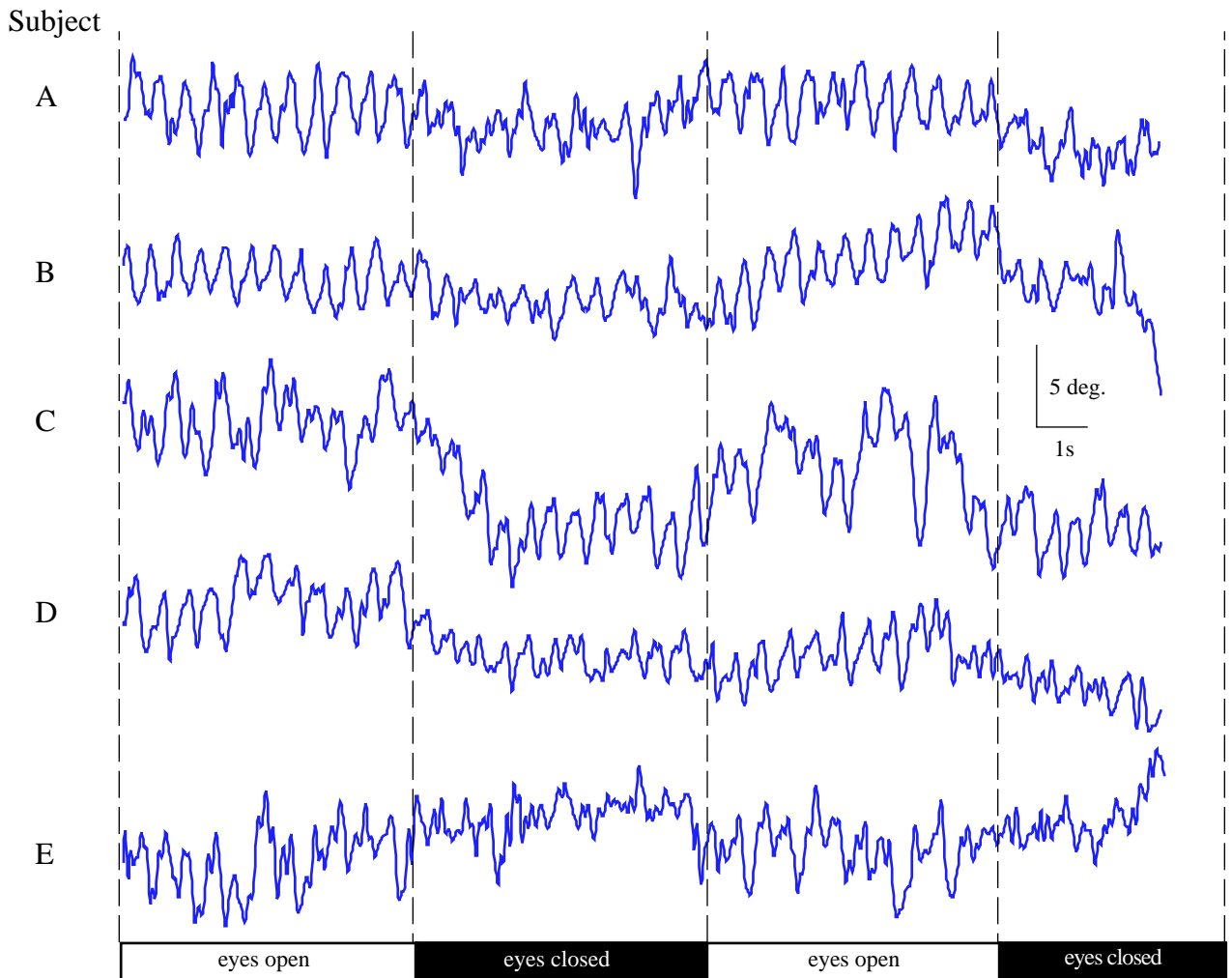


Figure 5.5-13. Waveforms showing pitch angular head displacement for 5 individual subjects (A-E) during the eyes open and eyes closed epochs of the IV condition obtained during one preflight trial. Note the reduction in amplitude and breakdown in waveform regularity during the Eyes Closed epochs.

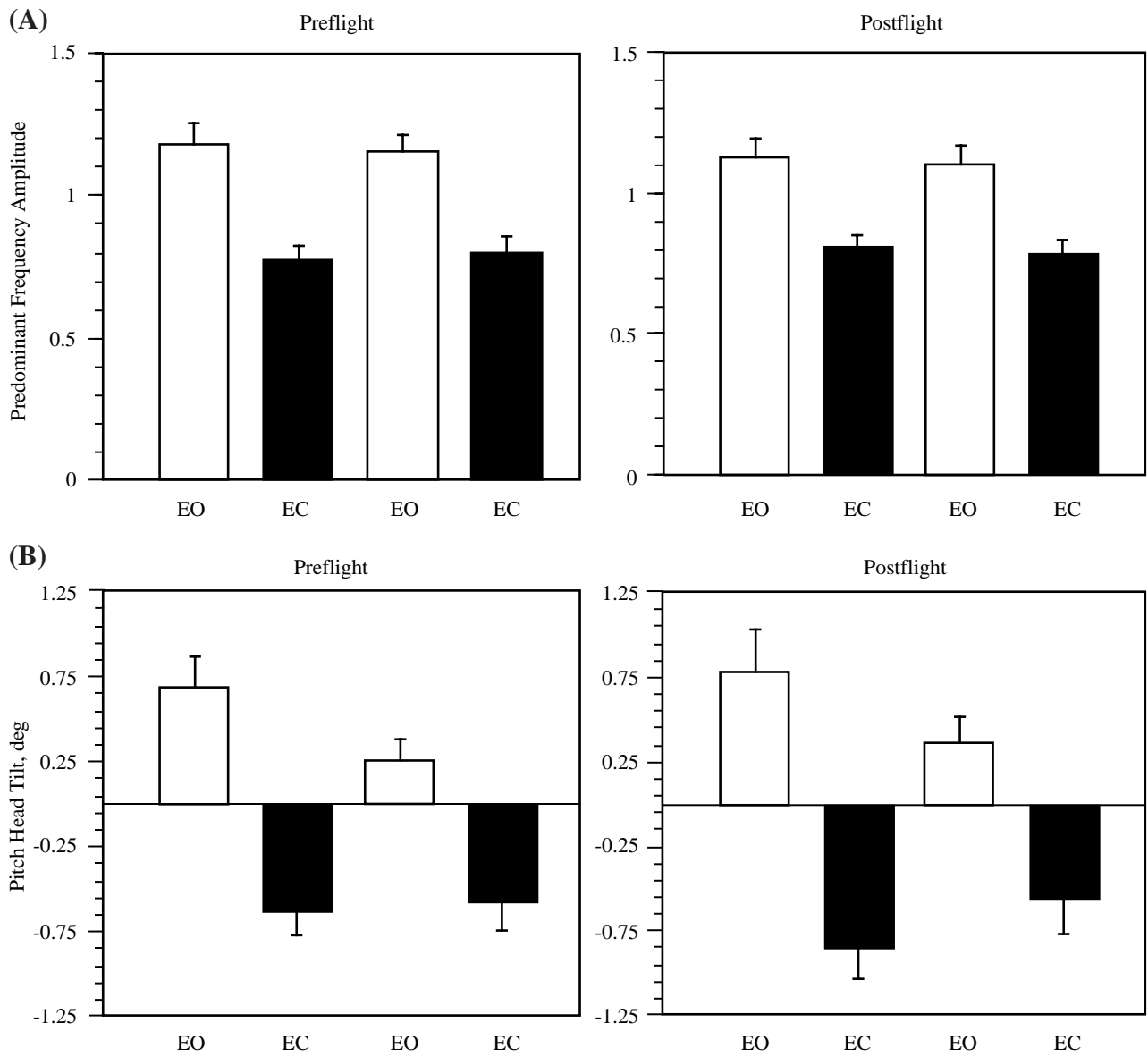


Figure 5.5-14. (a) Pre- and postflight mean (± 1 S.E.) predominant frequency amplitude for all subjects during the alternating 5 second eyes open/closed epochs of the IV condition. (b) Pre- and postflight mean (± 1 S.E.) head tilt relative to vertical in the sagittal plane for all subjects during the alternating 5 second eyes open/closed epochs. EO (eyes open); EC (eyes closed). During eye closure periods, both during pre- and postflight testing, pitch head movements were reduced and the head tilted forward.

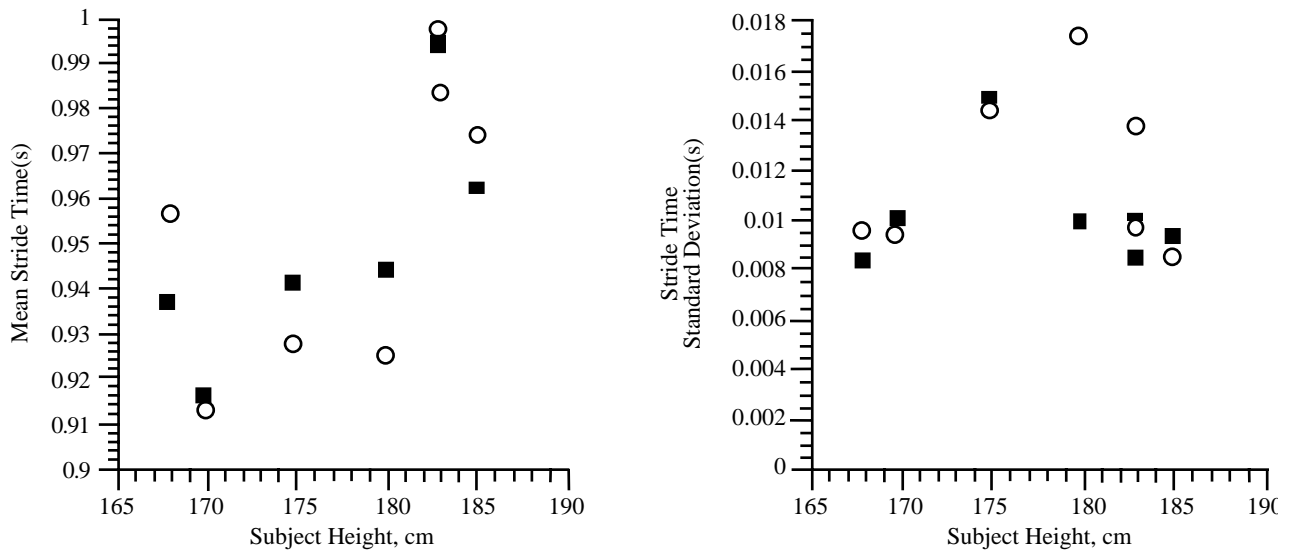


Figure 5.5-15. Mean and standard deviation of the preflight (filled square) and postflight (circle) trial stride time for each of the seven subjects plotted as a function of subject height.

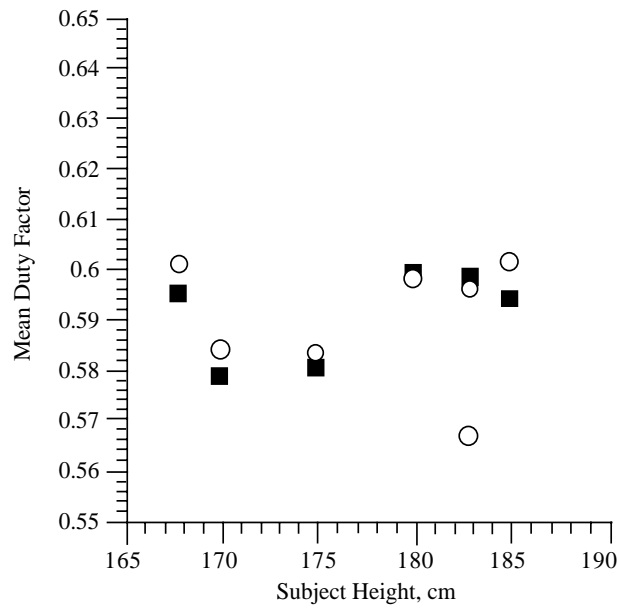


Figure 5.5-16. Preflight (filled square) and postflight (circle) mean duty factor presented for each subject as a function of subject height.

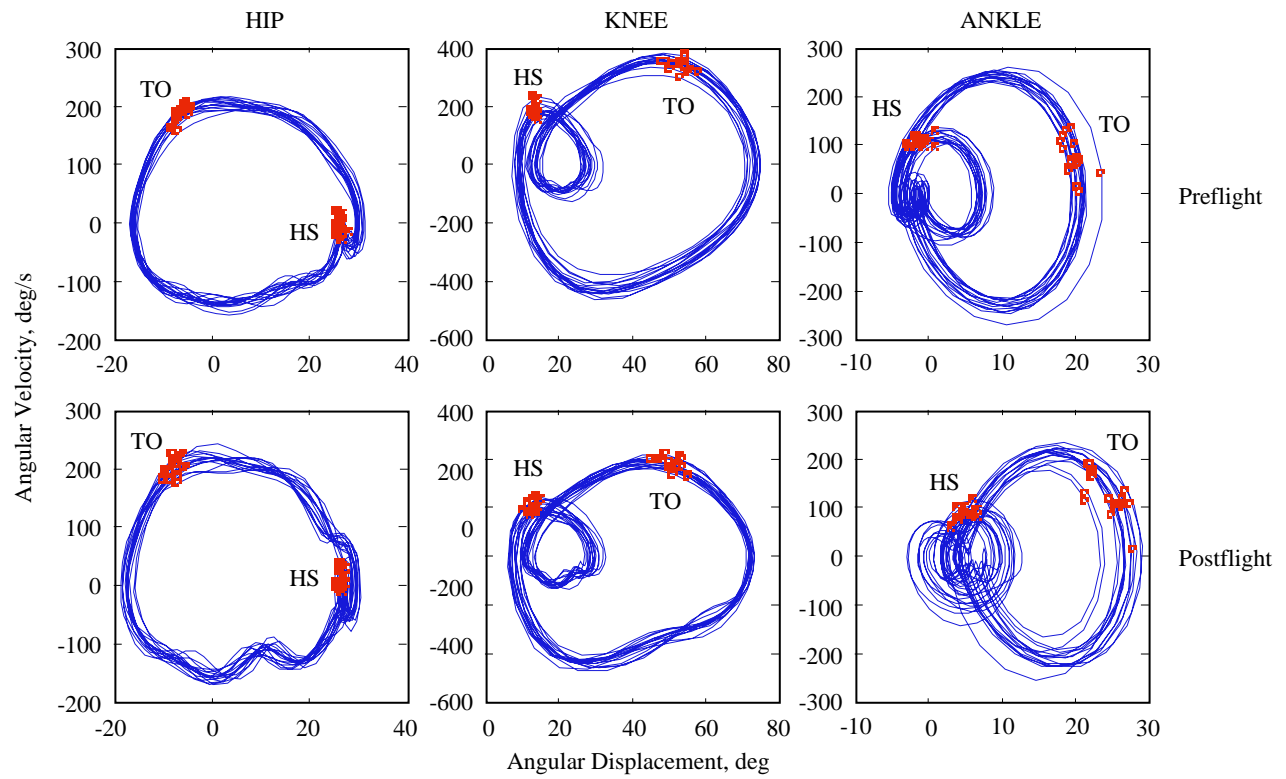


Figure 5.5-17. Exemplar phase portraits of three lower limb joints. These data are from one subject and illustrate 15 consecutive cycles from one preflight and one postflight trial. The location of heel strike (HS) and toe off (TO) for each cycle is indicated.

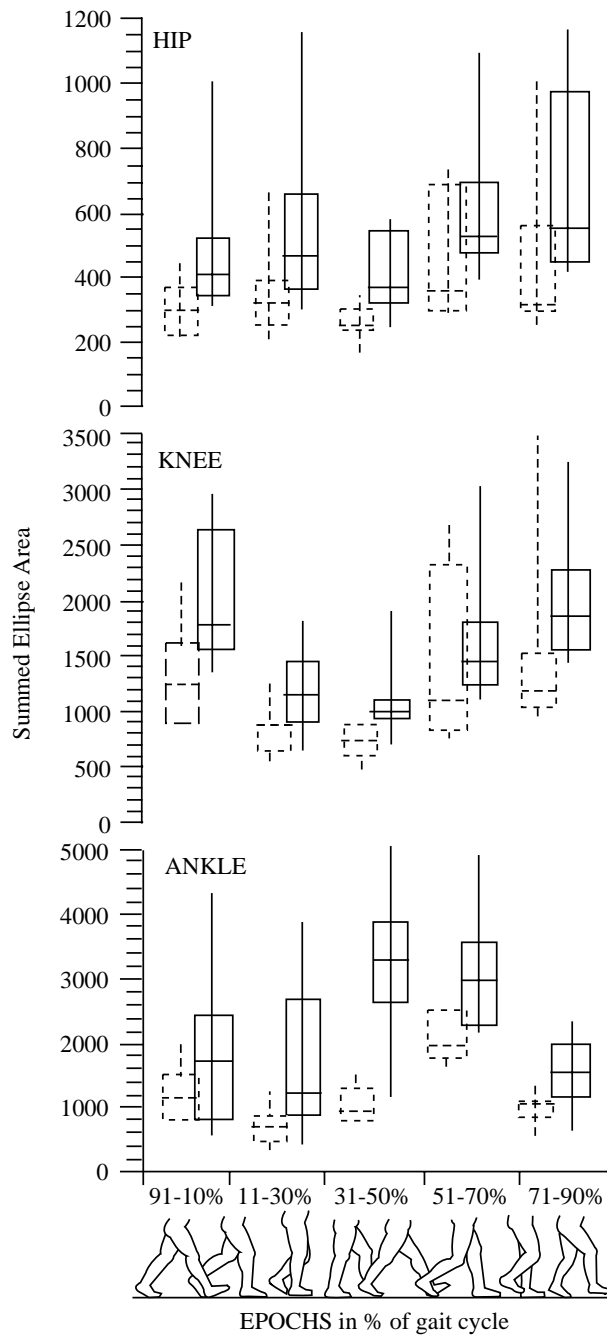


Figure 5.5-18. Box plots of phase plane variability as a function of stride epoch, from right heel strike to right heel strike. Epochs represent 91%-10%, 11%-30%, 31%-50%, 51%-70%, and 71%-90% of gait cycle. Dashed lines indicate preflight, solid lines indicate postflight. Boxes represent the 25th, 50th, and 75th percentile. Whiskers represent the 10th and 90th percentile.

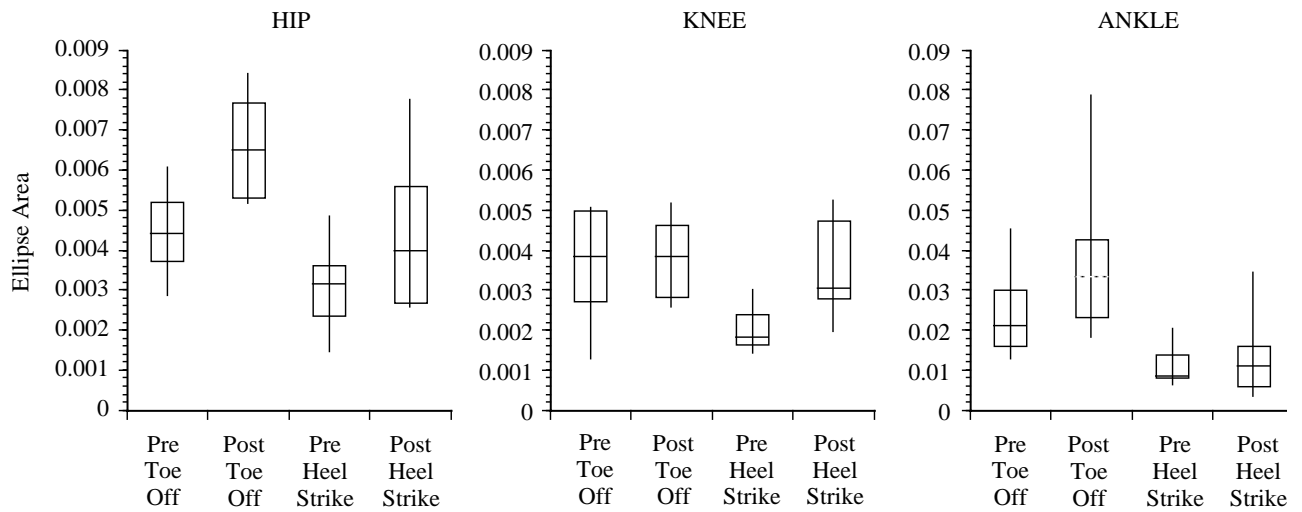


Figure 5.5-19. Box plots of phase plane variability of the preflight and postflight toe off and heel strike events for the hip, knee, and ankle angles.

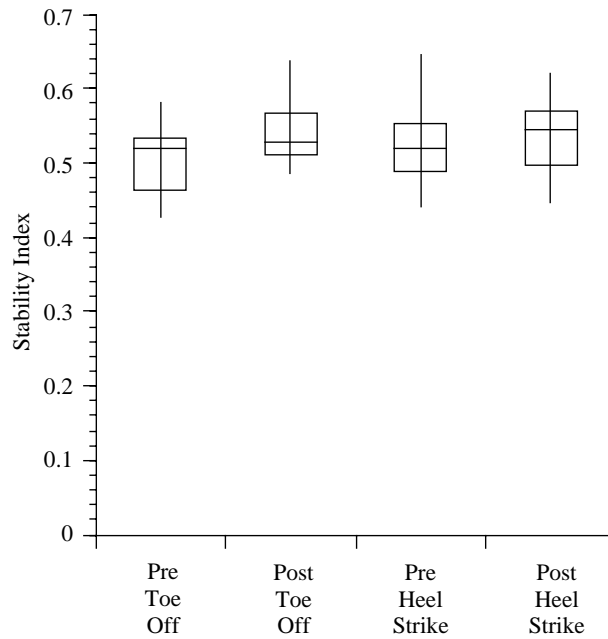
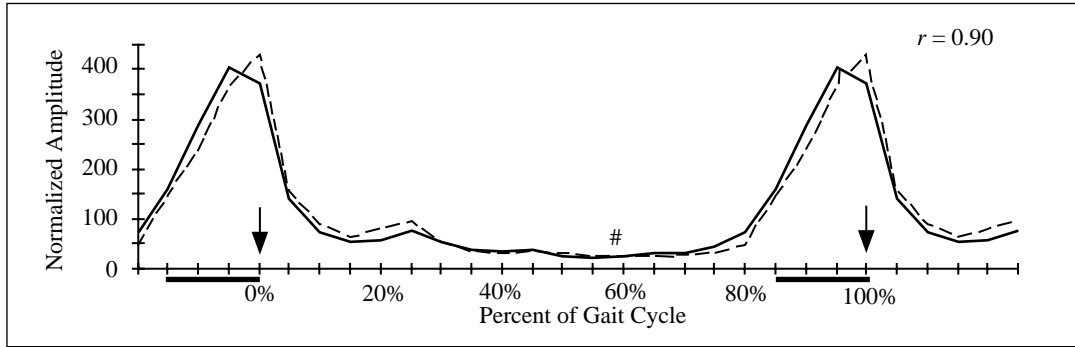
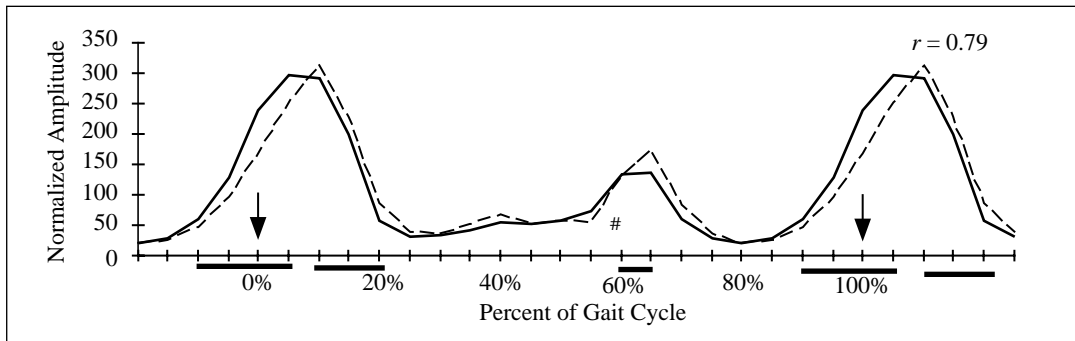


Figure 5.5-20. Box plots of the system stability index for the preflight and postflight toe off and heel strike events.

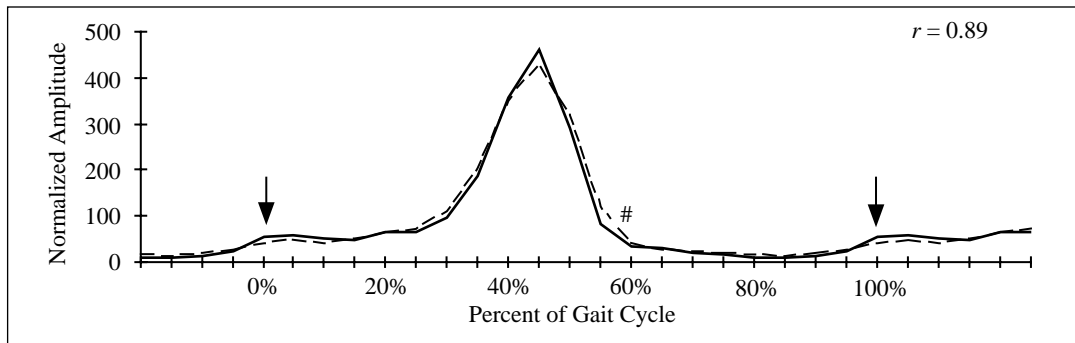
A. *Biceps Femoris*



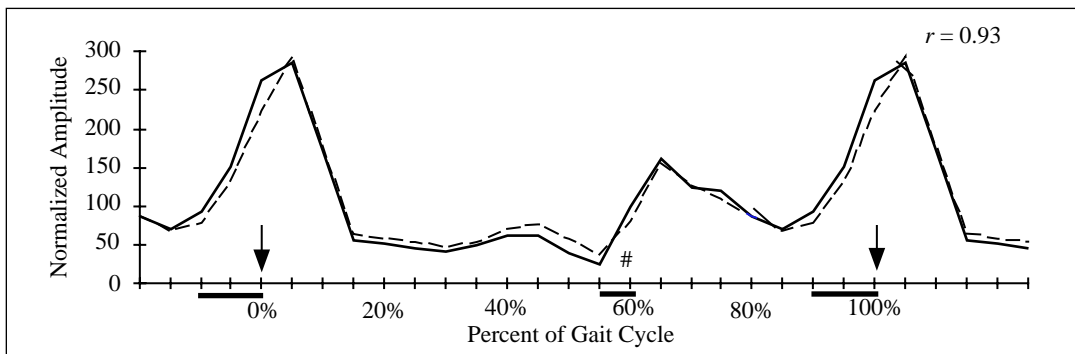
B. *Rectus Femoris*



C. *Gastrocnemius*



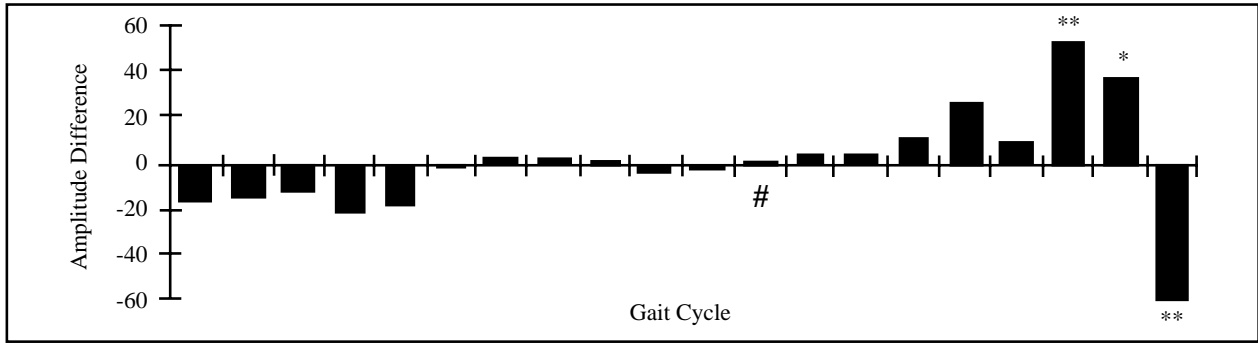
D. *Tibialis Anterior*



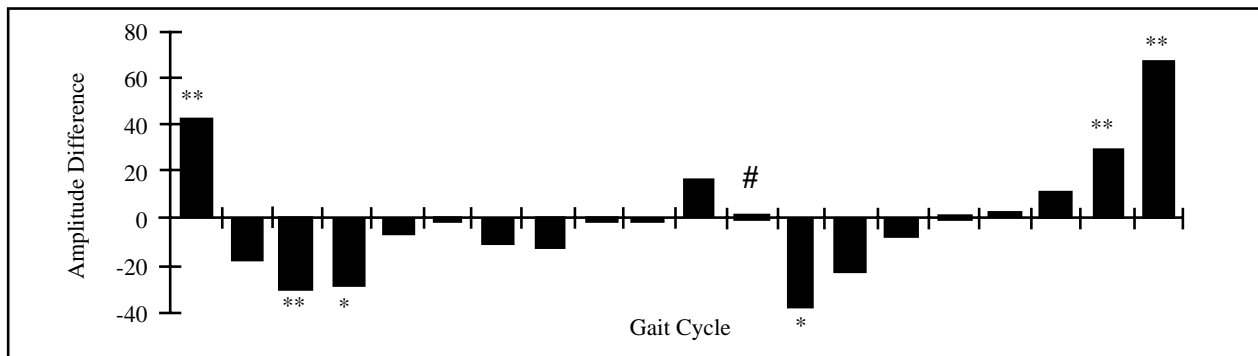
Indicating significant differences in normalized amplitude ——— Mean Waveform Preflight
 Indicating heel stroke - - - Mean Waveform Postflight
 # Indicating toe off

Figure 5.5-21. Grand ensemble average preflight and postflight waveforms for biceps femoris (A), rectus femoris (B), gastrocnemius (C) and tibialis anterior (D).

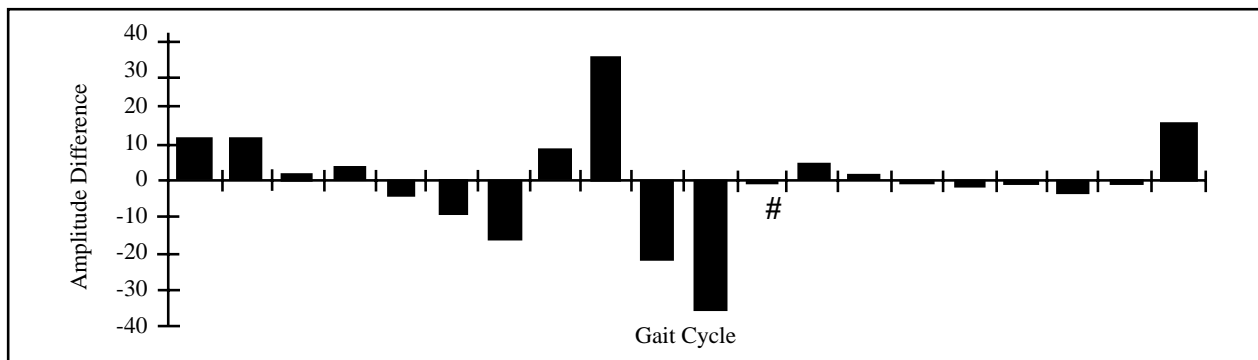
A. *Biceps Femoris*



B. *Rectus Femoris*



C. *Gastrocnemius*



D. *Tibialis Anterior*

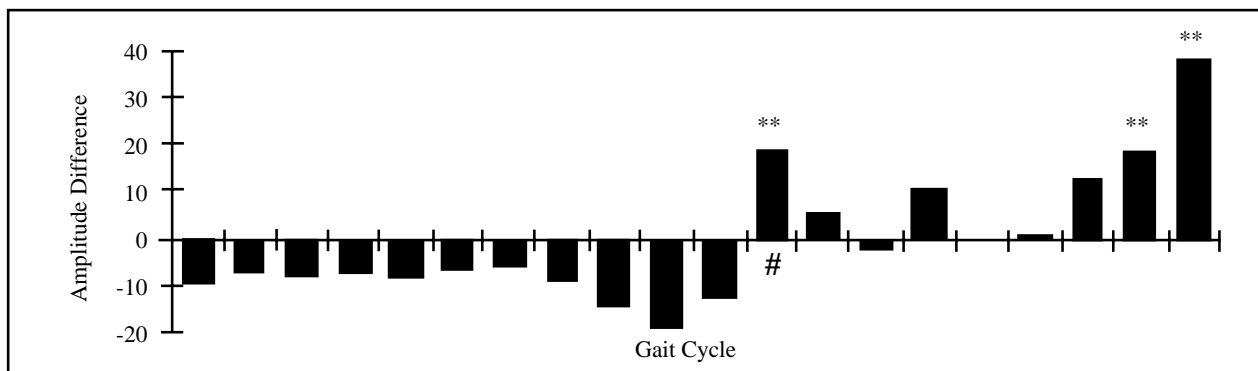


Figure 5.5-22. Differences in relative amplitude between preflight and postflight grand ensemble reduced wave forms at each 5% gait cycle epoch for: *biceps femoris* (A), *rectus femoris* (B), *gastrocnemius* (C) and *tibialis anterior* (D). Analysis epochs began at heel strike. # = Toe off. * = a significant statistical difference. ** = a significant functional difference.

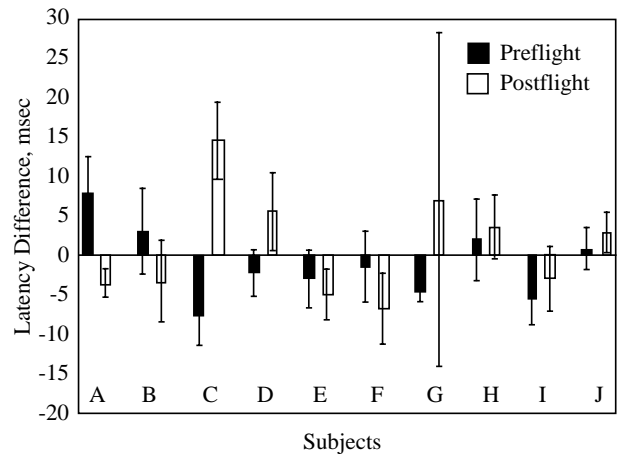
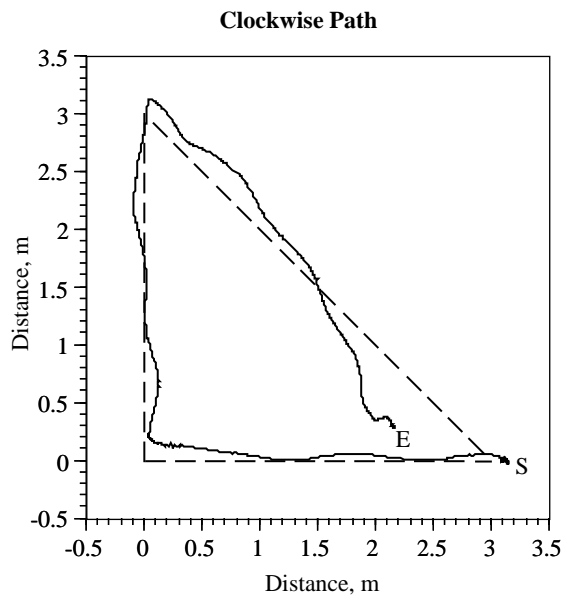
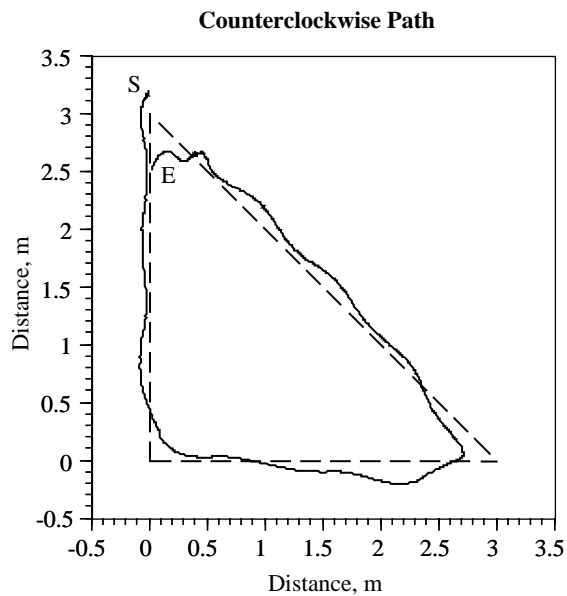
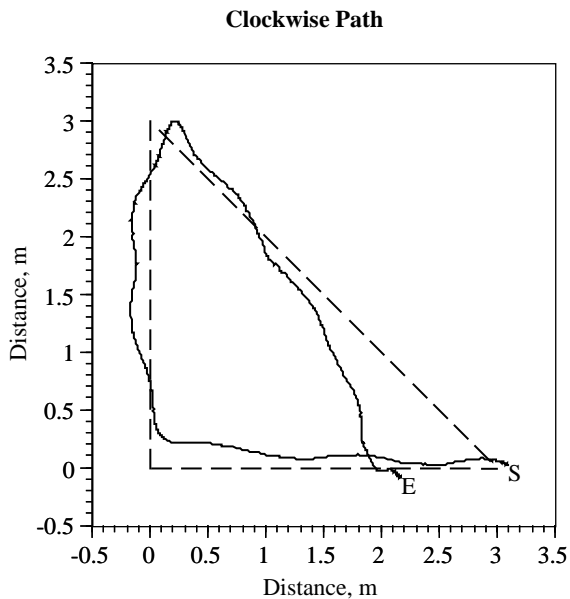
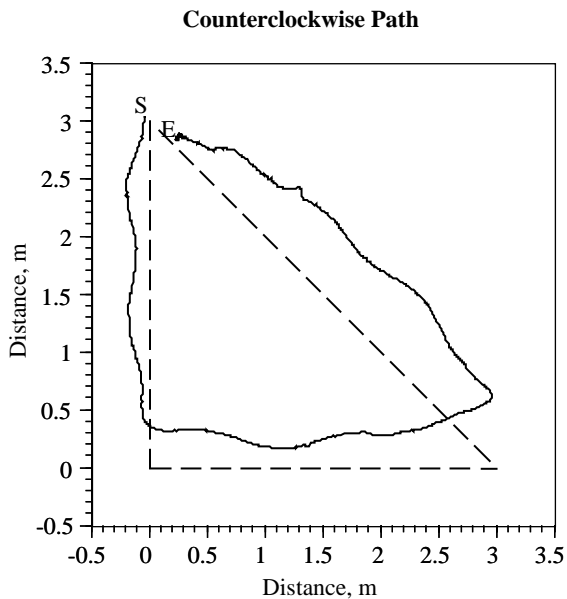


Figure 5.5-23. Preflight versus postflight latency average (± 1 S.D.) difference for each subject between GA offset and TA onset. Negative values indicate that the offset of the GA preceded the onset of the TA. GA = gastrocnemius. TA = tibialis anterior.

Preflight Locomotor Path Integration (without vision)



Postflight (R+0) Locomotor Path Integration (without vision)



— — Designated Path
 ——— Subjects Path

S Starting Point
 E Ending Point

Figure 5.5-24. Example of preflight and postflight walking trajectories (eyes closed condition). Dashed line = Map view of the path. Solid line = Trajectory performed by the subject.

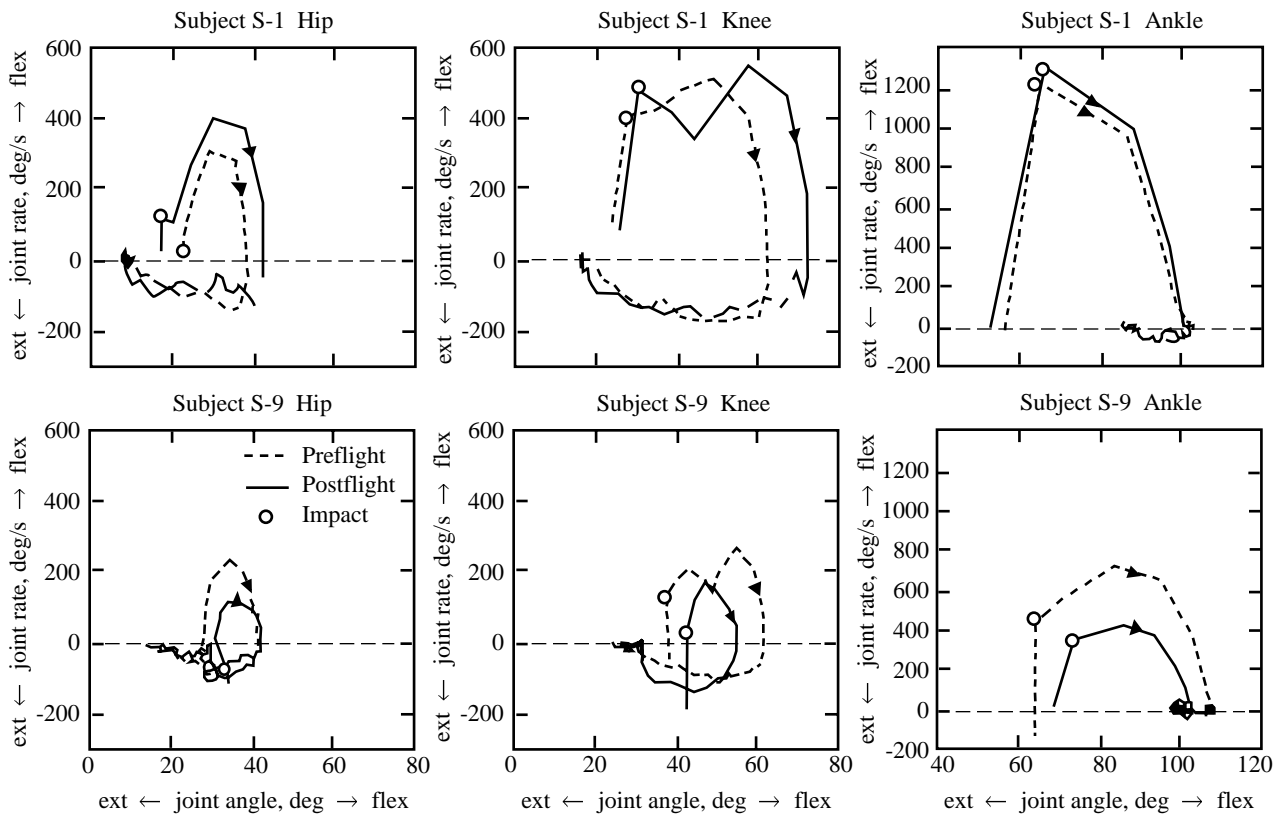


Figure 5.5-25. Comparison of preflight (dashed) and postflight (solid) joint angle phase-plane portraits for hip, knee and ankle. (Top) For subject S-1, the postflight phase is expanded with respect to the preflight diagram. (Bottom) In contrast, subject S-9 demonstrates postflight contraction of the phase portrait in comparison to preflight results.

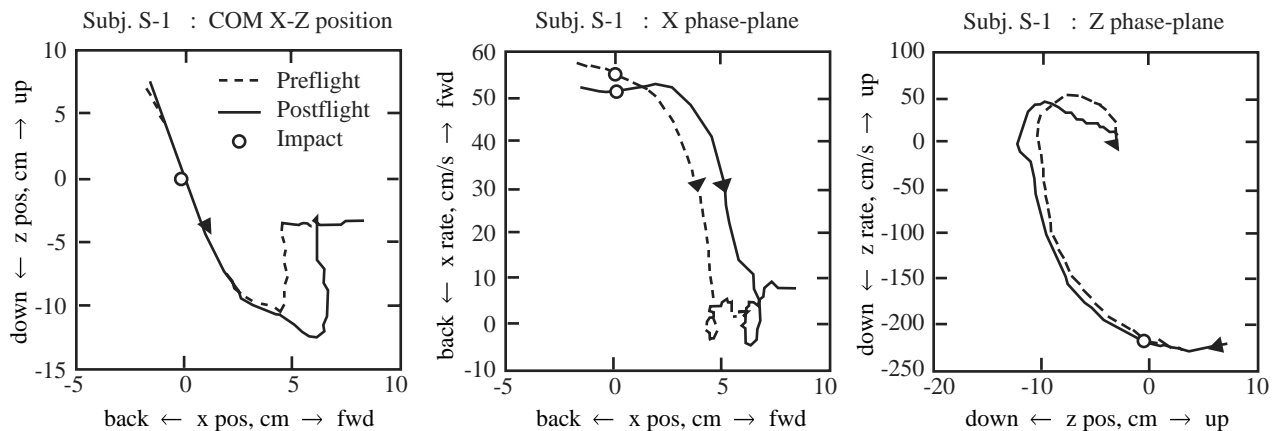
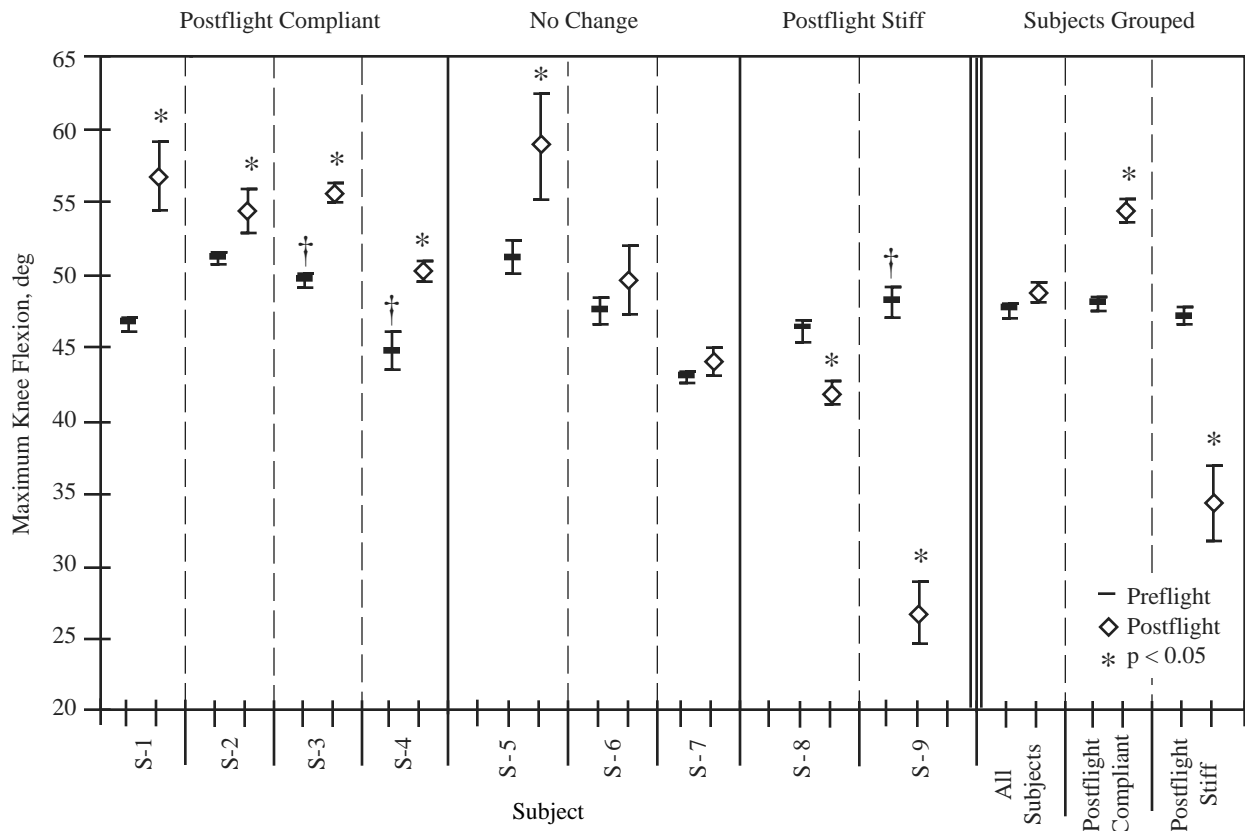
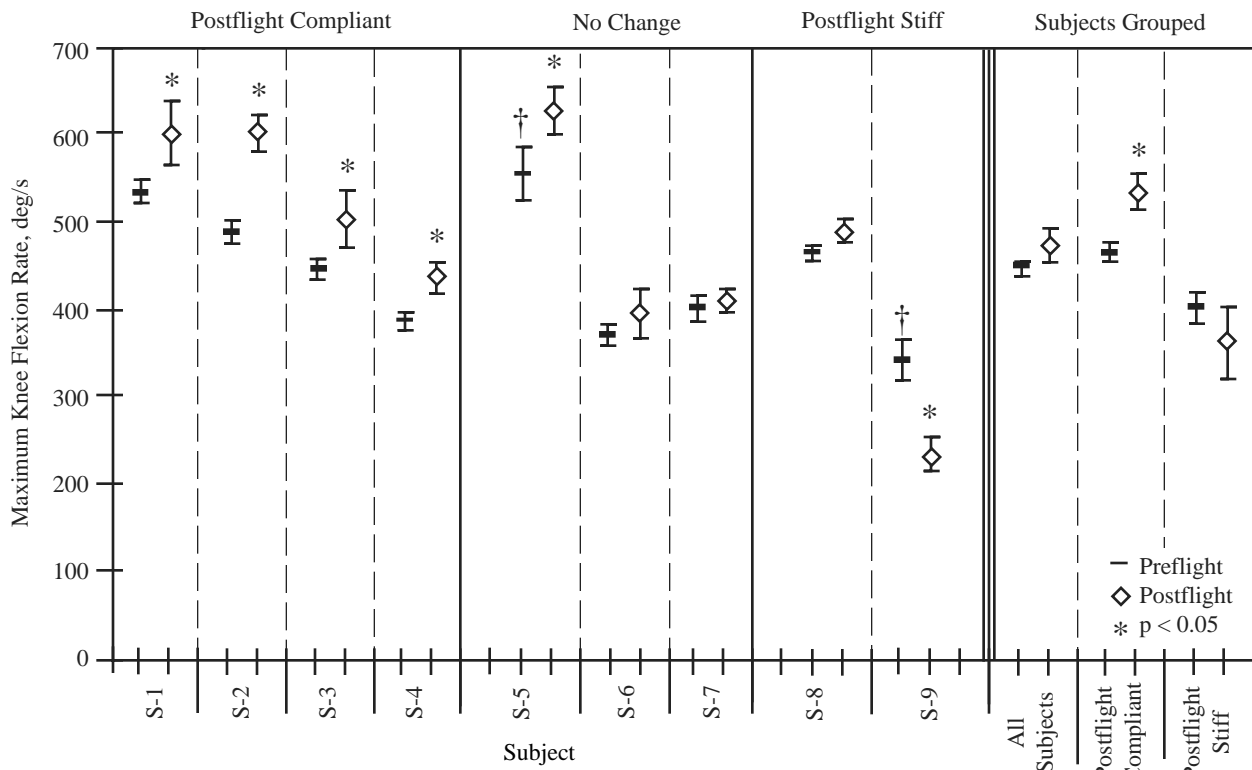


Figure 5.5-26. Comparison of preflight (dashed) and postflight (solid) COM motion for postflight-compliant subject S-1. (Left) The trajectory of the COM in the sagittal (X-Z) plane; peak deflection of the COM is greater postflight. (Middle) Phase-plane motion of the COM in the X (horizontal) direction is shown. (Right) Z (vertical) motion is shown in the phase-plane diagram, indicating greater downward deflection and slower upward recovery postflight.

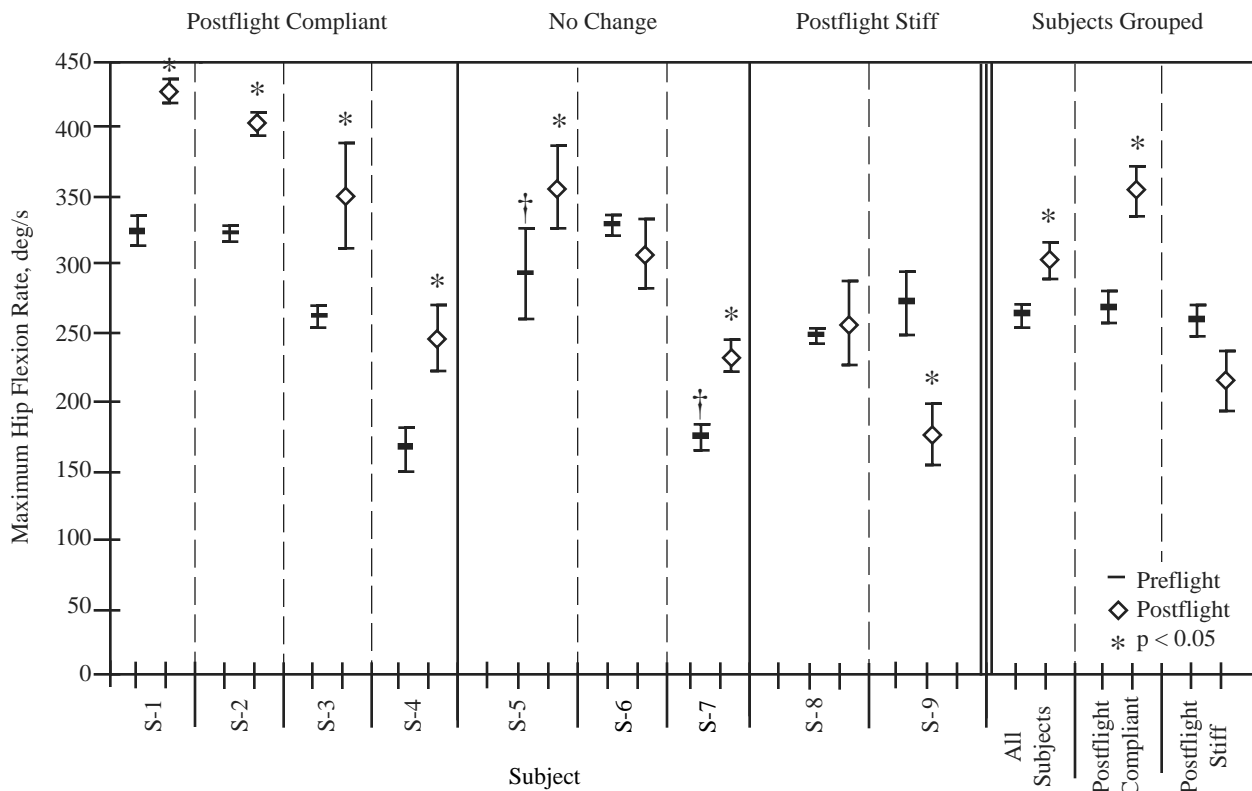


a. Joint flexion angles following impact from a 30 cm jump for the knee: postflight vs. preflight

Figure 5.5-27. Average preflight and postflight maximum values for nine astronaut subjects. Levels of statistical significance are denoted by $*p < 0.05$ and error bars indicate the standard error of the mean. A cross “†” indicates a significant test day effect for the contrast between the two preflight sessions.

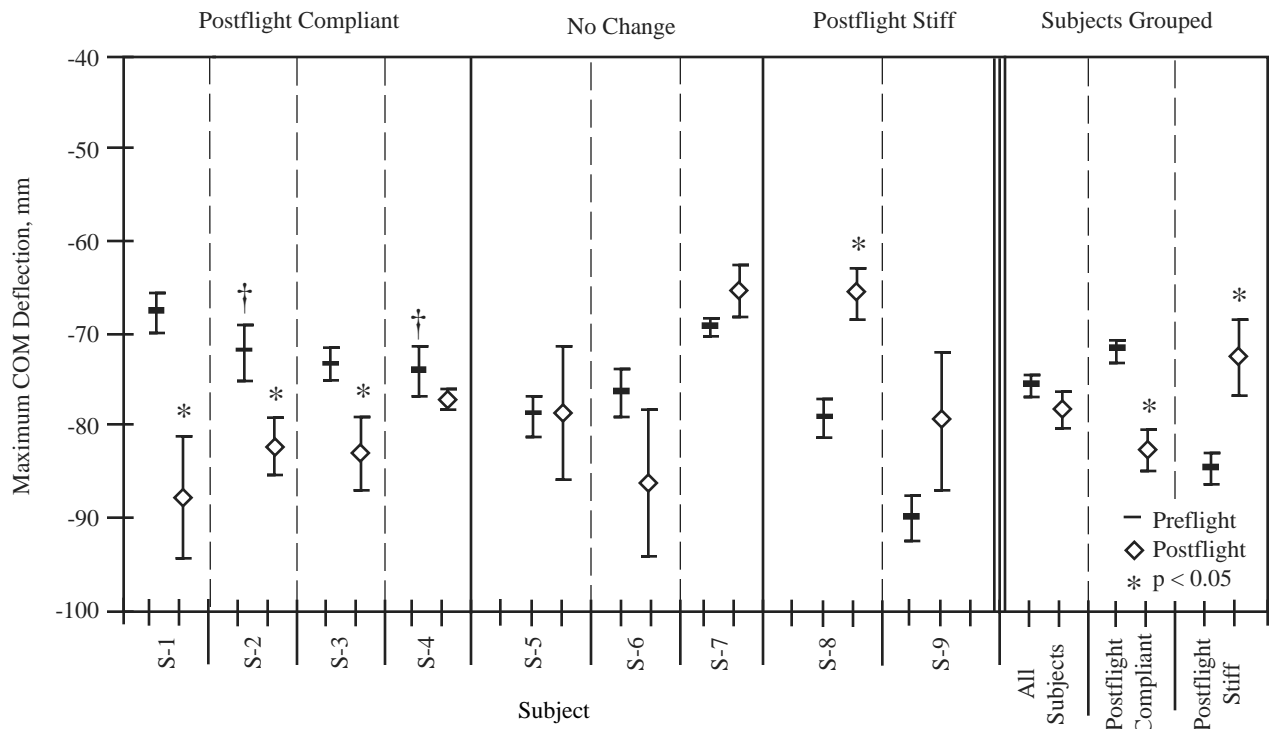


b. Peak joint flexion rate following impact for the knee: postflight vs. preflight

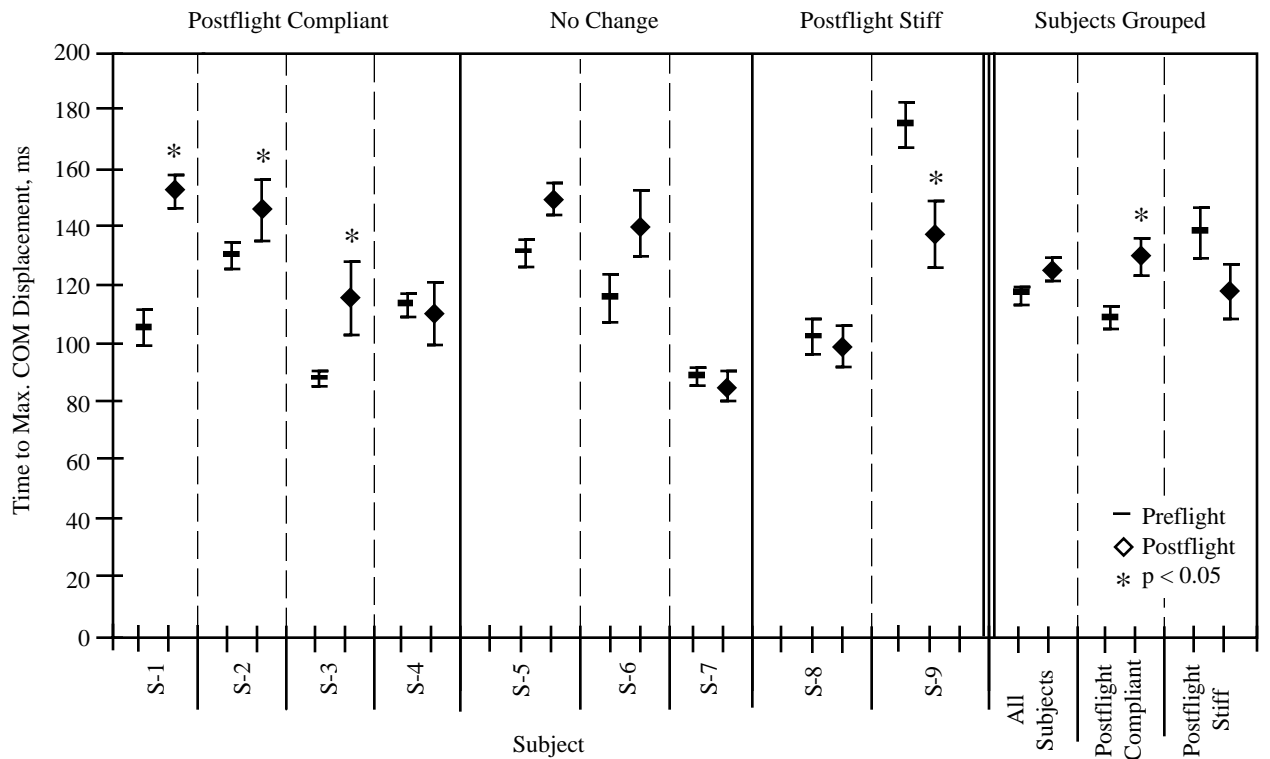


c. Peak joint flexion rate following impact for the hip: postflight vs. preflight

Figure 5.5-27. Concluded.

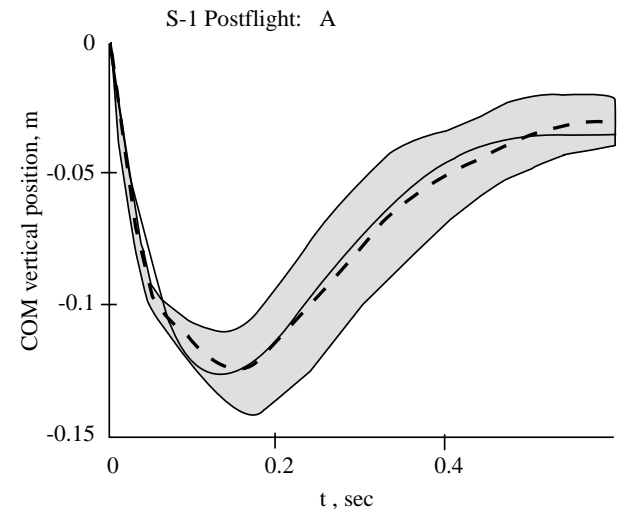
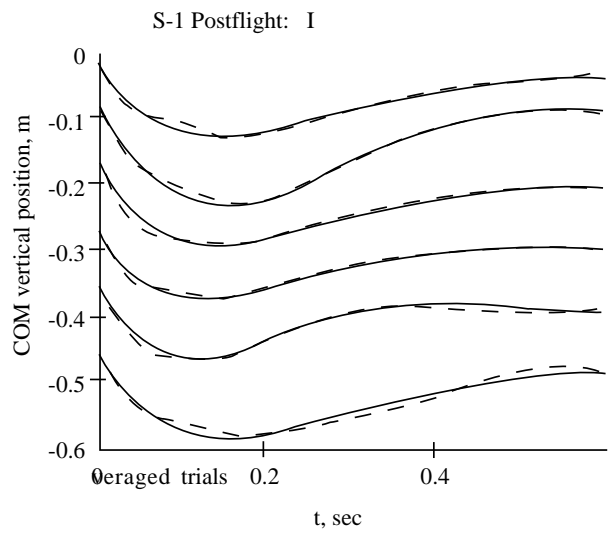
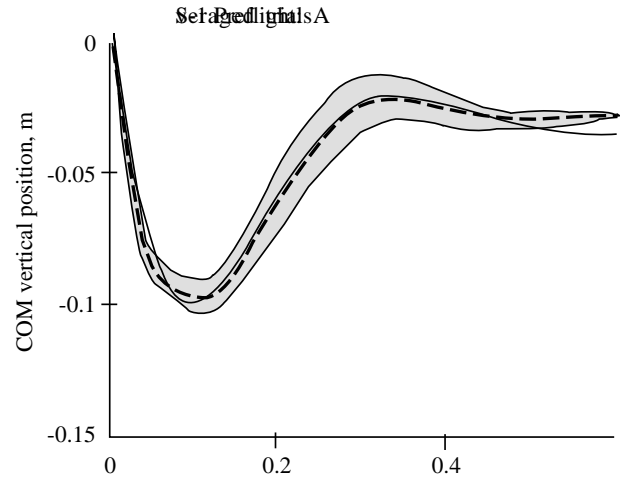
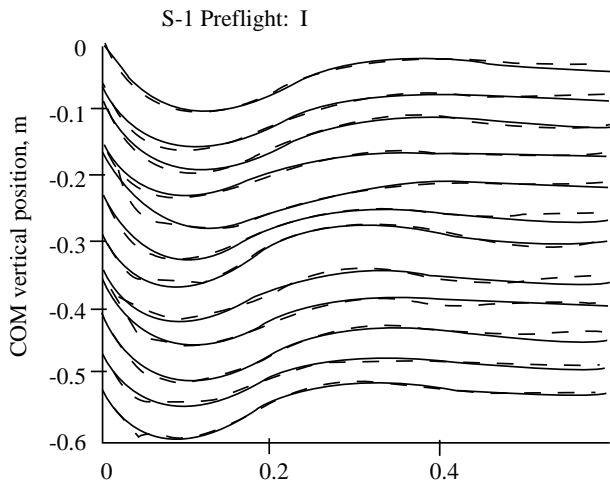


a. Maximum downward deflection of the COM following impact: postflight vs. preflight



b. Time from impact to maximum COM downward displacement: postflight vs. preflight

Figure 5.5-28. COM displacement. Levels of statistical significance are denoted by * $p < 0.05$ and error bars indicate the standard error of the mean. A cross “†” indicates a significant test day effect for the contrast between the two preflight sessions.



a. 12 individual preflight trials (upper) and 6 postflight trials (lower)

b. Corresponding averages for trials shown in (a). The origin represents time synchronization of jump landings at impact. The shaded region denotes ± 1 standard deviation.

Figure 5.5-29. Modeled COM vertical motion using stiffness and damping estimated for representative pre- and postflight for P-C subject S-1. Dashed lines are experimental data and solid lines represent model fits.

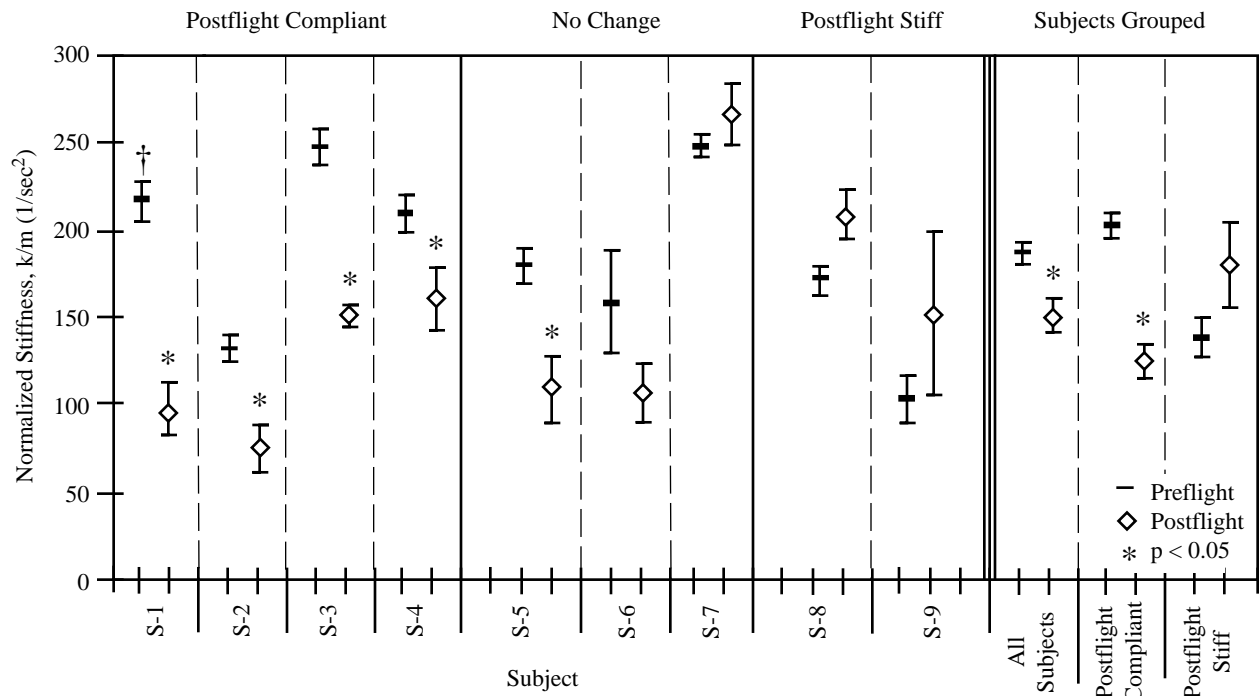


Figure 5.5-30. Mean preflight and postflight model vertical stiffness. Levels of statistical significance are denoted by * $p < 0.05$ and error bars indicate the standard error of the mean. A cross “†” indicates a significant test day effect for the contrast between the two preflight sessions.